Earth observation satellites have become one of the most important tools for monitoring the status of our planet. Among the tasks of the European Space Agency, satellite remote sensing has become a key element providing not only European societies with invaluable informations about their environment and its development.

With the ESA School Atlas, eoVision and ESA continue a long history of cooperation providing teachers and students of secondary schools with up-to-date teaching material introducing the use of satellite data and utilizing the huge potential of Earth observation in answering the important challenges of our time.

The ESA School Atlas consists of this printed atlas and an additional online version providing a wealth of case studies for a large variety of themes:

www.esa-schoolatlas.eu

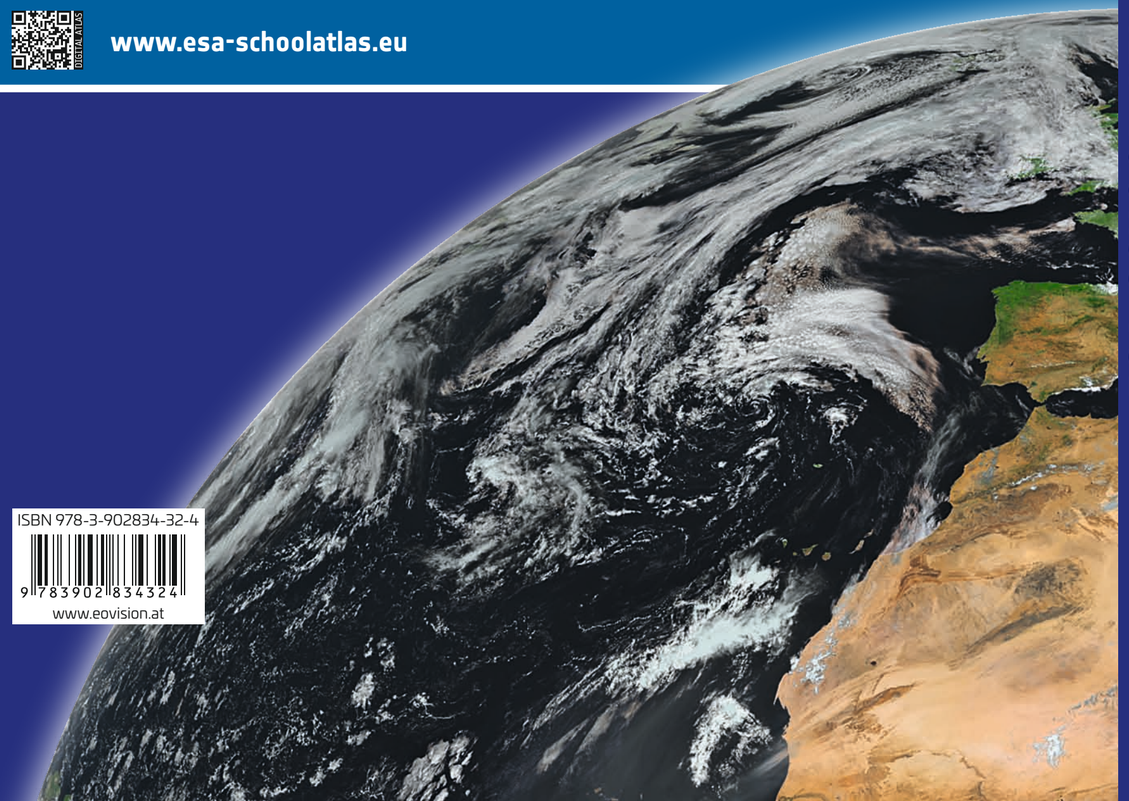

ISBN 978-3-902834-32-4
www.eovision.at

The Earth From Space

ESA SCHOOL ATLAS

eoVISION MEDIA

EUROPEAN SPACE AGENCY

ESA SCHOOL ATLAS

The Earth From Space

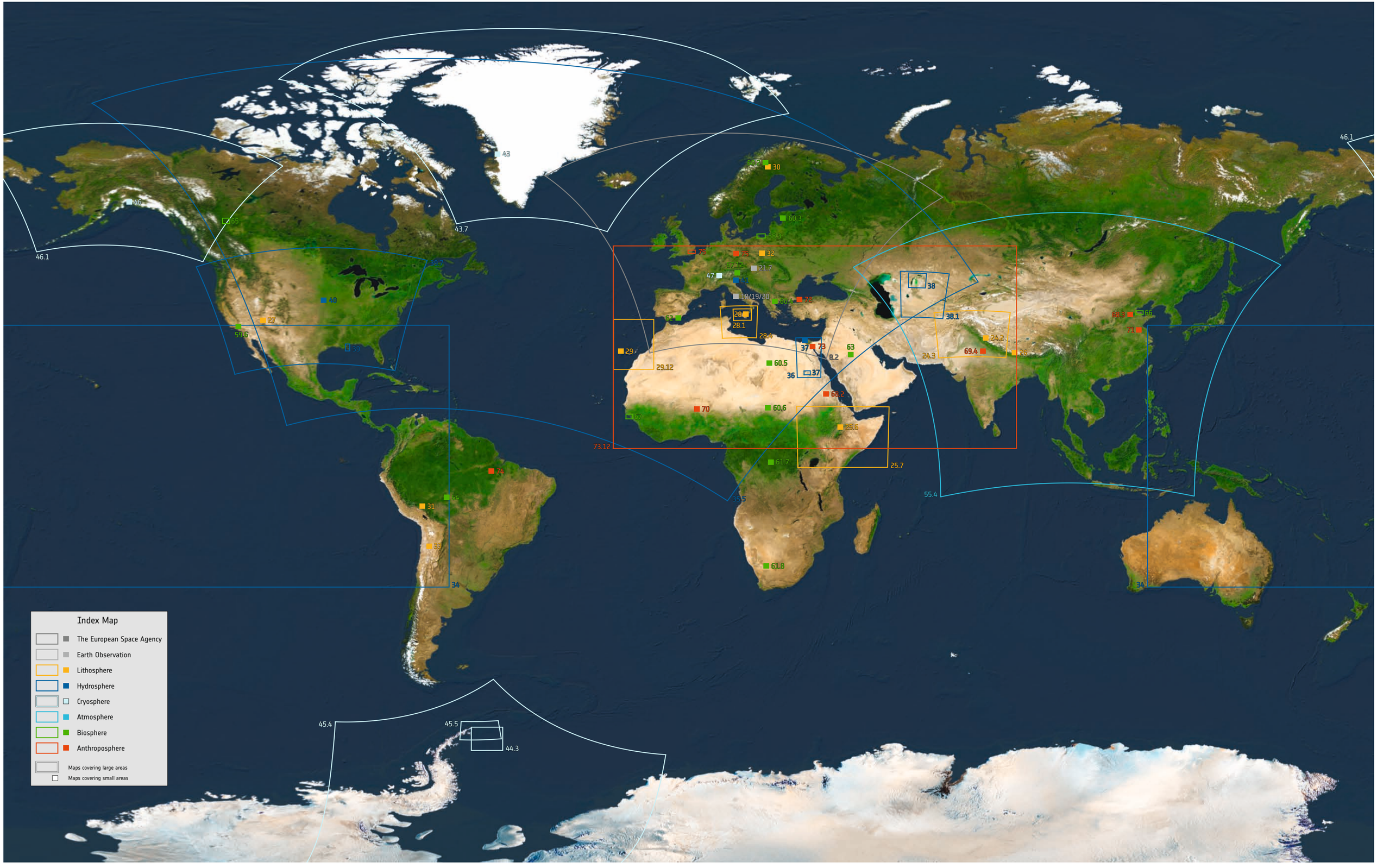
Index Map
The European Space Agency
Earth Observation
Lithosphere
Hydrosphere
Cryosphere
Atmosphere
Biosphere
Anthroposphere
Maps covering large areas
Maps covering small areas
46.1
43
43.7
46
65
39.7
40
27
59.6
39
74
64
31
38
34
30
60.3
58.9
75
75
32
21.7
47
19/19/20
60.4
72
32
28.1
28.4
29
29.12
60.5
37
73
63
8.2
36
37
68.2
70
60.6
67
73.12
25.6
61.7
25.7
35.5
61.8
38
38.1
24.2
69.4
24.3
28
58.3
66
71
55.4
34
45.4
45.5
44.3
46.1

ESA SCHOOL ATLAS

The Earth from Space

ESA SCHOOL ATLAS

The Earth from Space

1. Edition of Atlas, 2024

Franz-Josef-Strasse 19
5020 Salzburg, Austria
Tel.: +43 662 243217
office@eovision.at
www.eovision.at

Coordination
Markus Eisl

Image Editing
Markus Eisl, Gerald Mansberger

Idea and Concept
Markus Eisl, Gerald Mansberger

Editor
Markus Eisl

Layout
eoVision, Salzburg

Printed in the European Union

ISBN: 978-3-902834-32-4

Contents

Contents

The Earth from Space

Earth observation – or Remote Sensing – satellites have proven to be a game changer in helping us better understand the complexities of our planet while also responding to the challenges we face related to the environment, climate change, and sustainability. Satellite data is not only used to answer crucial Earth science questions but also to forecast the weather, assist in disaster response, and provide essential information to optimise agricultural practices, water management, and the siting of renewable energy plants.

Satellite data now forms the basis for evidence-based decision making and countless everyday applications. The European Space Agency (ESA), a world leader in Earth observation, is dedicated to fostering the development of cutting-edge space borne technology needed to further understand the planet, improve the daily lives of citizens, and support effective policy making for a more sustainable future, while also benefiting businesses and economies worldwide.

Space-based systems have seen significant advancements in recent years, driven by technological innovation and the increasing demand for accurate, timely, and comprehensive data about our planet. These innovations span various areas, including satellite technology, data processing, and information sharing. Copernicus – the world-leading Earth observation system and a key part of the European Union's Space Programme – is the result of many of these advancements.

Copernicus provides accurate, timely, and easily accessible information, available free of charge for a wide range of operational services and users, enabling improved management of the environment, the understanding and mitigation of the effects of climate change, and ensuring civil security.

Complementing Copernicus, the development of sophisticated science missions and high-resolution imaging satellites equipped with advanced sensors capable of capturing images of Earth's surface in unprecedented clarity and detail has given rise to multiple new applications such as urban planning and crop monitoring, in addition to supporting increased understanding of Earth's systems.

To foster wide use of satellite data and to raise awareness among citizens, ESA developed a wide variety of resources and activities that aim to inform teachers and students about Earth observation by providing easy access to materials that can be used in lessons. In the context of these activities, the first ESA School Atlas was published in 2005. Now, more than 15 years later, this updated Atlas – the Next Generation – is being published and will grant people the opportunity to learn more about the potential of digital maps and the online platforms delivering the information.

I sincerely hope that the readers and users of this School Atlas become inspired to learn more about satellite Earth Observation and to pursue studies and training on how to use this truly remarkable and valuable data.

Simonetta Cheli
Director of Earth Observation Programmes
European Space Agency

Using the School Atlas

The ESA School Atlas consists of two components: This printed Atlas and a digital Atlas, a web-based collection of materials accessible online via the URL

www.schoolatlas.esa.int

This printed Atlas contains a selection of overview material and case studies that provide offline access to important aspects of Earth observation with a selection of a few case studies highlighting the application of Earth observation techniques.

Structure of the Atlas

The structure of the Atlas follows the model of geophysical spheres comprising lithosphere, hydrosphere, cryosphere, atmosphere, and biosphere. Due to the complexity of our world and the specific importance of the human footprint and climate change, a chapter covering the anthroposphere has been added. Additionally, separate chapters provide background information about the European Space Agency and its activities, and describe basic issues concerning the principles and application of Earth observation tools.

In order to make it easy to change to the online version of the material, QR codes have been added. The QR codes encode the URL of the respective pages in the School Atlas web site.

Our world has become highly complex and involved. Phenomena on all levels have become interlinked and influence each other. In this context, the United Nations have developed the Sustainable Development Goals (SDGs), which provide a means of both categorising phenomena on Earth and of addressing important fields of activity, making it easier to define and to stick to priorities. This very helpful framework, which is seeing more and more widespread use, has been integrated into the Atlas. The icons indicating the relevant SDGs have been added to the respective case studies, making it easier for teachers and students to check the relevance of the case studies for their particular educational task.

UN Sustainable Development Goals

Created in 2016, the SDGs are a comprehensive framework addressing global challenges, from poverty and hunger to climate action and biodiversity conservation. Earth observation plays an important role in advancing these goals by providing critical data and insights.

Examples illustrating this are monitoring and assessing land cover changes, agricultural productivity, and water resources through satellites, which contribute to SDGs like Zero Hunger, Clean Water and Sanitation, and Life on Land. Earth observation data aids in disaster management, supporting SDG 11 (Sustainable Cities and Communities) by providing real-time information during emergencies. Earth observation also plays a crucial role in climate monitoring (SDG 13 – Climate Action) through the measurement of greenhouse gas concentrations, sea level rise, and temperature anomalies. Moreover, satellite imagery assists in mapping urban expansion, supporting sustainable urban planning (SDG 11). Biodiversity conservation efforts (SDG 15 – Life on Land) benefit from Earth observation by monitoring ecosystems, deforestation, and wildlife habitats.

Austria
Belgium
Czech Republic
Denmark
Estonia
Finland
France
Germany
Greece
Hungary
Ireland
Italy
Luxembourg
Netherlands
Norway
Poland
Portugal
Romania
Slovenia
Spain
Sweden
Switzerland
United Kingdom

1. Member states of the European Space Agency (ESA) as of 2024.

2. Member states, cooperating countries and ESA facilities.

The European Space Agency

The European Space Agency (ESA) was founded in 1975. Its mission is to shape the peaceful development of Europe's space capability and ensure that investment in space continues to deliver benefits to the peoples of Europe. ESA has 23 Member States today. By coordinating the financial and intellectual resources of its members, it can undertake programmes and activities far beyond the scope of any single European country.

For more than four decades the Member States of ESA have worked together and pooled their resources to open new pathways in space exploration, develop advanced technology and build a competitive industry able to compete at world-wide level.

ESA's programmes for science, launchers, telecommunications, Earth observation and human spaceflight have demonstrated a high level of competence and have already brought many benefits to everyday life. As well as working on its own independent projects, ESA regularly cooperates with other agencies and institutions in the United States, Russia, Canada, Japan, and China.

A European Vision

The idea of creating an independent space organisation in Europe goes back to the early 1960s when six European countries Belgium, France, Germany, Italy, the Netherlands, and the United Kingdom, associated with Australia formed ELDO (the European Launcher Development Organisation) to develop and build a heavy launcher called Europa. In 1962 the same countries plus Denmark, Spain, Sweden, and Switzerland formed ESRO (the European Space Research Organisation) to undertake scientific satellite programmes and to cover all kinds of space activities from telecommunication satellites to launchers, which were proposed at national level.

In 1975 a convention was endorsed at political level to set up the European Space Agency. In the same year Ireland became a member of ESA and in 1979 the first of a series of Cooperation Agreements was signed to allow Canada to participate in certain ESA programmes and sit on the ESA Council. The convention entered into force on 31 October 1980. Since then, the founding members have been joined by twelve additional European countries. In addition to the regular members, Latvia, Lithuania, and Slovakia have joined as non-full members.

As an important European institution, ESA is closely cooperating with the European Commission and institutions such as the European Environmental Agency EEA and EUMETSAT, e.g. in the context of the Copernicus Programme.

ESA's Activities

Following the strategy defined by ESA, its activities cover a wide range of diverse fields, which all are related to research into and utilisation of space. Among the most important of the activities are:

- Earth Observation
- Human and Robotic Exploration
- Launchers
- Navigation
- Space Science
- Space Engineering & Technology
- Operations
- Telecommunications & Integrated Applications
- Preparing for the Future
- Space for Climate.

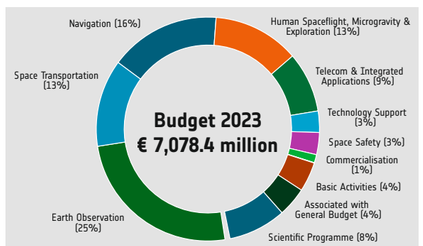

3. About two thirds of ESA's budget are spent for Earth Observation, Navigation, Space Transportation, and Human Spaceflight.

4. ESRIN, Frascati, Italy.

5. ECSAT, Harwell, UK.

6. ESOC, Darmstadt, Germany.

7. ESTEC, Nordwijk, The Netherlands.

8. ESEC, Redu, Belgium.

ESA Headquarters. The Director General and cabinet have their offices in the Headquarters located in Paris, France. It is the organisation's administrative centre and contains the main offices for staffing, legal affairs, finance, budget, internal audit, strategy, international relations and communications.

ESA ESTEC. The European Space Research and Technology Centre in Noordwijk, the Netherlands, is ESA's largest establishment, a test centre and hub for European space activities, responsible for the technical preparation and management of ESA space projects and providing technical support to space activities.

ESA ESOC. The European Space Operations Centre in Darmstadt, Germany, ensures the smooth working of spacecraft in orbit. Linked to ground stations all over the world, it tracks and controls satellites, and carries out payload operations and systems monitoring.

ESA ESRIN. ESA's centre for Earth observation in Frascati, near Rome, manages the ground segment for ESA and third-party Earth observation satellites, maintaining the largest archive of environmental data in Europe and coordinating over 20 ground stations and ground segment facilities in Europe.

ESA EAC. The European Astronaut Centre in Cologne, Germany, is a training facility and home base for all European astronauts. It is a centre of excellence for astronaut training and medical support.

ESA ESAC. The European Space Astronomy Centre at Villafranca de la Cañada, Spain, hosts the scientific operations centres for ESA's astronomy and planetary missions and their archives. It provides services to astronomical research projects worldwide.

Europe's **Spaceport** in French Guiana, is Europe's gateway to space. Covering over 96 000 hectares, it is ideally sited for launching satellites, in particular because it is close to the equator. ESA is the owner of the launch and launch vehicle production facilities.

ESA ESEC. European Space Security and Education Centre at Redu, Belgium, is a centre of excellence for space cyber security services, home to the Space Weather Data Centre, the ESA Education Training Centre dedicated to the training of teachers and students within the ESA Education programme, and part of ESA's ground station network.

ESA ECSAT. The European Centre for Space Applications and Telecommunications in Harwell, UK, supports activities related to telecommunications, integrated applications, climate change, technology and science.

9. ESA Headquarter in Paris, France.

10. European Spaceport, Kourou, French Guiana.

11. EAC, Cologne, Germany.

12. ESAC, Villafranca, Spain.

1. Selection of ESA space science missions for planetary science and astrophysics.

Planetary Science Missions
[2024] Hera
[2023] Juice
[2018] BepiColombo
[2016] ExoMars TGO & Schiaparelli
[2004] Rosetta
[2005] Venus Express
[2003] Mars Express
[2003] Double Star
[2003] SMART-1
[2000] Cluster
[1997] Cassini-Huygens
[1985] Giotto

Astrophysics Missions
[2021] JWST
[2019] CHEOPS
[2013] Gaia
[2009] Planck
[2009] Herschel
[2002] INTEGRAL
[1999] XMM-Newton
[1995] ISO
[1990] Hubble
[1989] Hipparcos
[1983] EXOSAT
[1978] IUE
[1975] Cos-B

Exploring the Solar System

Space science addresses some of the most basic scientific questions of mankind, such as how our Earth formed, why it provides the environment required for our existence, and whether there are other places in the universe, where life exists.
Planetary science deals with our solar system. Originally done solely with the use of telescopes, space technology now allows for travelling to the sun, the planets and other objects in our solar system. In addition to missions acquiring data while passing or orbiting these objects, a number of explorers have landed on some of them. More than this, rovers have roamed Moon and Mars.
The information collected by the planetary science missions helps not only understand the other planets in the solar system, but allows getting deeper insight into the development of the Earth system, for example with respect to climate change.

Towards the Frontiers of the Universe

Other ESA missions aim at targets far beyond the solar system. Light reaching us from a distance of billions of light years is used to investigate the conditions of the early universe e.g. by the James Webb Space Telescope (JWST). A glimpse into a time, when the universe was only 380,000 years old, was obtained with the Planck mission, which measured the cosmic microwave background (CMB) radiation with unprecedented accuracy.
These missions at the edge of what is technologically possible are very expensive. As a consequence, a part of them is done in cooperation with other space organisations. Examples are the Hubble Space Telescope (HST) and the JWST, which have been developed and are operated in cooperation with the U.S. space agency NASA.

4. Combined data taken by the Hubble and the James Webb Space Telescopes provide unprecedented views of deep space, such as this cluster of hundreds of galaxies.

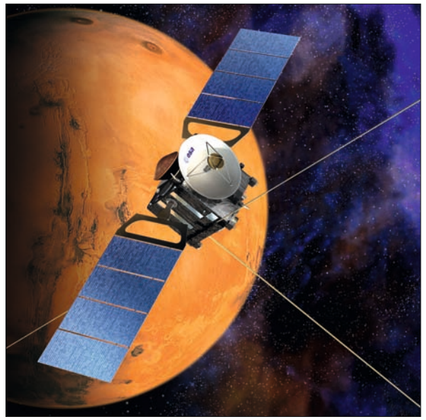

2. Launched in 2003, Mars Express is one of the most successful missions to our neighbour planet.

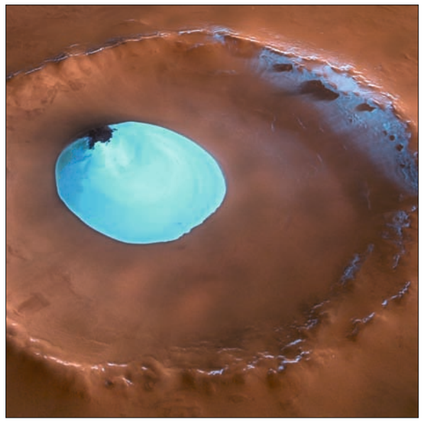

3. Residual water ice in Vastitas Borealis Crater. Data from Mars Express changed our view of the existence and amount of water on the planet.

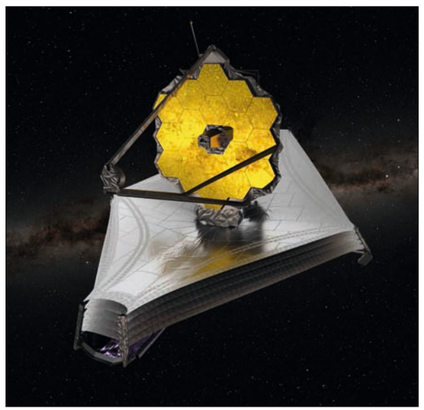

5. Placed in an orbit in a distance of 1.5 million kilometres from Earth, the James Webb Space Telescope is equipped with a primary mirror with a diameter of 6.5 metres. It is protected from solar radiation by a set of screens about 21 x 14 metres large.

Launchers

Satellites as well as human space flight rely on technologies that allow them to reach their "working places" in space. Through the Ariane launcher programme, ESA has provided Europe with autonomous access to space, a strategic key to the development of all space applications. Having been developed initially for the sake of European independence, the Ariane launcher family has become Europe's most spectacular commercial space success by virtue of the volume of business and the share of world market. It has become an important factor in Europe's credibility as a space power.
Europe's activities in this field benefit from the best placed and most efficient launch base in the world near Kourou, in French Guyana, South America.

Arianespace, the international company formed to market the European launcher, has secured more than half of the world market for launching commercial communications satellites into geostationary transfer orbit. Whilst ESA continues to finance improvements to Ariane and a small launcher called Vega, the Agency is also alert to more radical long-term possibilities, such as reusable launchers.

Ariane 5 and 6 — The Ariane 5 heavy-lift launcher was conceived by ESA to ensure that Europe maintained its competitive edge in the worldwide launcher market. It replaced the successful Ariane 4 series and made about five missions every year. Ariane 5's principal mission is to put satellites into geostationary orbit. Its versatility provides adaptability, allowing it to meet a wide range of launch needs, including deployment of satellite constellations, exploration of planets in our solar system, and orbiting cargos for the Space Station. The ECA version of Ariane 5 carries payloads of up to 10 tonnes into orbit.
Ariane 6 has been developed as the successor to Ariane 5 with the main goal to significantly reduce the launch cost. The first launch took place on July 9th, 2024.

Vega — In 2012 a new European small launcher called Vega started its first flight. Vega was planned to place mainly scientific and Earth observation satellites weighing up to 2500 kg into polar and low-Earth orbits.

Human Spaceflight

The International Space Station (ISS), the world's largest ever technical co-operation in peacetime history is a powerful science laboratory, a testbed for future technologies and a facility for advanced medical, biological, physical and material research in the special environment of space. Europe has a substantial share in the ISS and ESA's main hardware contributions are Columbus, a multipurpose science and technology laboratory, and the Automated Transfer Vehicle (ATV). European astronauts are making regular visits during the construction phase and serve as long duration crew members of the ISS, which is continuously manned since late 2000.

6. Ariane 5 lift off from Kourou.

7. Size comparison of Vega, Vega-C, Ariane 5 ECA, Ariane 62, and Ariane 64 (from left to right).

Research and Development

The ISS provides a unique capability to study how gravity affects biological, physical and chemical processes. The effective absence of gravity on the Space Station allows new insights into human health, disease prevention and treatment.

8. Space walk of ESA astronaut Luca Parmitano during a mission on board of the ISS.

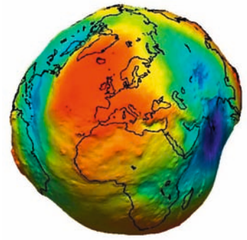

1. GOCE provided valuable information about Earth's gravity field (blue to red: from lower to higher gravity).

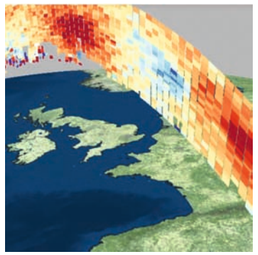

2. Aeolus measures wind speeds in different altitudes (from blue to red: from low to higher wind speeds).

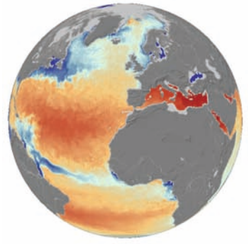

3. SMOS measures ocean salinity and soil moisture content (blue to red: low to higher salt concentration).

4. The Earth Explorer satellites are important platforms for developing Earth observation tools.

Earth Observation Research

From its beginning, research has played an important role for the European Space Agency (ESA). This holds true not only for the exploration of the solar system and space science, as ESA's research activities have a special focus on Earth observation.

In this context, ESA is actively involved in the fields of satellite and sensor technology, and the development of data analysis methods and Earth observation applications. A wealth of research projects have been performed covering a wide range of scientifically important issues.

Launched in 1991 and 1995, respectively, the radar satellites ERS-1 and ERS-2 were ESA's first Earth observation satellites and an important step to gain expertise in this field. The enormous scientific value of these missions is reflected by the fact that they were the basis for about 5000 research projects resulting in about 4000 publications.

In 2002, the Envisat satellite was launched, a milestone in the history of Earth observation. Operational until 2012, this bus-sized satellite weighed more than 8 tonnes, making it the largest Earth observation satellite ever built. Envisat was a research laboratory in an orbit 800 km above the Earth's surface. Numerous sensor and data processing technologies were tested with respect to their applicability in operational services.

Earth Explorers

GOCE (2009-2013) — The Gravity field and steady-state Ocean Circulation Explorer (GOCE) mission provided data to determine global and regional models of Earth's gravity and geoid. This is advancing research in areas of ocean circulation, physics of Earth's interior, geodesy and surveying, and sea-level change.

SMOS (launched 2009) — The *Soil Moisture and Ocean Salinity* mission is making global observations of soil moisture and ocean salinity. By mapping these variables, SMOS supports our understanding of exchange processes between Earth's surface and atmosphere and helps to improve weather and climate models.

CryoSat (launched 2010) — The CryoSat mission is monitoring centimetre-scale changes in the thickness of ice floating in the oceans and of the ice sheets covering Greenland and Antarctica. This helps to understand how the volume of Earth's ice is changing and how ice and climate are interrelated.

Swarm (launched 2013) — Swarm is a constellation of three satellites to measure precisely magnetic signals from the magnetosphere, ionosphere, Earth's core, mantle, crust and the oceans. This will lead to an improved understanding of the processes that drive Earth's 'dynamo'.

Aeolus (2018-2023) — The Aeolus mission made advances in global wind-profile observation and provided information to improve weather forecasting. Demonstrating novel laser technology, Aeolus paved the way for the future operational meteorological mission dedicated to measuring Earth's wind fields.

EarthCARE (launched 2024) — The *Earth Clouds Aerosols and Radiation Explorer* is a European-Japanese mission to improve the representation and understanding of Earth's radiative balance in climate and numerical weather forecast models.

Biomass (planned for 2025) — The Biomass mission will provide information about the state of our forests and how they are changing. The data will be used to improve our knowledge of the role forests play in the carbon cycle.

FLEX (planned for 2025) — The *Fluorescence Explorer* will map vegetation fluorescence to quantify photosynthetic activity. This will improve our understanding how photosynthesis affects the carbon and water cycles.

FORUM (planned for 2027) — The *Far-infrared Outgoing Radiation Understanding and Monitoring* mission will provide insight into the planet's radiation budget, thus improving climate models.

Harmony (planned for 2029) — In tandem with the Sentinel-1 satellites, the Harmony satellites will deliver high-resolution observations of motion occurring at or near Earth's surface, providing information about our oceans, ice, earthquakes and volcanoes.

ESA Education Programme

In the ESA Convention, the ESA Education Programme is a mandatory activity. Education is fundamental to prepare the future workforce that will turn Europe's space strategy and ambitions into reality. Moreover, it helps building generations of future citizens who are informed, able to decide and to act responsibly, and who are equipped to face the challenges of the future, whatever profession they choose.
Space is used as an asset in support of STEM (Science Technology, Engineering and Mathematics) education. Space is an important part of contemporary culture, it is a societal and economic driver and enabler. Learning by using space means accessing top-edge knowledge, learning to collaborate, create, innovate. In other words, it means being accompanied on an inspired, unique path to developing so called 21st century skills – everything that a young person should be given the possibility to develop to be successful in a career and to contribute to a better future.
Inspired education is a fundamental part of the ESA strategy for Europe's future in space – Agenda 2025. In December 2022 the ESA Member States approved the *Space for Education 2030* (S4E 2030) vision and plan, giving their green light for the ESA Education Programme to go wider, more innovative, more inspirational, and reaching much further than before.

Space for Education 2030 targets a wide age spectrum, from early ages up to the very first career stages, through the STEM Learning and Inspiration programme, for the education and inspiration of 3-18 years-old children and pupils, and the ESA Academy programme, for the skill-building and engagement of students in higher education.
The new *STEM Learning and Inspiration* programme consists of two activity sets. *Learn with Space* is strictly educational, with activities designed with specific learning objectives in mind, both for youngsters and their educators. The second, *Let Space Inspire You*, is strictly inspirational; it is aimed at using the 'wow' factor generated by space to spark children and teenagers' curiosity and imagination, and to stimulate their interests towards STEM and space studies and careers. Synergy of activities within the two sets is pursued, so to mutually reinforce the learning and inspirational elements of the experience proposed.
All these activities are solidly rooted and implemented at national level through the ESA ESERO *(European Space Education Resource Office)* framework, a network of national offices and consortia of partners established by ESA in its Member and Associate States.

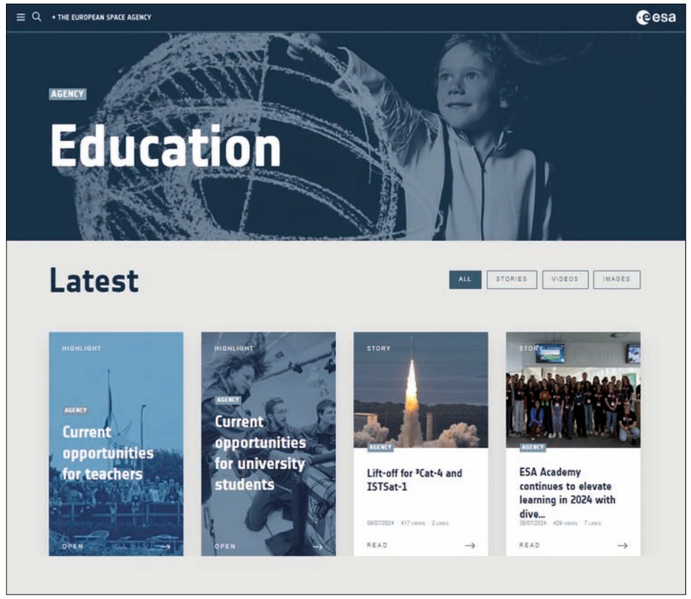

5. The websites of ESA Education and of the ESEROs offer large amounts of multi-lingual space related resources for teachers.

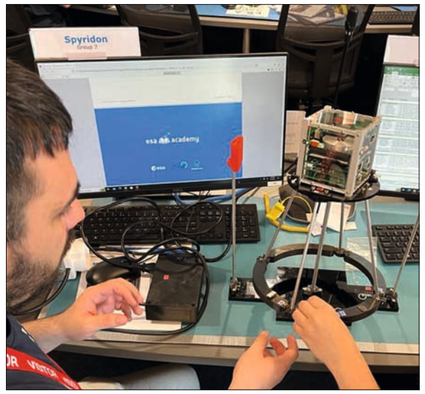

6. In special courses students can develop their own nanosats, small satellites performing specific tasks.

7. In the CanSat competitions, teams from schools all over Europe design their projects, in which sensors are launched for short flights during which the measured data are recorded and transmitted to a ground station.

1. Within the space component of the Copernicus programme a wealth of Earth observation satellites have been launched and are planned to be launched during the next years.

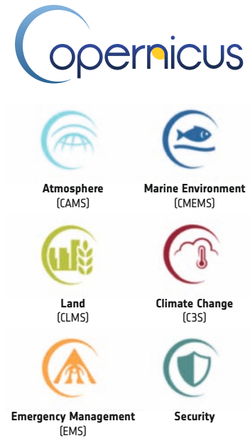

2. The Copernicus browser gives access to a wealth of Earth observation data. The example shows a search result of Sentinel-2 data of the British Channel.

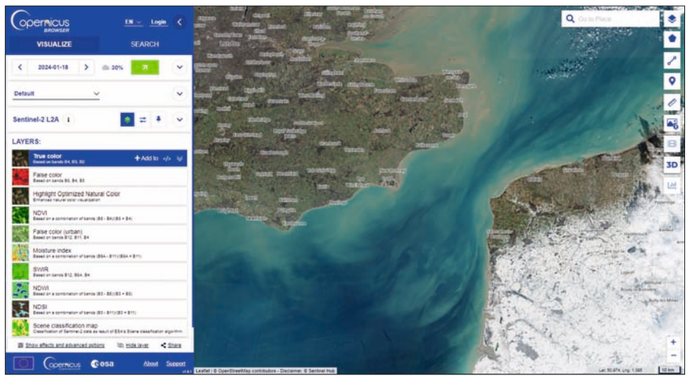

Copernicus — Monitoring the State of Earth

The Copernicus programme, funded by the European Commission, is a highly successful initiative for monitoring the state of Earth. Providing accurate, timely and easily accessible information to improve the management of the environment, understand and mitigate the effects of climate change and ensure civil security, Copernicus is the most ambitious Earth observation programme to date.

The name of the programme pays homage to the great European scientist and observer, Nicolaus Copernicus. His theory of the heliocentric universe made a pioneering contribution to modern science. The Copernicus programme is implemented in partnership with the Member States, the European Space Agency (ESA), the European Organisation for the Exploitation of Meteorological Satellites (EUMETSAT), the European Centre for Medium-Range Weather Forecasts (ECMWF), EU Agencies and Mercator Ocean International.

Vast amounts of global data from satellites and ground-based, airborne and seaborne measurement systems provide information to help service providers, public authorities, and other international organisations improve the lives of citizens from Europe and beyond. The information services provided are free and openly accessible to users via the Copernicus Data Space Ecosystem *(https://dataspace.copernicus.eu/)*.

Copernicus Information Services

Raw data as acquired by the satellites is the basis of all Earth observation information. However, in all applications processed data or information is needed. Copernicus Information Services provide comprehensive data across six thematic areas: Atmosphere, Marine, Land, Climate Change, Emergency Management, and Security. These services leverage a sophisticated infrastructure that integrates data from Earth observation satellites, airborne sensors, and in-situ measurements:

The **Atmosphere service** focuses on monitoring key atmospheric components such as CO_2, the ozone concentration, and UV radiation levels. By providing real-time and historical data, the Atmosphere service contributes to the identification of pollution sources, the evaluation of air quality trends, and the formulation of effective policies.

The **Marine service** offers data concerning ocean conditions, including sea surface temperature, ocean colour, and sea ice extent. These datasets are crucial for applications such as maritime safety, fisheries management, the conservation of marine ecosystems, and climate research.

The **Land service** focuses on monitoring land cover, land use changes, and vegetation health. This service is used in applications ranging from agriculture and forestry management to urban planning and biodiversity conservation.

The C**limate Change service** provides essential information on climate parameters, including greenhouse gas concentrations, temperature anomalies, and sea level rise. This service aids scientists, policymakers, and researchers in assessing the impacts of climate change, and developing mitigation and adaptation strategies.

The **Emergency service** offers rapid mapping and early warning capabilities. During natural disasters or humanitarian crises, these services provide timely and accurate geospatial information, aiding in disaster response coordination, damage assessment, and resource allocation.

The **Security service** focuses on border control and maritime surveillance, utilizing Earth observation to monitor and analyse activities in sensitive regions. This service contributes to the overall safety and stability of both land and maritime borders.

The Sentinel Satellite Fleet

The Sentinel satellites are the backbone of the space-borne information retrieval part of the Copernicus programme, providing a wealth of Earth observation data of different types and resolutions. The satellites come in pairs to ensure a permanent delivery of data even if one satellite fails. Moreover, it is planned to replace Sentinels once they have reached the end of their life cycles. This is important to allow for a long-term use of the applications developed in the Copernicus programme. Currently the following Sentinels are operational or planned:

Sentinel-1 (since 2014): All-weather, day-and-night radar imaging capability for Copernicus land and ocean services with ground resolutions down to 5 metres.

Sentinel-2 (since 2015): high resolution optical image data to support Copernicus Land monitoring studies, including the monitoring of vegetation, soil and water cover, as well as observation of inland waterways and coastal areas. Depending on the wavelength, the ground resolution of the provided data is between 10 and 60 metres per pixel.

Sentinel-3 (since 2016): multi-instrument capability to support the accurate measurements of topics such as land-surface temperature and land colour. The optical instrument of this medium-resolution system acquires data with a resolution in the range around 300 metres per pixel. An altimeter measures e.g. sea level, wave heights, and sea ice.

Sentinel-4 (since 2023, on board of Meteosat MTG): Ultraviolet Visible Near-infrared (UVN) spectrometer and data from Eumetsat's thermal InfraRed Sounder (IRS), both on board of the MTG-Sounder (MTG-S) satellite.

Sentinel-5P (since 2017) and -5 (launch planned for 2024): dedicated atmospheric monitoring mission, which measures air quality, ozone and ultraviolet radiation, and provides data for climate monitoring and forecasting applications.

Sentinel-6 Michael Freilich (since 2020): Altimetry mission performed in cooperation with EUMETSAT and NOAA for monitoring the sea surface level. This mission continues the data acquisition started by TOPEX-Poseidon 20 years ago.

In addition to maintaining this fleet of satellites, it is planned to launch additional Sentinels dedicated to CO_2 monitoring, high resolution temperature measurements, and ice and snow monitoring.

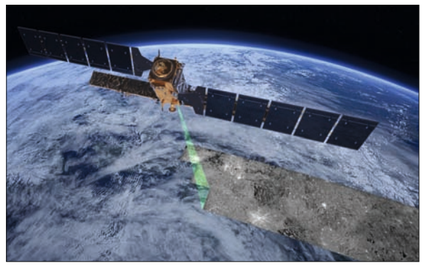

3a. Sentinel-1 radar satellite, artist impression.

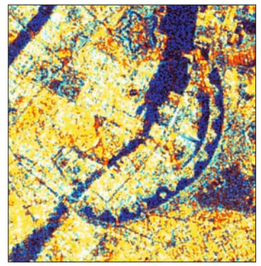

3b. Colour composite radar image of Copenhagen. Data: Sentinel-1.

4a. Sentinel-2 high resolution optical satellite, artist impression.

4b. True colour satellite image of Copenhagen. Data: Sentinel-2.

5a. Sentinel-3 medium resolution satellite, artist impression.

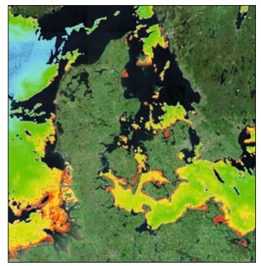

5b. Denmark, algal pigment concentration in the sea. Data: Sentinel-3.

6a. Sentinel-5 atmospheric monitoring satellite, artist impression.

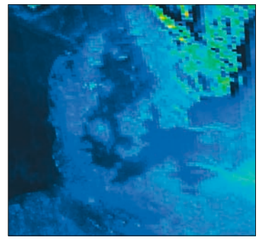

6b. SO_2 concentration above Denmark and south Sweden. Data: Sentinel-5P.

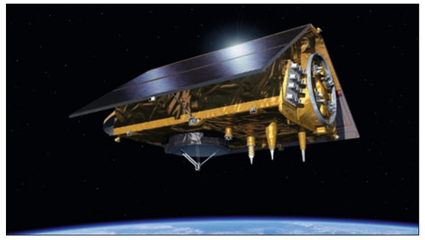

7. Sentinel-6 altimetry mission satellite, artist impression.

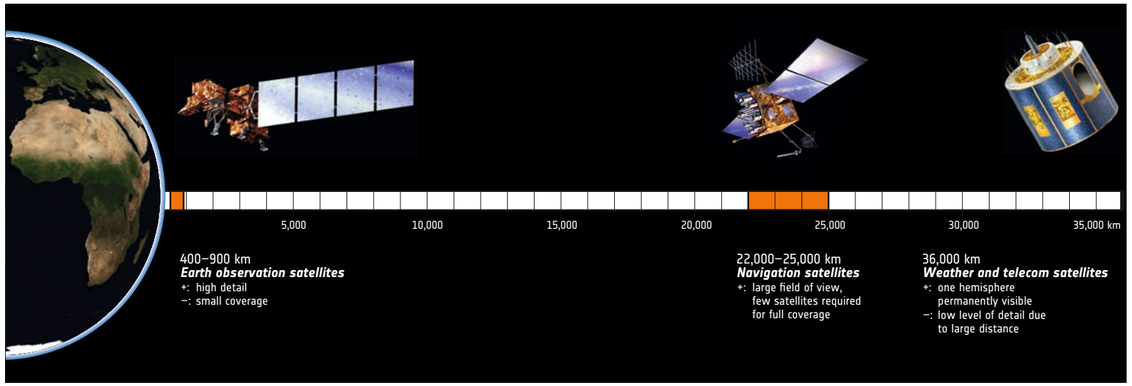

1. Depending on their purpose, satellites operate in orbits at different distances from Earth.

Types of Satellites

There are various types of satellites, each designed for specific purposes, including Earth observation, communication, navigation, and scientific research. Depending on their tasks they are operating in different orbits at different distances from Earth.

Communication satellites facilitate global telecommunications by relaying signals between ground stations, allowing for the transmission of data, voice, and video across vast distances. Positioned in geostationary or low Earth orbits, these satellites provide essential services for television broadcasting, internet connectivity, and mobile communication. Prominent examples include the Intelsat and the Iridium satellite constellations and, more recently, the Starlink constellation with several thousand satellites.

Navigation satellites form the backbone of global navigation satellite systems (GNSS), enabling precise location determination and navigation on Earth's surface. These satellites transmit signals that are received and triangulated by GNSS receivers, providing users with accurate positioning data for navigation, mapping, and surveying purposes. The GPS constellation operated by the United States, along with other systems like Galileo (Europe), GLONASS (Russia), and Beidou (China) comprise navigation satellite networks. Navigation satellites operate in a distance of 20,000 to 25,000 kilometres from Earth.

Earth observation satellites are equipped with sensors and cameras to monitor the planet's surface, atmosphere, and oceans. These satellites capture high-resolution imagery, detect changes in land cover, track weather patterns, and monitor environmental phenomena such as deforestation, urbanisation, and sea level rise. Examples include the Sentinel series for land imaging and the Meteosat series for weather monitoring. Such satellites provide data relevant both for scientific research (such as the Earth Explorers) and for operational applications.

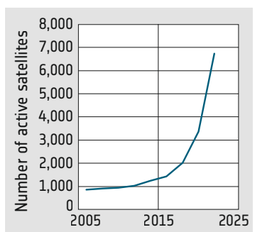

2. During the last years the number of active satellites has grown quickly.

3. Space around Earth has become a crowded place, in which several thousand operational and defunct satellites as well as numerous pieces of debris from all types of missions orbit the planet.

Scientific satellites are designed to explore the cosmos and study celestial objects and phenomena. These satellites are equipped with specialized instruments for conducting astronomical observations, measuring cosmic radiation, and studying celestial bodies such as stars, galaxies, and black holes. Examples include the Hubble Space Telescope for optical astronomy, the James Webb Space Telescope for infrared astronomy, and the Chandra X-ray Observatory for studying X-ray emissions from celestial objects.

Satellites on their way around Earth

Based on specific mission objectives and applications, Earth observation satellites are deployed in various orbits, each offering its advantages and trade-offs. The choice of orbit type influences parameters such as revisit time, spatial resolution, and coverage area. The most important orbit types used by Earth observation satellites are the Low Earth Orbits and the Geostationary orbits.

Low Earth Orbits (LEO) are the most common orbits for Earth observation satellites, ranging from about 180 to 2,000 kilometres above the Earth's surface. LEO satellites have short orbital periods, allowing for frequent revisits to specific areas. This results in high temporal resolution, making them ideal for applications such as weather monitoring, disaster response, and environmental surveillance. Due to their low altitude, the area covered during each pass is limited.

Sun-Synchronous Orbit (SSO): Sun-synchronous orbits are a subtype of LEO designed to maintain a constant angle between the satellite, the sun, and the Earth's surface. This results in consistent lighting conditions during each pass, which is crucial for optical sensors that rely on sunlight. SSO satellites are commonly used for imaging and remote sensing applications, providing regular, well-illuminated images for tasks like land cover mapping and vegetation monitoring.

Polar Orbit: Polar orbits pass over the Earth's poles, allowing satellites to observe the entire surface as the Earth rotates beneath them. This orbit type is common for Earth observation satellites that aim to achieve global coverage. Satellites in polar orbits provide comprehensive views of the planet, making them well-suited for tasks such as climate monitoring, ice mapping, and environmental change detection.

Geostationary Orbits (GEO) are the second important orbit type used for Earth observation and located at an altitude of 35,786 kilometres above the equator. A satellite in a GEO orbits the Earth above the equator, at the speed of Earth's rotation, making it appear stationary relative to a specific point on the Earth's surface. This enables continuous monitoring of that area. While GEO satellites offer continuous coverage, their spatial resolution is lower compared to LEO satellites due to their larger distance from Earth. They are often employed for weather monitoring, communication, and environmental surveillance.

Other orbit types, which are very important for specific purposes, are:

Medium Earth Orbit (MEO): Medium Earth Orbits are positioned between low and geostationary orbits, typically ranging from 2,000 to 35,786 kilometres above the Earth. Navigation satellite constellations like GPS and Galileo use MEO orbits to provide global positioning services.

Highly Elliptical Orbit (HEO): Highly Elliptical Orbits have an elongated shape, with one end closer to the Earth and the other farther away. These orbits are suitable for missions requiring extended dwell times over specific regions, such as high-latitude areas. HEO satellites offer prolonged observation periods, making them valuable for monitoring phenomena like auroras and the Earth's magnetosphere.

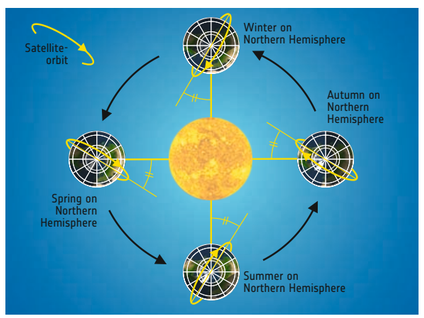

4. Many Earth observation satellites operate in sun-synchronous orbits, in which they cross every point at the same solar time.

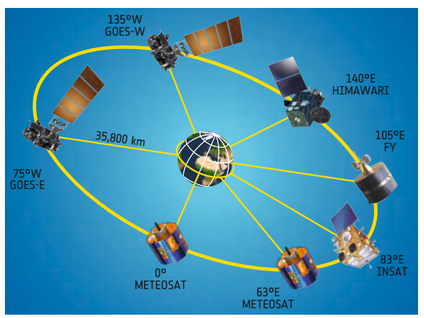

5. The main advantage of geostationary orbits is that satellites remain over the same point of the Earth surface.

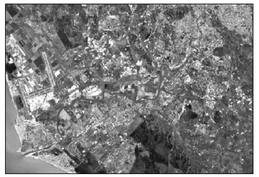

1a. Sentinel-2, band 2 (490nm, blue).

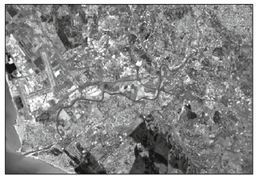

1b. Sentinel-2, band 3 (560nm, green).

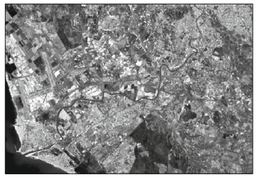

1c. Sentinel-2, band 4 (665nm, red).

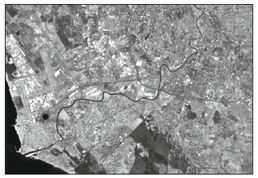

1d. Sentinel-2, band 5 (705nm, red).

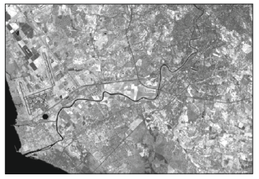

1e. Sentinel-2 band 8 (865nm, IR).

4. Electromagnetic spectrum, atmospheric transmission, properties of selected sensors.

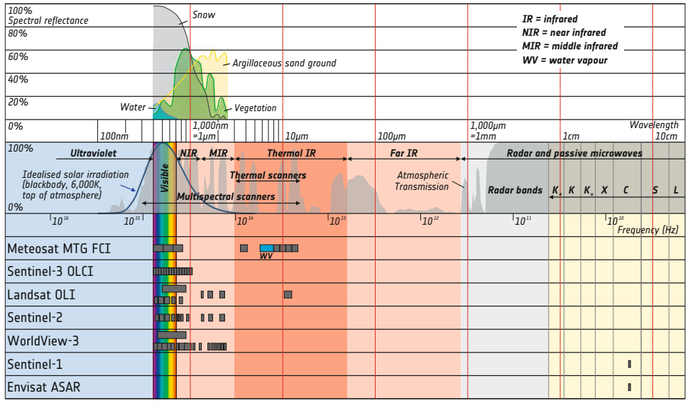

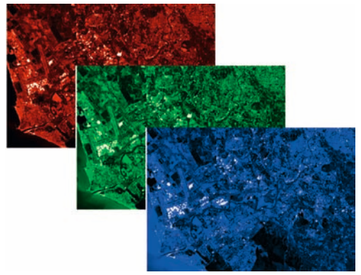

2a. Sentinel-2, bands 4, 3, and 2 prepared for combination into a true colour image.

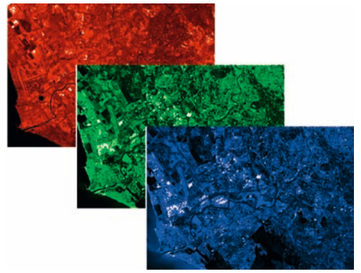

2b. Sentinel-2, bands 8, 4, and 3 prepared for combination into a false-colour infrared image.

From Data to Images

Most Earth observation satellites do not deliver standard colour images. They rather acquire series of greyscale images in different parts of the electromagnetic spectrum. These image bands are used for scientific evaluations, and, similar to the procedures applied in printing and display technology, they are combined to produce colour images of various types.
Different from usual photography, the greyscale image bands are combined in various ways. Depending on the application, images are produced in natural colours (true-colour image), false-colour infrared and other band combinations.

3a. True colour image of the region west of Rome produced using the bands 4, 3, and 2. Data: Sentinel-2, 2022-03-21.

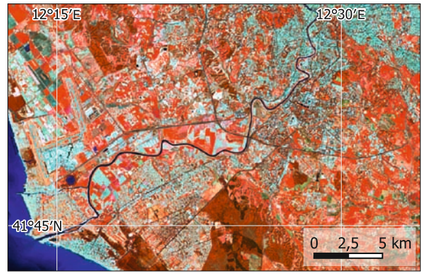

3b. False-colour infrared image of the region west of Rome produced using the bands 8, 4, and 3. Sentinel-2, 2022-03-21.

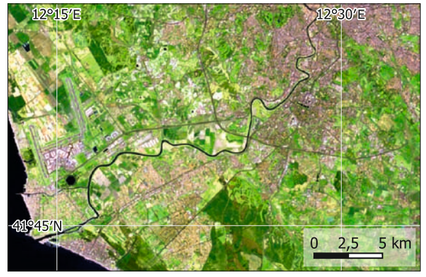

3c. False colour infrared image of the region west of Rome produced using the bands 12, 11, and 4. Sentinel-2, 2022-03-21.

True colours and False-colour infrared Images

While true colour images are used to show the Earth "as it is" (i.e. as it would appear to the human eye) for mapping and illustration purposes, other representations are used to highlight specific properties of the displayed area.
Important additional information is contained especially in the infrared image bands. This information is used e.g. to highlight and to analyse properties of plants, because the chlorophyll contained in the leaves reflects the infrared part of the sunlight very well. This makes this data a valuable information source for applications in agriculture and nature protection.
Other uses for false-colour infrared representations using other infrared bands include analyses of fires and volcanic activities, and of properties of urban spaces.

Radar Satellites

Radar satellite data provide a very special perspective on Earth's surface, capturing information beyond what optical sensors can reveal. In contrast to optical data, which relies on the reflection of sunlight, radar sensors actively emit microwave pulses and measure the return signal. This active sensing capability allows radar satellites to operate independently of external illumination by sunlight, making them suitable for a wide array of Earth observation tasks.

One key advantage of radar satellite data is its ability to penetrate cloud cover, a significant limitation for optical sensors. SAR can "see" through clouds because of its longer wavelength, providing continuous monitoring in regions prone to persistent cloud cover, such as tropical rainforests or high-latitude areas. Together with its independence of daylight conditions, this enables consistent monitoring. This is crucial for applications like disaster monitoring, where real-time information is essential. This constant observational capability proves invaluable for applications like maritime surveillance, where tracking vessels in remote or poorly lit regions can be challenging for optical sensors.

Another distinctive feature of radar data is its ability to measure topography and surface deformation with high precision. Interferometric SAR (InSAR) techniques are used to analyse the phase difference between multiple radar images, allowing for the detection of ground subsidence, elevation changes, and even millimetre-level deformations. This makes radar data indispensable for monitoring ground stability in earthquake-prone regions or tracking subtle shifts in infrastructure.

Radar data's ability to penetrate vegetation provides a unique advantage for forestry applications. While optical sensors are limited in their ability to see through dense canopies, radar can penetrate vegetation layers and capture information about forest structure, biomass, and even detect illegal logging activities.

As for every technology, radar data has its limitations. The spatial resolution of radar imagery is generally coarser than that of high-resolution optical data. While optical sensors can provide detailed information about surface features, radar data may lack the ground resolution needed for specific applications addressing fine-scale details. In addition, the interpretation of radar data is less intuitive than that of optical data and requires sophisticated software tools to extract and evaluate the subtle information contained in the data.

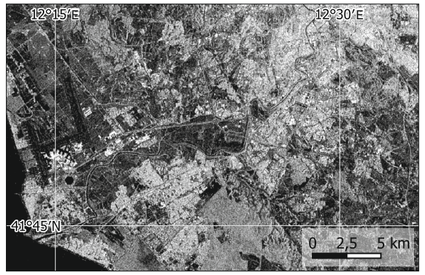

5. Radar image of the region southwest of Rome. Single polarisation image. Data: Sentinel-1, 2022-03-23.

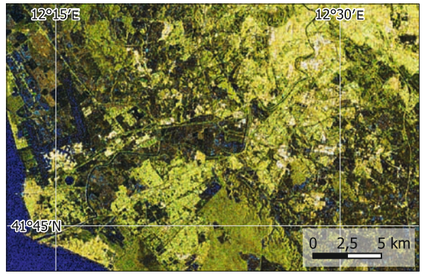

6. Radar image of the region southwest of Rome. Multi-polarisation image. Data: Sentinel-1, 2022-03-23.

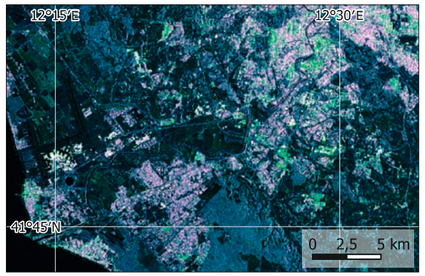

7. Radar image of the region southwest of Rome. Multi-polarisation image optimised for urban analyses (built-up areas appear in violet colour). Data: Sentinel-1, 2022-03-23.

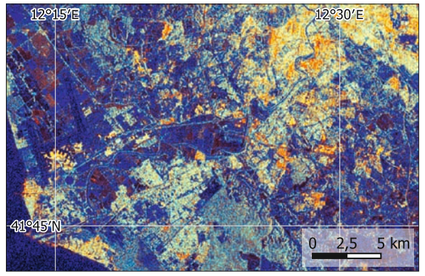

8. Radar image of the region southwest of Rome. Multi-polarisation image optimised for good discrimination of different landcover classes. Data: Sentinel-1, 2022-03-23.

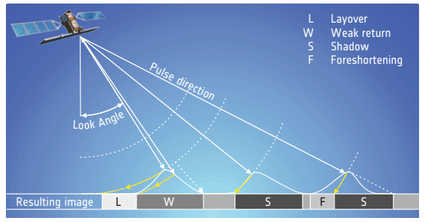

9. Radar satellites send radiation pulses to the surface of Earth and measure the reflected signal. From the time the signal takes to return to the satellite, the distance of the reflecting point is calculated. This allows to produce radar image maps.

Satellite Data Interpretation — Indices

Interpreting satellite data to derive insights about Earth's surface features and changes is a complex task. Index-based analysis has emerged as a powerful tool to extract information from satellite data. Various indices, derived from combinations of spectral bands, highlight specific features, patterns, and environmental conditions:

Vegetation: Vegetation indices are fundamental in monitoring plant health, biomass, and land cover changes. Indices like the Normalized Difference Vegetation Index (NDVI) use the contrast between the reflectance in the red and near-infrared bands to quantify vegetation density. High NDVI values typically indicate healthy and dense vegetation, while lower values may suggest stressed or sparse vegetation. These indices are crucial for applications ranging from agriculture monitoring to ecosystem health assessments.

Urbanisation: Urbanisation indices help analyse and monitor the extent and characteristics of urban areas within satellite imagery. The Urban Heat Island Index (UHII), for example, compares the temperature of urban and rural areas, highlighting the increased heat in urban environments. Other indices, like the Normalized Difference Built-Up Index (NDBI), focus on the built-up areas within the landscape, aiding in urban planning and infrastructure development studies.

Water: Satellite data are used to assess water quality through specific indices. The Normalized Difference Water Index (NDWI) is used to identify surface water bodies, while indices like the Water Quality Index (WQI) use multiple bands to assess parameters such as chlorophyll concentration and sediment loads, offering insights into aquatic ecosystems and water resource management.

Burned Area: Monitoring and assessing burned areas and wildfires are critical applications of satellite data. Indices like the Normalized Burn Ratio (NBR) highlight changes in vegetation cover after a fire. With them, analysts can quantify the severity and extent of the burned area, aiding in post-fire recovery planning and ecological restoration.

Snow and Ice: In polar and mountainous regions, monitoring snow and ice cover is vital for understanding climate change impacts. Indices like the Normalized Difference Snow Index (NDSI) help differentiate between snow and other surfaces. These indices contribute to snowpack assessments, glacier monitoring, and water resource predictions.

Minerals: Satellite data is used in mineral exploration and resource mapping. Indices help e.g. identifying minerals associated with water bodies, facilitating the detection of potential mineral deposits. These indices assist in geological surveys and resource management.

1. True colour image of the region southwest of Rome, showing the mouth of the Tiber, Ostia, and the Fiumicino airport. Data: Sentinel-2, 2022-03-21.

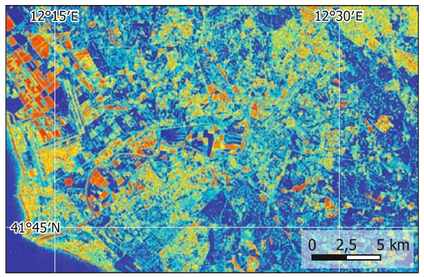

2. Soil moisture index map of the region southwest of Rome. Red colours show dry areas such as built-up areas and bare land, dark blue highlights moist, mostly vegetated areas. Data: Sentinel-2, 2022-03-21.

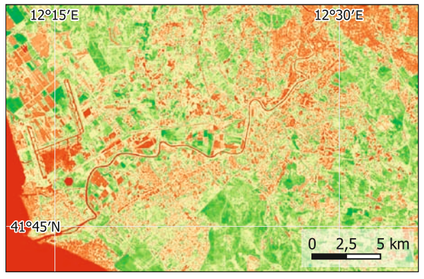

3. NDVI (Normalised difference vegetation index) map of the region southwest of Rome. From red to green the intensity or vitality of the vegetation increases. Data: Sentinel-2, 2022-03-21.

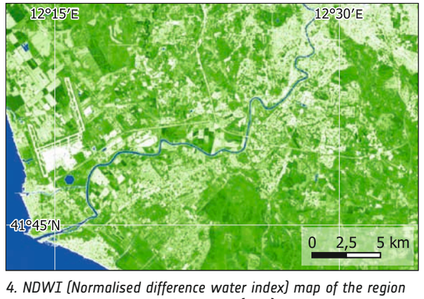

4. NDWI (Normalised difference water index) map of the region southwest of Rome. Water bodies (blue) can be clearly identified, from green to white the water content of the surface decreases. Data: Sentinel-2, 2022-03-21.

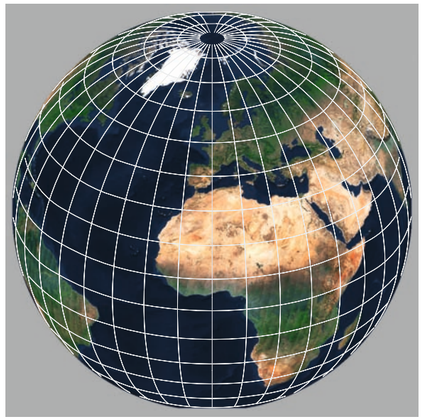

5. The Earth is a three-dimensional body. Representing its surface in two dimensional maps necessarily is accompanied by distortions, leading to errors in the displayed distances, angles, or areas.

From Satellite Data to Maps

The production of accurate and reliable maps from satellite data relies on two critical factors: georeferencing and map projections. These aspects play a fundamental role in ensuring that satellite imagery is not only visually interpretable but also spatially accurate and compatible with existing geographic datasets. This makes it possible to create time series and to use satellite data for updating maps with older information.

Georeferencing is the process of assigning geographic coordinates to each pixel in satellite imagery, establishing a spatial relationship between the image and the Earth's surface. This step enables the integration of satellite data with other geographic information, facilitating accurate analysis and interpretation. Important aspects of georeferencing are:

Ground Control Points (GCPs): Georeferencing is often achieved by identifying ground control points, which are well-defined features with known geographic coordinates. These points act as reference markers, allowing the satellite image to be aligned with a coordinate reference system.

Transformation Methods: Various transformation methods, such as polynomial transformations or affine transformations, are applied to warp the satellite image to match the known locations of the ground control points.

Accuracy Assessment: The accuracy of georeferencing is crucial for reliable mapping. Accuracy assessments compare the mapped coordinates of selected points to their true ground coordinates.

Map Projections: Earth's surface is three-dimensional, but maps are two-dimensional representations, requiring the use of map projections. A map projection is a systematic method for representing the curved surface of the Earth on a flat map.

Selecting an appropriate map projection is crucial to minimize distortions in shape, area, distance, or direction. Therefore it depends on the specific requirements of the mapping project. Important types of projections are:

- *Geographic projection*, providing easy access to the coordinates of a point,
- M*ercator projection*, preserving angles, often used for navigation,
- Equal-area projections like the *Albers Equal Area projection* or the *Mollweide projection*, maintaining accurate representations of relative areas.

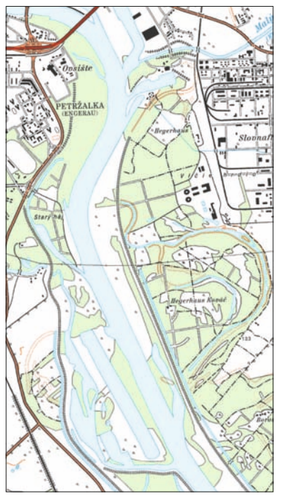

7. Showing recent changes, satellite data is an important tool used to update topographic maps (left: map from 1972, centre: Sentinel-2 image from 2023, right: map from 2023).

6a. In the geographic projection, the lines of constant latitude and longitude form straight lines.

6b. The Mercator projection is an angle-preserving projection with large distortions in higher latitudes.

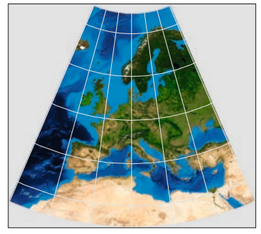

6c. The Albers Equal-Area projection drapes the Earth's surface on a cone.

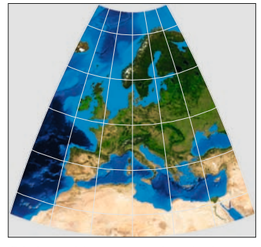

6d. Around its centre point, the Lambert Azimuthal Equal-Area projection shows relatively small distortions.

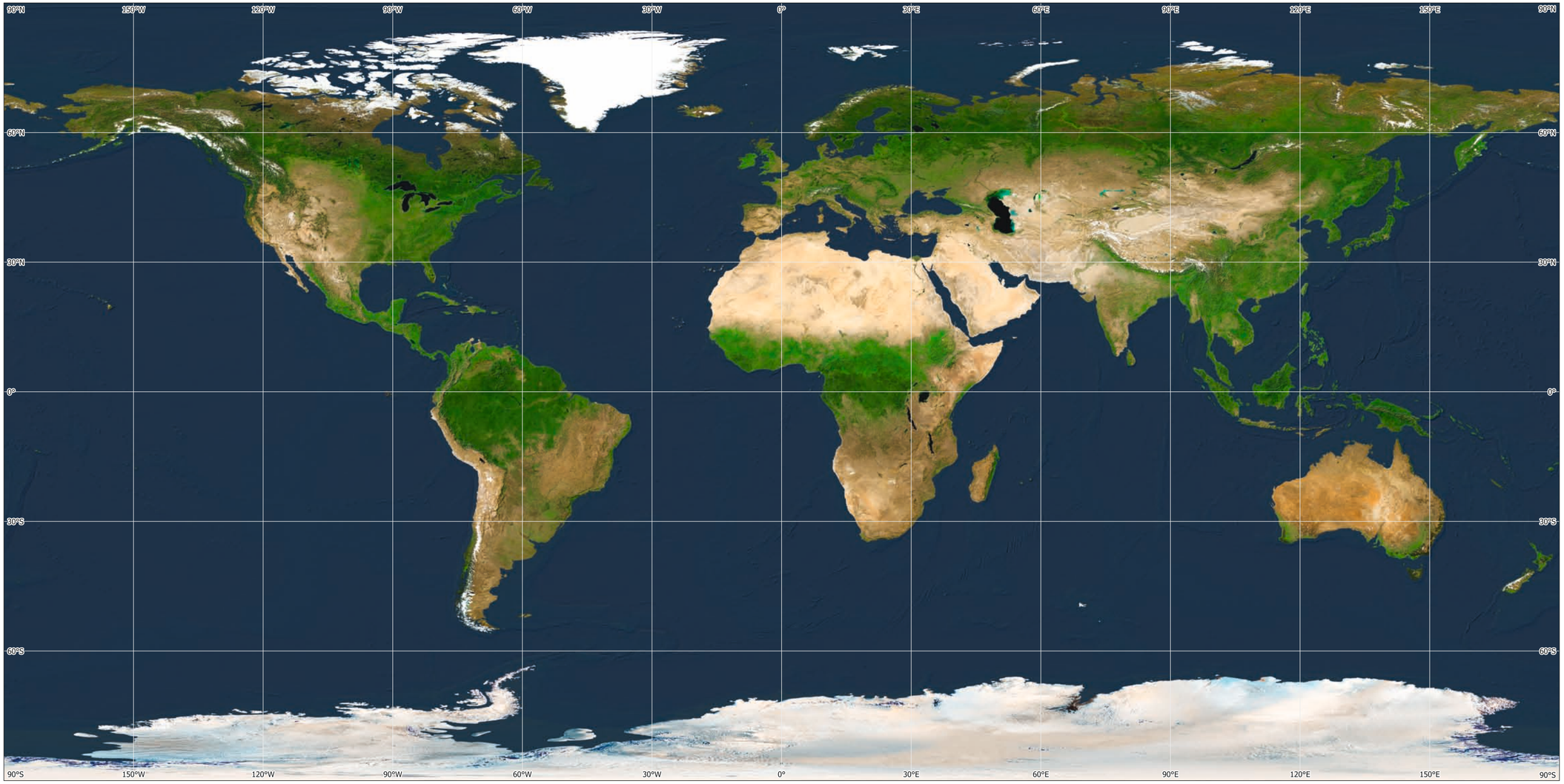

1. Global Daylight Satellite Image Map derived from a large collection of satellite images acquired by the SPOT Vegetation sensor.

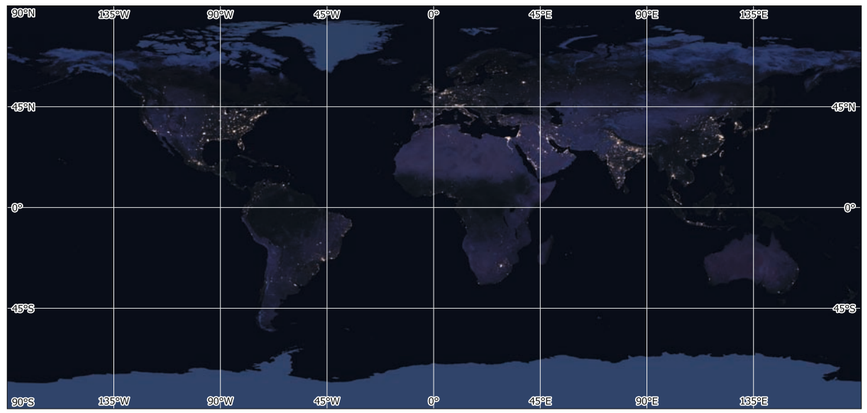

2. Global Nighttime Satellite Image Map (Black Marble). Data: DMSP – Operational Linescan System.

3. Space view of Earth, taken on December 7, 1972, by the crew of the Apollo 17 spacecraft on its way to the Moon at a distance of about 29,400 kilometres.

Global Satellite Views

Earth observation satellites allow viewing the Earth in a homogeneous manner. Usually large parts of the Earth's surface are covered by clouds. To get the full view it is necessary to combine cloud-free images, ideally from the same time within the vegetation period.

Global satellite image maps are produced not only to present the daylight, natural colour situation, they can give an overview of many aspects. Temperature maps, precipitation maps and trace gas maps are examples for the wide range of information produced. A special application are nighttime maps highlighting human activity on Earth.

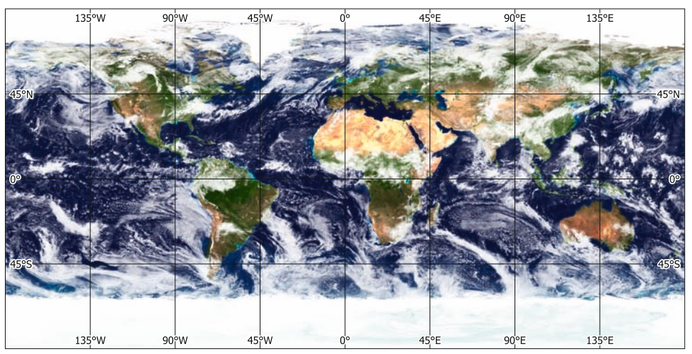

4. This global daytime satellite image mosaic shows the Earth with clouds, which at any time cover a large part of the planet.

LITHOSPHERE

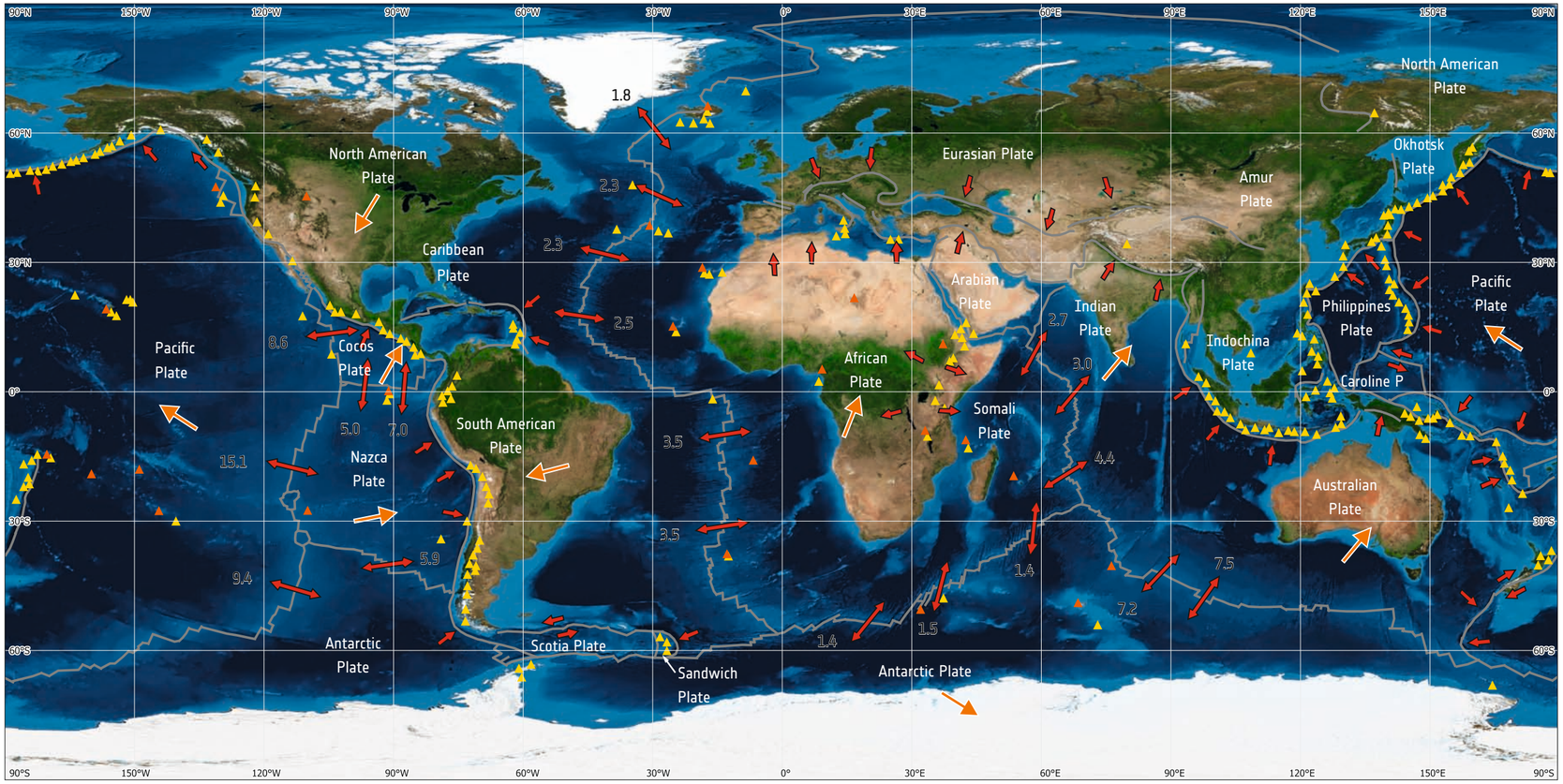

1. Tectonic plates

Tectonic Activities shape the Earth

The crustal movements and deformations driven by the movement of tectonic plates are powerful processes, shaping the surface of the Earth over millions of years. The Earth's lithosphere, comprising the crust and upper mantle, sees immense forces related to the movement and interaction of these plates, leading to the formation of mountains, rift valleys, earthquakes, and other geological phenomena. Examples illustrating tectonic processes are the Himalayas and the East African Rift Valley.

The Himalayas, stretching across South Asia, are the result of the collision between the Indian and Eurasian tectonic plates. This ongoing collision began around 50 million years ago and continues to shape the landscape of the region. The converging plates have caused the uplift of mountain ranges, including Mount Everest, the world's highest peak. The Himalayas exhibit a wealth of geologic processes, including folding and erosion.

In contrast, the East African Rift Valley is the result of divergent forces tearing apart the African continent. The Earth's crust is being pulled apart along a system of rifts, resulting from tectonic plates moving away from each other. This so-called continental rifting is the initial stage of plate boundary evolution. Magma from the mantle contributes to the thinning and eventual separation of continental landmasses. The rift valley's landscape is characterized by steep cliffs, volcanic activity, and lakes.

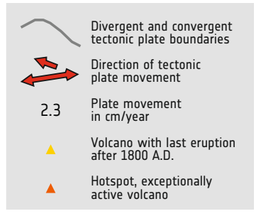

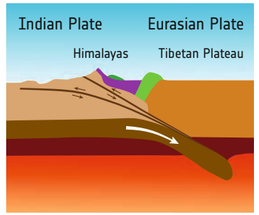

4. Schematic cross section of the Himalayas and the Tibetan Plateau, showing the formation of the mountain chain by the collision of the Indian and the Eurasian Plates.

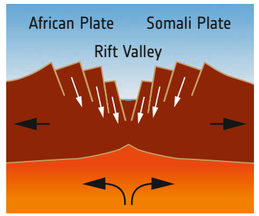

5. Schematic cross section of the East African Rift Valley, showing the formation of the valley due to the divergence of the African and the Somalian Plates.

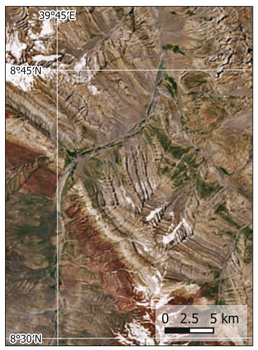

2. Typical fold structures at the northern slope of the Himalayas, showing rock layers in different colours. Data: Sentinel-2, 2023-08-02.

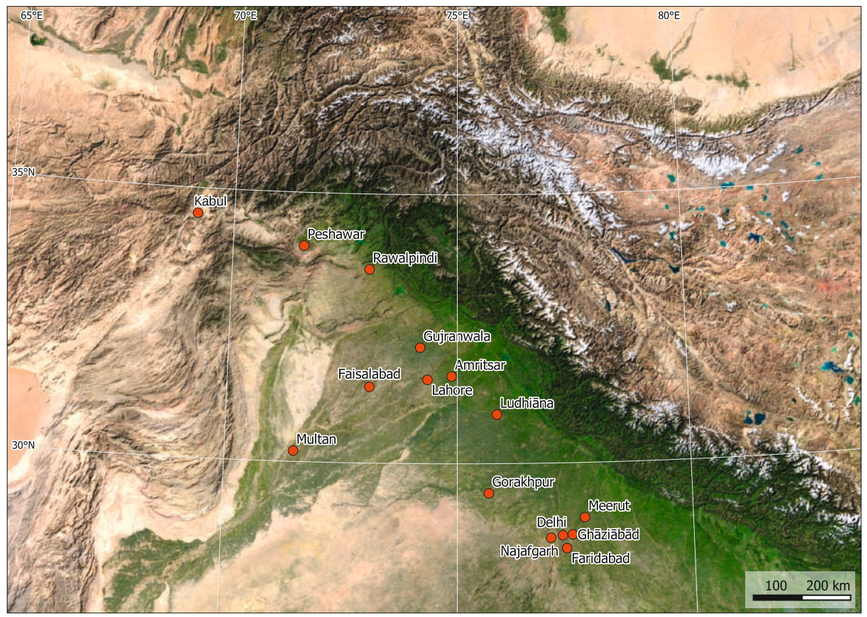

3. The Himalayas are characteristic fold mountains. They are the result of the movement of the Indian Plate towards north, where it collides with the Eurasian Plate.

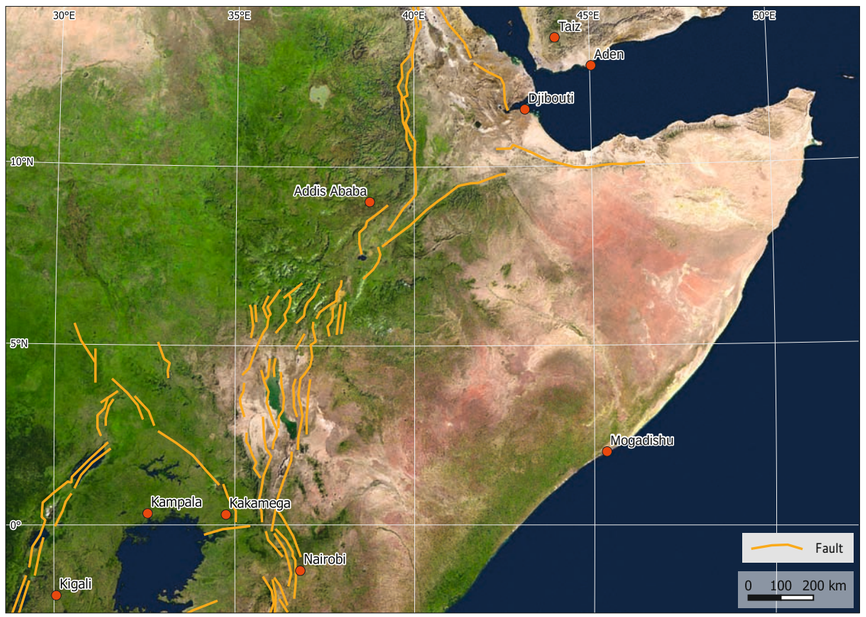

6. Detail view of rifts of the East African Rift Valley east of Addis Ababa, Ethiopia. Data: Sentinel-2, 2023-08-26.

7. The East African Rift Valley is formed by the ongoing separation of the Somalian Plate from the African plate, leading to a thinning of the Earth crust around the separation line.

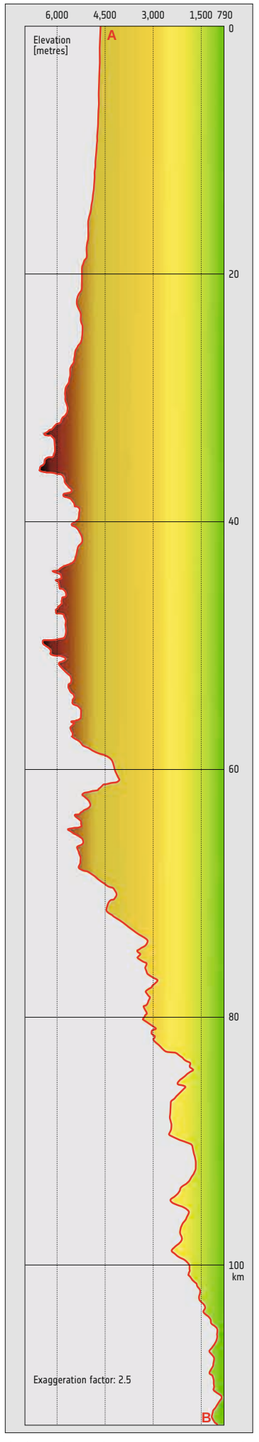

1. *A north-south cross-section through the Himalayas.*

2. *The Himalayas separate the green lowlands in the south from the arid Tibetan Plateau in the north. Sentinel-2, 2023-10-22.*

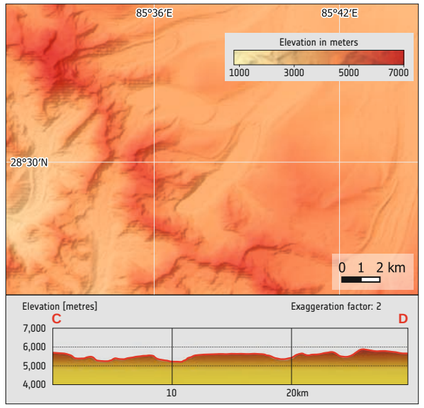

3. *Typical smooth, U-shaped valleys formed by glaciers are accompanied by moraines and glacial lakes.*

Landscapes shaped by Erosion

The slopes of the Himalayas are tectonically active. The collision between the Indian Plate and the Eurasian Plate results in crustal uplift and the formation of the Himalayan mountain range. Different erosion processes are slowing down the uplift of the mountain range.

The northern slope of the Himalayas, the Tibetan Plateau, is characterized by high plateaus, deep valleys, and rugged terrain. This area is largely arid and has a higher average elevation compared to the southern slope. Here the erosion is largely governed by glaciers, leading to the typical U-shaped valleys and moraines of glacial erosion.

The southern slope of the Himalayas is generally more varied in relief, with lower valleys and higher peaks. This region includes the foothills of the Himalayas, which gradually transition into the vast plains of the Indian subcontinent. Here mainly fluvial erosion is seen. The landscape is formed by rivers and landslides, leading to V-shaped valleys.

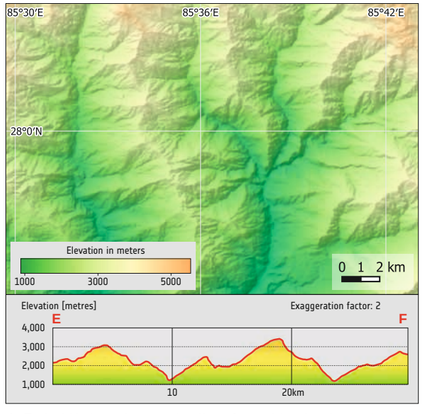

4. *Typical V-shaped, rugged valleys formed by the rivers along the southern slopes of the Himalayas.*

Carved into Sediment Layers

The Colorado Plateau in the south-west of the United States is intersected by the Colorado River. The Kaibab Plateau in the west appears in a green colour as it is vegetated with aspens, spruce-firs and juniper woodlands. The Painted Desert in the east consists of bands of petrified sand dunes parallel to the surface. The Colorado flows from its headwaters in the Rocky Mountain National Park to the south-west, passing the Marble Canyon. At the southern end of the canyon, the river is joined by the Little Colorado River. Over millions of years the erosive force of the water has cut the Grand Canyon through the layers of sediments as the Colorado Plateau has been uplifted.

The detail maps highlight the specific geological and geomorphologic situation of the region, resulting from the fluvial erosion of the otherwise mostly undisturbed sediment layers. The terrain map and the profile illustrate the gorge character of the canyon carved into the surface of the Colorado Plateau.

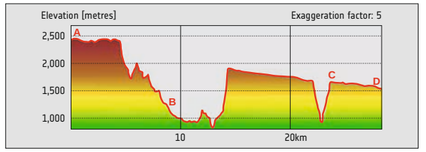

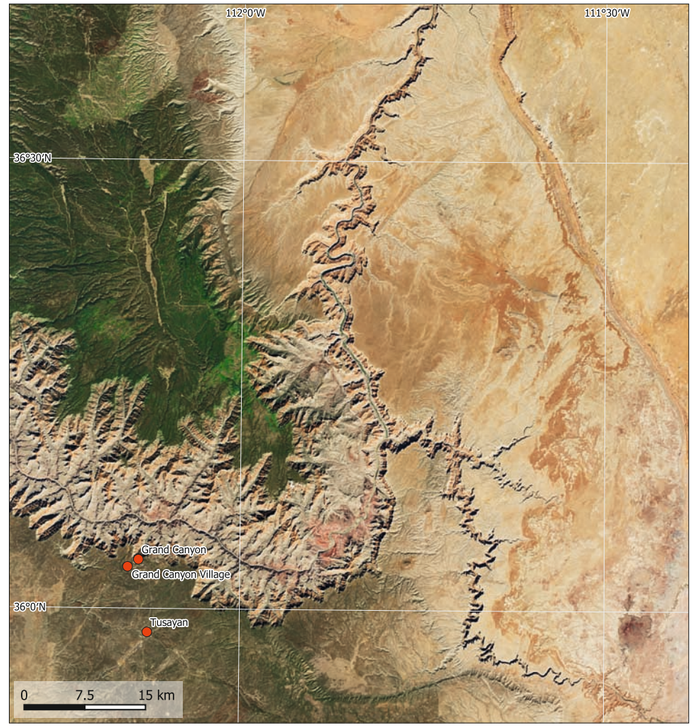

5. *The Colorado River has carved the Grand Canyon up to 1500 metres deep into the layers of sediment rock forming the Colorado Plateau. Data: Sentinel-2, 2023-09-24.*

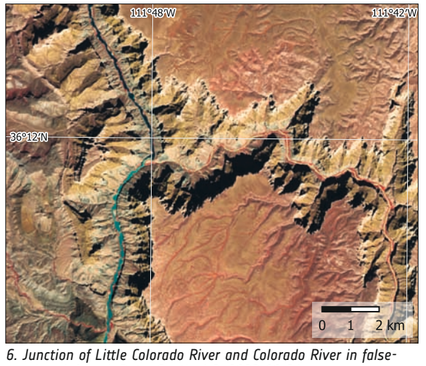

6. *Junction of Little Colorado River and Colorado River in false-colour infrared. Data: Sentinel-2, 2023-09-24.*

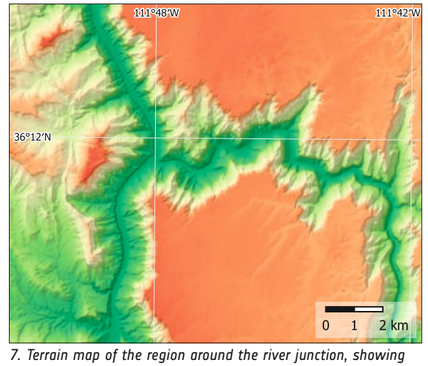

7. *Terrain map of the region around the river junction, showing the ragged canyon cut into the smooth Colorado Plateau.*

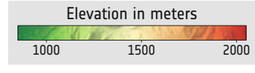

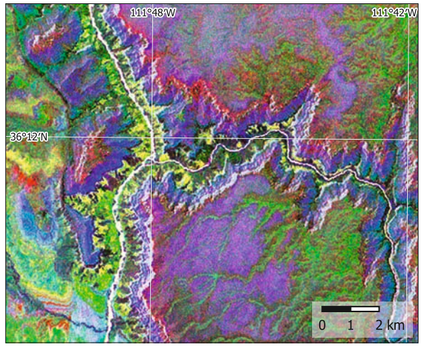

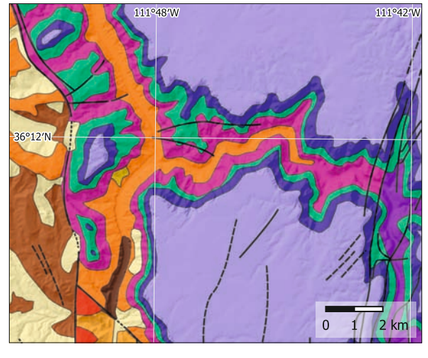

8. *A principle component analysis of the satellite data allows to separate the geological layers (left).*

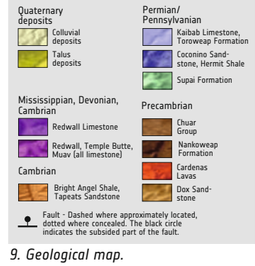

9. *Geological map.*

1. Sicily, overview satellite image mosaic. Data: Sentinel-2 in June 2023.

6. Mount Etna during an eruption.

Mount Etna, Italy

Mount Etna, located on the island of Sicily in Italy, is the largest volcano in Europe and one of the most active volcanoes on Earth. This is reflected in a high frequency of eruptions. People living at and near the slopes of the volcano are used to being repeatedly disturbed by volcanic activities. They make use of the advantages of the situation, particularly the fertile volcanic soil and the role of the volcano as a tourist landmark.

Satellite data is used to closely monitor and quantify damages caused by this natural event. Satellite technology plays a crucial role in tracking the eruption's progress, providing real-time insights into the volcano's behaviour, allowing to map the lava flows, ash plumes, and gas emissions. These observations enable timely warnings to protect nearby communities and air traffic.

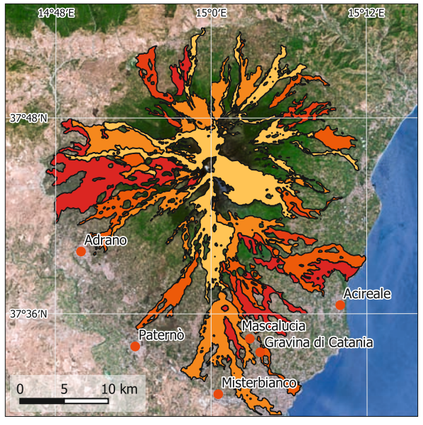

5. Map of the age of the lava fields covering the slopes of Mount Etna. Data: Sentinel-2, 2022-07-06.

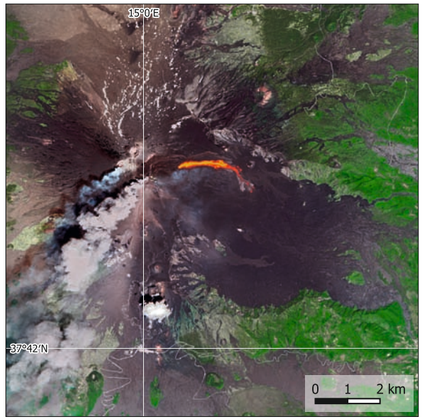

2. Enhanced true colour image of the beginning of the June 2022 eruption of Mount Etna, showing a lava flow east of the summit. Data: Sentinel-2, 2022-06-03.

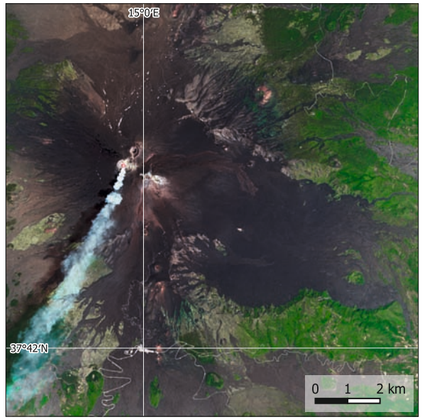

3. The June 2022 eruption of Mount Etna after the lava flows have stopped. Data: Sentinel-2, 2022-06-21.

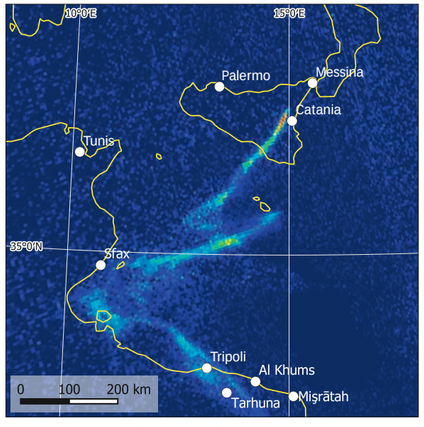

4. SO_2 concentration (total column) showing the plume of the eruption transported bywinds towards south. Data: Sentinel-5B, 2022-06-21.

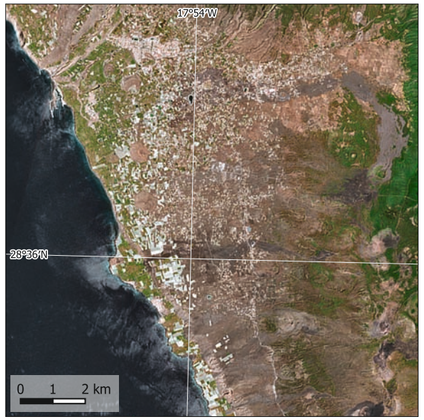

7. True colour image of La Palma, Spain, showing the region around Los Llanos de Ariadne before the eruption in the Cumbre Vieja ridge. Data: Sentinel-2, 2021-08-21.

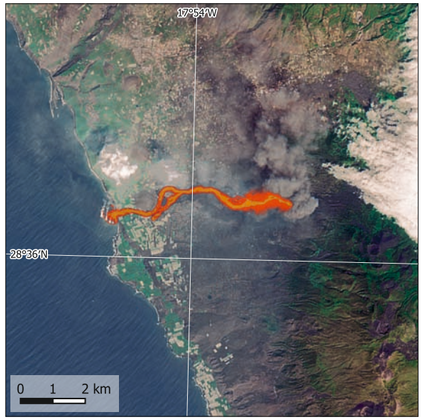

8. True colour satellite image of La Palma, Spain, highlighting the lava flow during the eruption. Data: Sentinel-2, 2021-09-30.

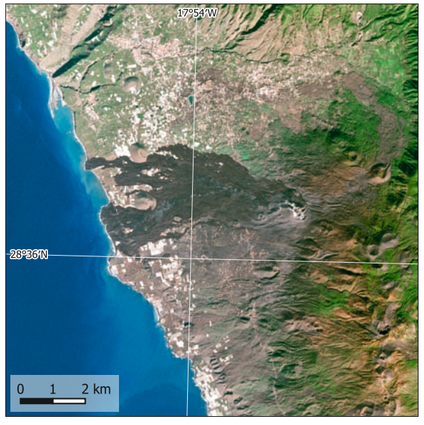

9. La Palma, Spain, showing the new lava cover. Comparison with the image before the eruption reveals the loss of settlements and fields. Data: Sentinel-2, 2022-01-03.

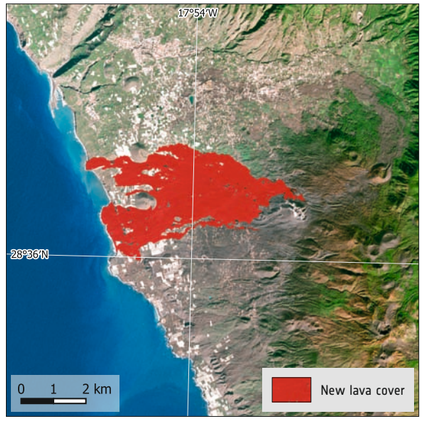

10. La Palma, Spain, after the eruption. The overlay highlights in red the new lava cover as derived from the satellite data. Data: Sentinel-2, 2021-09-30.

Hot Spot Volcanism

Hotspots are regions of the Earth's crust that are located above so-called mantle plumes, regions in the Earth mantle where magma rises due to convection processes. As a consequence, the Earth crust above the plume can be thinned and the volcanic activity of the region can be increased. When the Earth crust moves across the hotspot, the zone of volcanic activity wanders and can create chains of volcanos. Hawaii and the Canary Islands are prominent examples of hotspot volcanism.

La Palma, Spain

The Canary islands are located above the so-called Canarian hotspot, a hotspot and volcanically active region off the north-western coast of Africa. In the autumn of 2021, the island of La Palma, part of the Spanish Canary archipelago off the coast of West Africa, saw a spectacular volcanic eruption.

On September 19th, the Cumbre Vieja volcano, dormant for decades, erupted violently. In a devastating spectacle it unleashed ash and molten lava. Rivers of red-hot lava flew down the volcano's slopes, engulfing homes, farms, and roads. Although the eruption did not claim any lives, the total damage was huge. It was estimated at over 800 million Euros, including the destruction of infrastructure, residential areas, and agriculture. More than 2,800 buildings were destroyed.

La Palma heavily relies on tourism, which suffered from the eruption. Tourism revenue plummeted by approximately 60%, temporarily causing significant job losses and business closures. Additionally, the destruction of farmland and infrastructure disrupted the island's agricultural and transportation sectors.

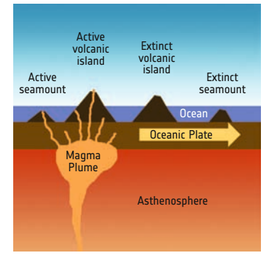

11. Mechanism of the formation of volcanic island chains by hotspot volcanism.

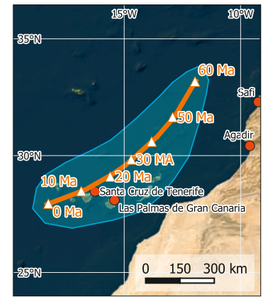

12. Canary Islands hotspot. During the last 60 million years (Ma) the seafloor has moved almost 1000 km across the hotspot, leaving the chain of the Canary Islands behind.

13. La Palma is the youngest of the larger Canary Islands. Its surface exhibits typical volcanic structures such as craters and lava fields. Data: Sentinel-2, 2022-01-03.

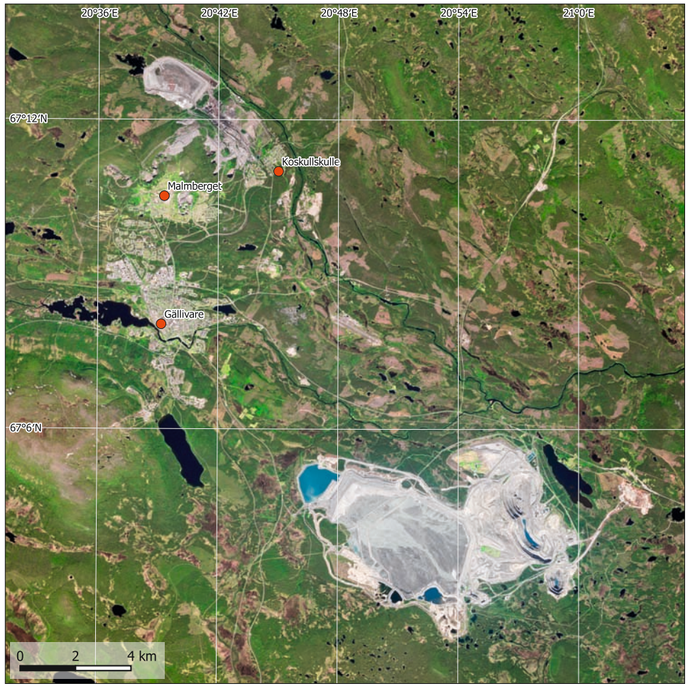

1. True colour image of the Aitik Mine (lower right in the image) in 2023. Data: Sentinel-2, 2023-06-15.

Copper Mine in Aitik, Sweden

Located near the town of Gällivare, Aitik is an open-pit copper mine. Put into production in 1968, it covers now over 450 hectares as one of Europe's largest and the world's most efficient copper mines. Satellite imagery illustrates change in the scale of its operations between 1992 and 2023. During this period the extraction of ore was extended to approximately 39 million tonnes annually.

3. View of the terraced structure of the Aitik open pit mine.

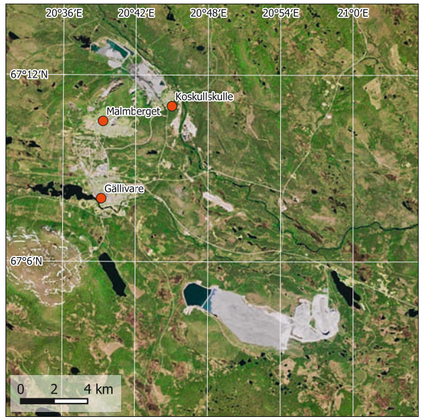

2. True colour image of the Aitik Mine in 1992. Data: Landsat 5, 1992-06-05.

The economic importance of Aitik is high, as it contributes significantly to Sweden's mineral exports, accounting for nearly 40% of the nation's copper production. Additionally, smaller amounts of Gold, Silver and Molybdenum are produced. With its activities the mining hub provides employment opportunities for thousands in the local community.

With its impact on the environment, Aitik's mining activities have raised sustainability concerns, necessitating environmentally responsible practices. The mine employs cutting-edge technology to minimize its ecological footprint, with measures in place to mitigate water and air pollution.

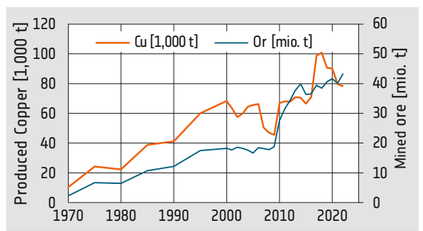

4. Development of copper production in the Aitik mine. Over the years, the copper concentration of the ore has roughly halved, meaning that more ore has to be mined for the same amount of copper.

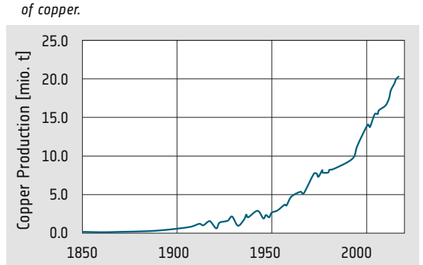

5. The development of the global copper production since 1850 shows an almost exponential trend.

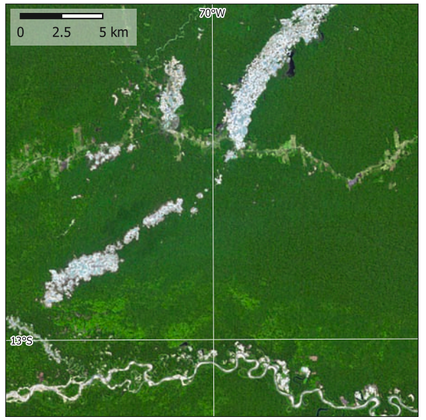

6. Gold mining in Madre de Dios, Peru in. In this region, small-scale mining has intensified since its start around 2000. Data: Landsat 5, 2011-09-03.

Gold Mining in Madre de Dios, Peru

The region along the Rio Madre de Dios in the part of the Amazon Basin located in Peru has seen a significant increase in informal and illegal mining activities during the last two decades.

The mining activities have had negative environmental and social consequences, including deforestation, mercury pollution, and habitat destruction, endangering wildlife and indigenous communities. The extraction of gold involves the use of poisonous mercury. Released into the environment, it contaminates rivers and aquatic ecosystems. Between 30 and 40 tons of mercury are released into the food chain every year. This poses serious health risks to residents and to the environment. About 80 percent of the local population have enhanced mercury concentrations.

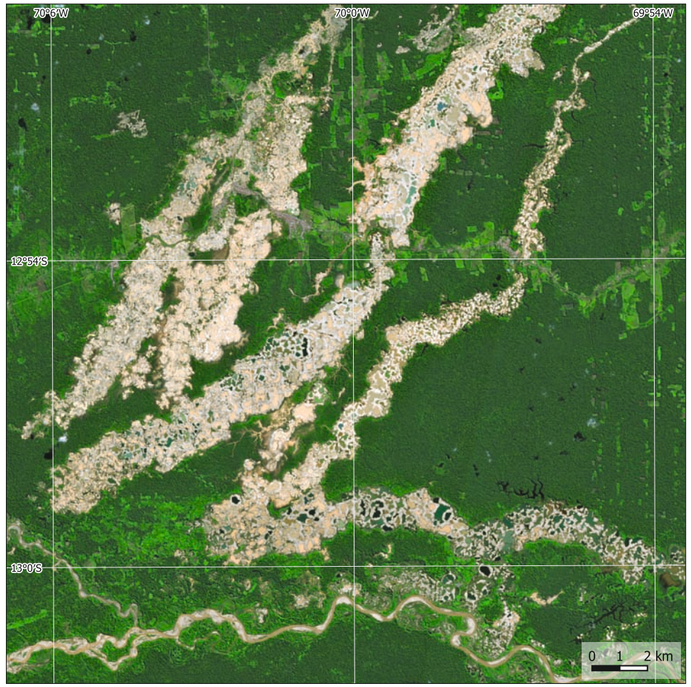

7. Gold mining in Madre de Dios. The satellite image shows the areas directly affected by mining. Additionally, new settlements and agricultural land can be seen. Data: Sentinel-2, 2023-06-03.

Efforts have been made by the government to combat these issues by regulating the mining activities. Satellite imagery plays an important role in monitoring and assessing the impact of these initiatives, helping to find a balance between economic development, public health, and the preservation of one of the world's most biodiverse regions. The future of gold mining in Madre de Dios hinges on finding sustainable practices that protect the environment and support local livelihoods.

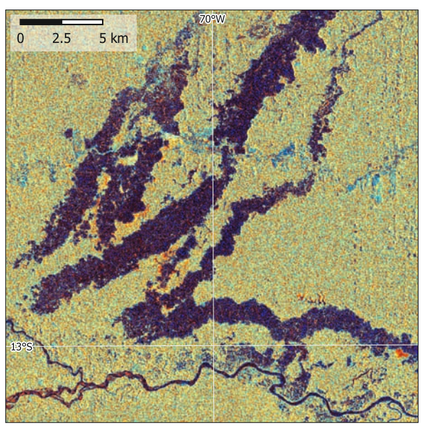

8. Radar satellite data is a valuable tool for analysing land use changes, especially in tropic regions, where often clouds prevent from using optical data. Data: Sentinel-1, 2023-05-25.

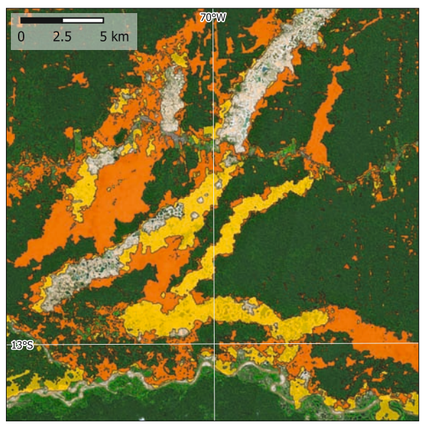

9. Forest area change between 2011 and 2023 as derived from satellite data (yellow: forest loss between 2011 and 2016, orange: forest loss between 2016 and 2023).

10. Aerial view of the ponds remaining from gold mining activities in the Rio Madre de Dios region. The colours of the water reflect different concentrations of sediments and algae.

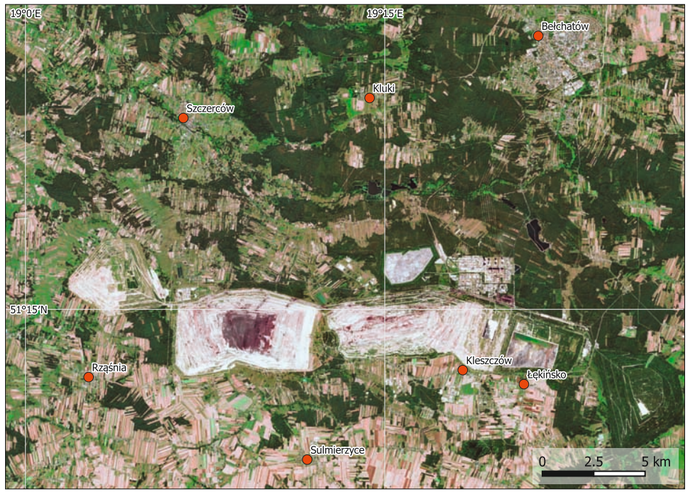

1. True colour image of the Bełchatów lignite mine in 2023. Data: Sentinel-2, 2023-08-15.

The Bełchatów Coal Mine, Poland

The Bełchatów lignite mine, located in central Poland, covers an area of more than 12,500 hectares. It is one of the largest in Europe and has been operational since the mid-1970s.

The mine has reserves exceeding 2 billion tons of lignite, a low-grade coal used for electricity generation. The produced lignite is provided to the adjacent Bełchatów Power Plant, which consumes more than 40 million tons lignite per year. With its capacity of more than 5.3 GW this power plant is one of Europe's largest thermal power stations.

As the satellite maps show, the mine has been shifted westwards, following the coal deposits. It faces environmental challenges due to the extraction of fossil fuels and greenhouse gas emissions. With emissions of 30 million tons of CO_2 in 2020, the adjacent power plant was the biggest single emitter of this greenhouse gas in Europe.

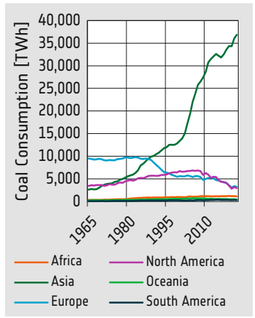

7. Development of the coal consumption (hard coal and lignite) for energy production.

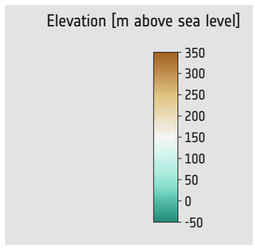

6. Mining activities have changed the relief of the area by several hundred metres.

2. True colour image of the Bełchatów lignite mine in 2020. Data: Sentinel-2, 2020-07-01.

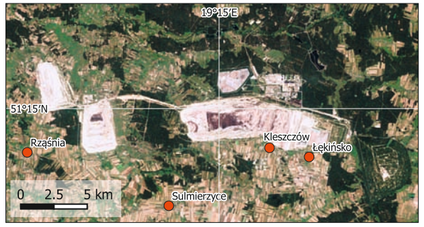

3. True colour image of the Bełchatów lignite mine in 2010. Data: Landsat 5, 2010-08-22.

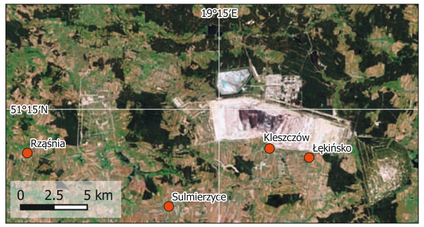

4. True colour image of the Bełchatów lignite mine in 2001. Data: Landsat 5, 2001-07-28.

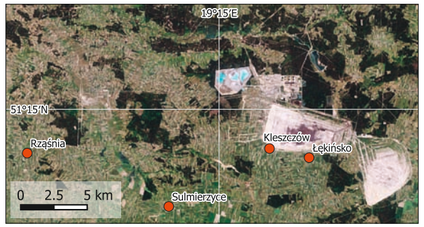

5. True colour image of the Bełchatów lignite mine in 1990. Data: Landsat 4, 1990-06-12.

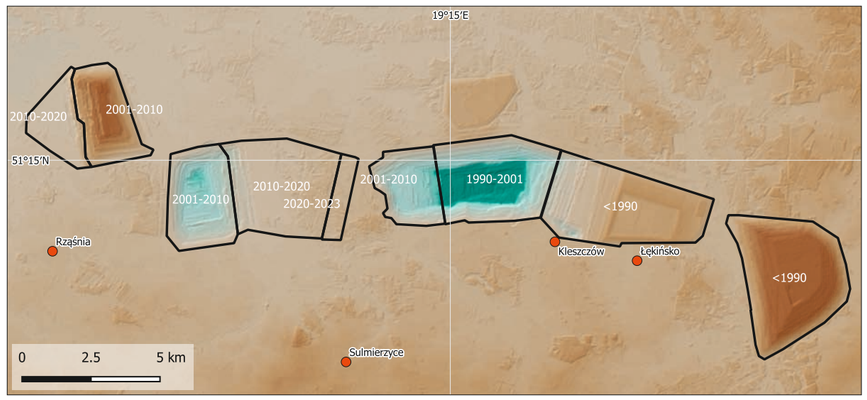

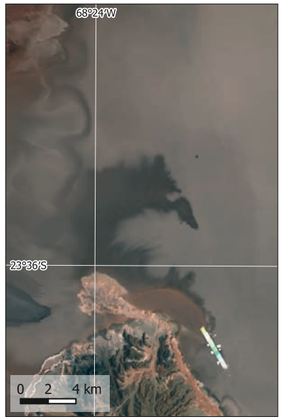

8. The 1985 image shows first mining activities. Data: Landsat 4, 1985-01-25.

9. The areas of the evaporation pans in 2000. Data: Landsat 5, 2000-01-03.

10. The area of the evaporation pans in 2023. Data: Sentinel-2, 2023-01-18.

11. View of the salt crust forming the surface of the Salar de Atacama.

Salar de Atacama, Chile

With its area of about 3050 km² the Salar de Atacama is the largest salt flat or saltpan of Chile. Located in the Andes at an elevation of 2300 m above sea level, the salar consists of salts mixed with sand.

The region receives extremely small amounts of precipitation. With only 2 mm rain per year it is among the driest regions in the world. Water from the surrounding mountains is enriched with minerals and salts and flows to the lowest point, the saltpan, where the water evaporates. This process has formed a body of brine reaching down to 1.7 km below the surface. It consists mostly of sodium chloride and is rich in lithium, potassium, magnesium, and boron. The brine is pumped to the surface, where the water evaporates and the salts are further enriched. The Salar de Atacama is one of the most important lithium production sites, with about 36 percent of the global lithium production and about 27 percent of the worldwide known lithium reserves.

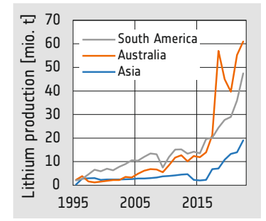

12. In the course of a few years, the growing demand for battery electric vehicles has led to a significant increase of lithium production.

13. The false colour infrared satellite image shows vegetation in red. In this barren environment only small patches of vegetation along the eastern rim of the salt flat are visible. Data: Sentinel-2, 2023-01-18.

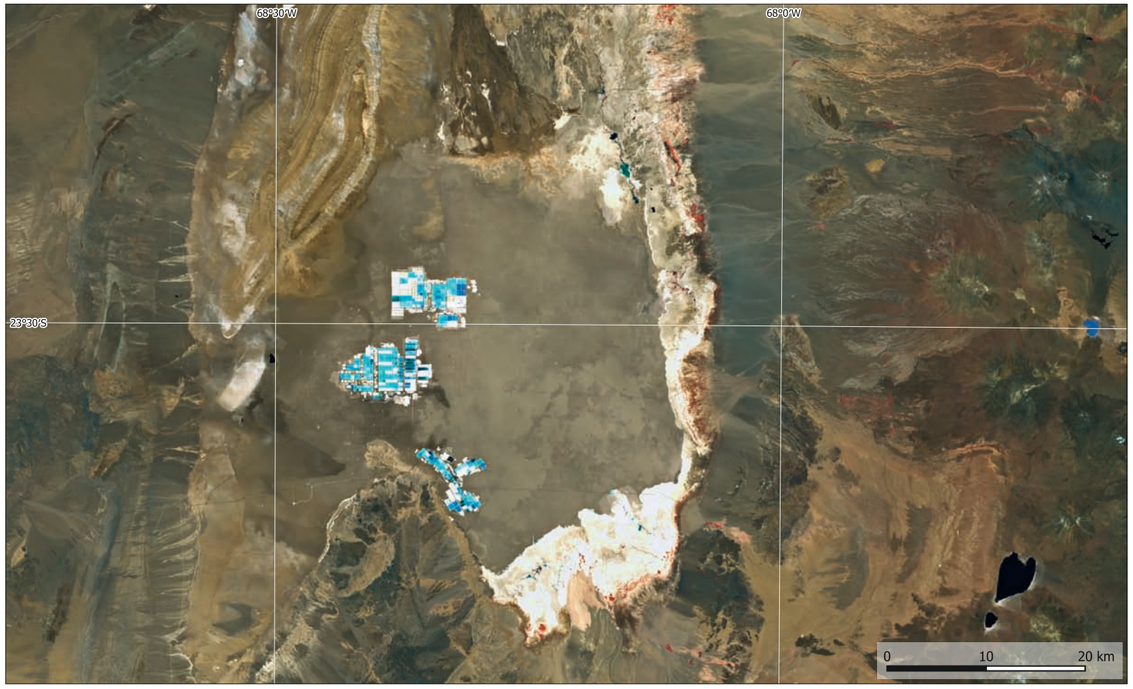

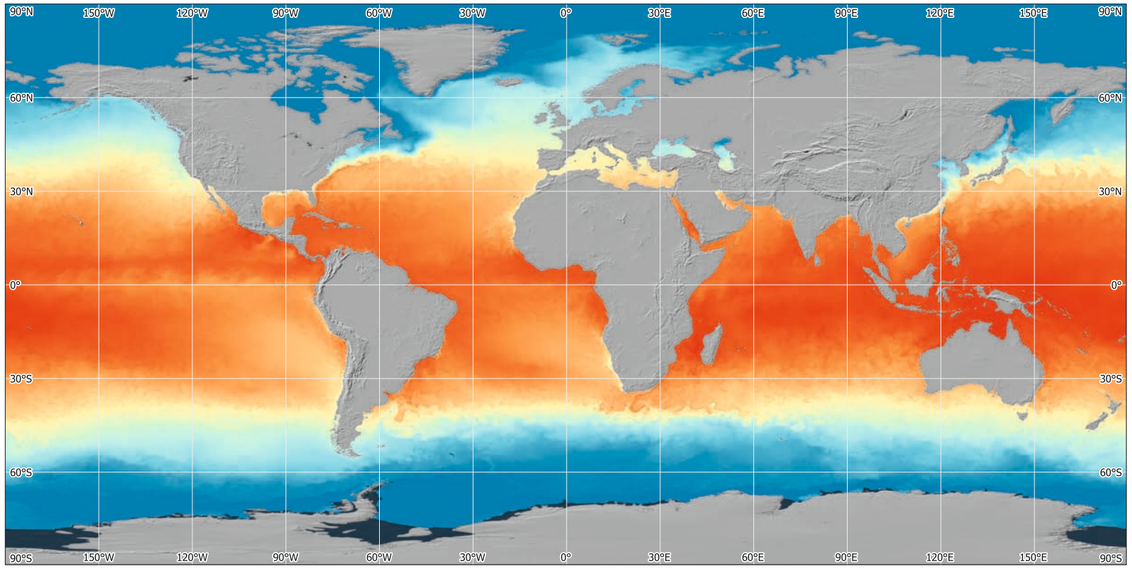

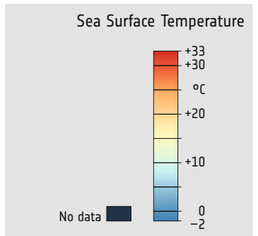

1. Global Sea Surface Temperatures, 2023-01-01.

Sea Surface Temperature (SST)

Global sea surface temperatures (SST) are a critical component of Earth's climate system, influencing weather patterns, ocean circulation, and ecosystem dynamics. The SST shows a zonal pattern, with warmer temperatures near the equator and cooler temperatures toward the poles. In a seasonal change these zones are shifted towards north or south. The temperature differences drives atmospheric and oceanic circulation and shapes climate patterns.

Compared to the atmosphere, water bodies can store large amounts of thermal energy and act as an important energy buffer in the context of climate change. Although at a smaller rate, the water temperatures of the oceans have risen by about 0.8 °C between 1950 and 2020. Increasing temperatures cause a thermal expansion of the water, which is one of the most important drivers of the global sea level rise.

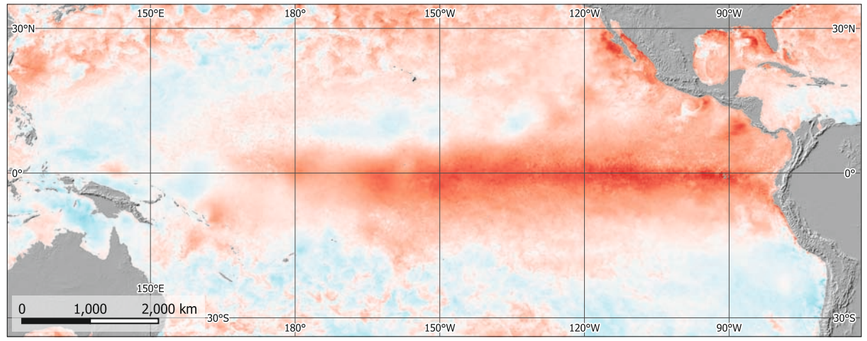

3. Sea Surface Temperature Anomaly of the equatorial Pacific Ocean during an El Niño event, 2015-12-25.

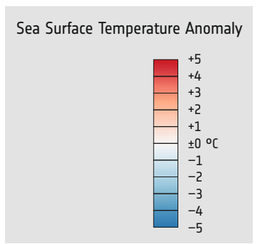

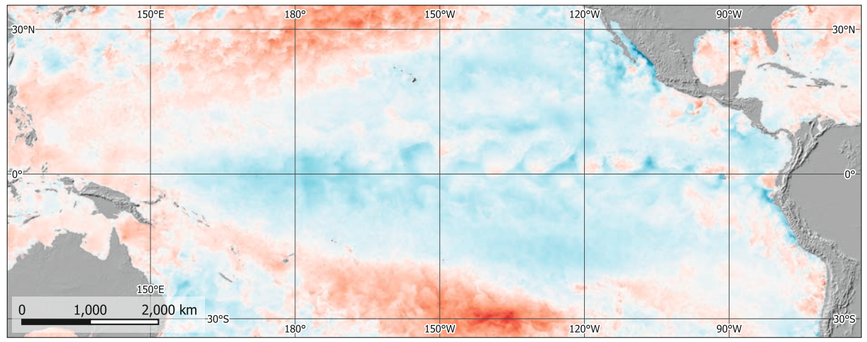

4. Sea Surface Temperature Anomaly of the equatorial Pacific Ocean during a La Niña event, 2011-12-25.

El Niño and La Niña

A significant phenomenon related to the SST is the El Niño-Southern Oscillation (ENSO). ENSO is a natural climate cycle characterized by the periodic warming (El Niño) and cooling (La Niña) of sea surface temperatures in the equatorial Pacific Ocean. During El Niño events, warmer-than-average SSTs develop in the central and eastern Pacific, altering atmospheric circulation patterns and influencing weather across the globe. Conversely, La Niña events feature cooler-than-average SSTs in the same region, leading to contrasting climate impacts, such as increased rainfall in some regions and drought in others.

Gulf Stream and North Atlantic Current

The Gulf Stream is a powerful ocean current in the North Atlantic Ocean, transporting warm water from the Gulf of Mexico toward the northeastern United States and western Europe. This warm current significantly influences SSTs along its path, contributing to the relatively mild climates of coastal regions in these areas. The Gulf Stream also plays a crucial role in regulating global climate by redistributing heat from the tropics to higher latitudes, affecting weather patterns and ocean circulation far beyond its immediate vicinity.

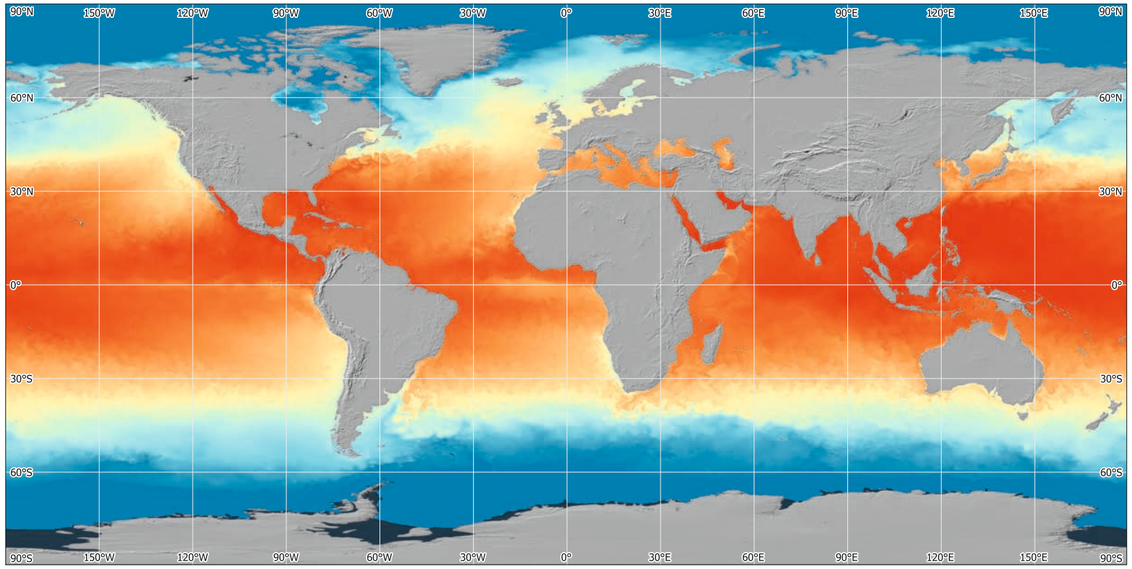

2. Global Sea Surface Temperatures, 2023-07-01.

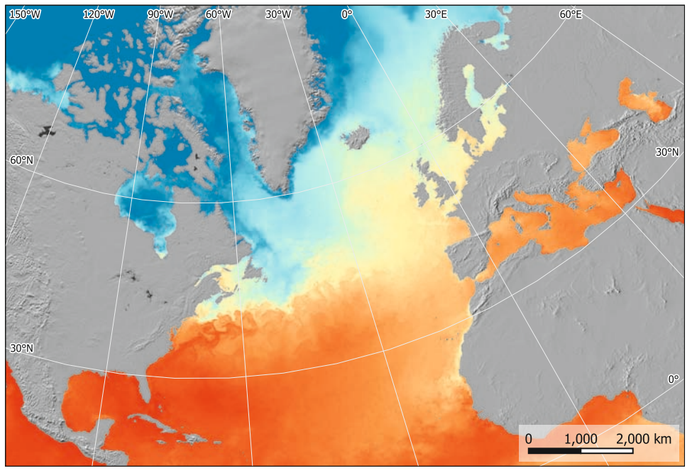

5. The Gulf Stream and the North Atlantic reaching from Florida in North America to Scandinavia in northern Europe are visible in the Sea Surface Temperature (2014-01-01).

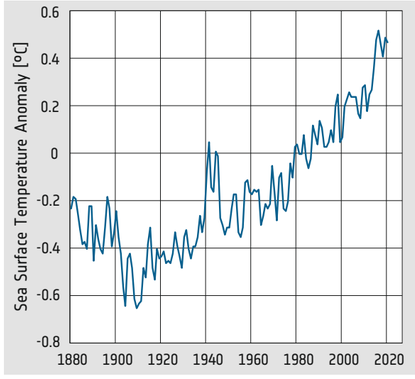

6. The global average Sea Surface Temperature shows a clear rise. During the last 50 years the increase was about 0.8 degree Celsius.

1. Overview satellite image of the Nile Valley. Data: Sentinel-2.

The Nile River

The coastline at the Nile mouth near Alexandria is defined mainly by the balance of sediment deposition by the Nile River and its removal by the Mediterranean Sea.

The sediment load of the Nile River was significantly reduced by the Aswan High Dam located about 1000 km upstream, which was completed in 1970. Before the construction of the dam, the Nile Delta received an annual sediment load of approximately 130 million tons. Today, this figure has dwindled to around 16-20 million tons, leading to reduced natural replenishment of the coastline.

Over the past century, the Mediterranean Sea has seen an average sea level rise of about 3.4 millimetres per year due to global warming. This leads to an additional substantial increase in coastal erosion and vulnerability to storm surges.

Based on satellite data, coastal erosion around Alexandria has been estimated at around 1 metre per year in certain areas. This rapid rate of erosion threatens infrastructure, coastal communities, and agricultural lands. Alexandria is Egypt's second-

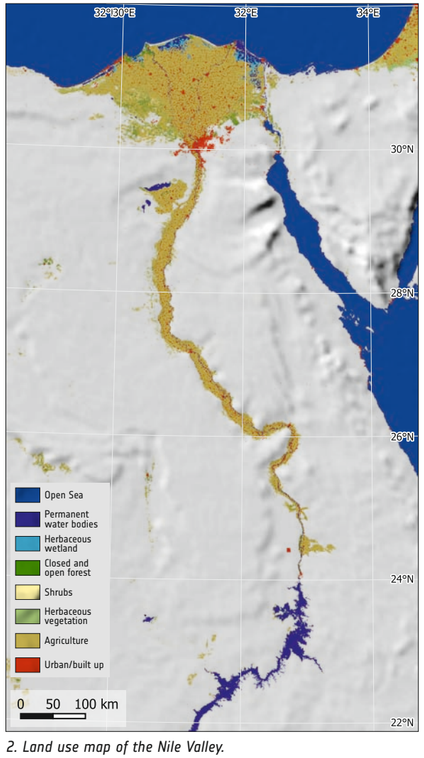

2. Land use map of the Nile Valley.

3. Nile Delta, Egypt, near Rosetta in 1985. Data: Landsat 5, 1985-06-10.

4. Nile Delta near Rosetta. Overlay: Change of the coastline from 1985 to 2023. Data: Sentinel-2, 2023-06-25.

5. View of Damiette at the shore of the Nile river.

largest city and home to over 5 million people. Many of the residents rely on agriculture, fisheries, and tourism, all of which are directly or indirectly affected by changes in the coastline. Therefore, Egypt combats coastal erosion around Alexandria and has, for example, spent 21 million Euro in 2018 for this task.

Large Scale Projects along the Nile River

The New Valley, covering an area of around 440,000 square kilometres, has undergone a significant agricultural development. Encompassing the Toshka Depression and adjacent lands along the Nile River, the valley was the focus of the Toshka Project, which was initiated in the late 20th century.

This project aimed to divert water from the Lake Nasser storage lake to irrigate approximately 540,000 hectares of desert land in the New Valley, with the goal of creating new agricultural land. The project involved the construction of canals and infrastructure to facilitate irrigation. After initial successes, the Toshka Project faced a series of challenges, and by 2011, it was estimated that only a fraction of the intended area was under cultivation. In the meanwhile, the efforts have been increased again and have led to a significant growth of the cultivated area.

To understand the scale and impact of the project, satellite images are a valuable tool. Over the years, satellite technology has been instrumental in monitoring changes in land use and vegetation. Satellite images are used to analyse how the landscape transforms, providing a visual representation of successes and setbacks of the agricultural initiatives in the New Valley.

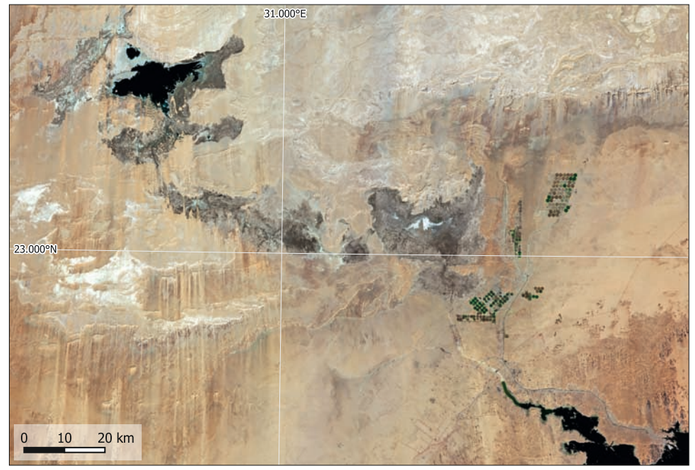

6. New Valley, Egypt, in 2017. Data: Sentinel-2, 2017-11-05.

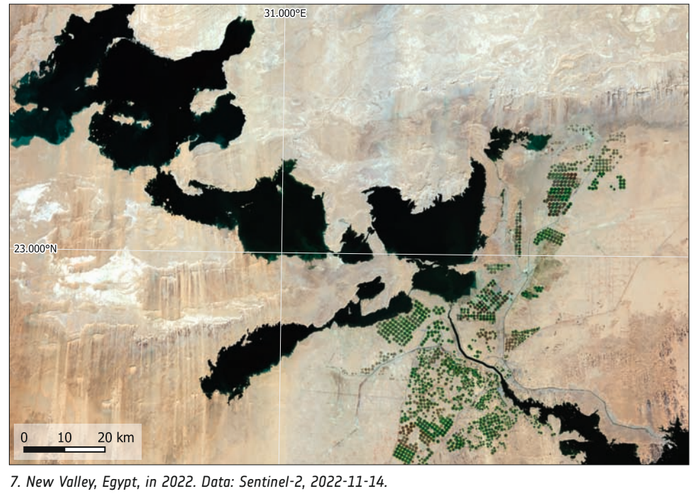

7. New Valley, Egypt, in 2022. Data: Sentinel-2, 2022-11-14.

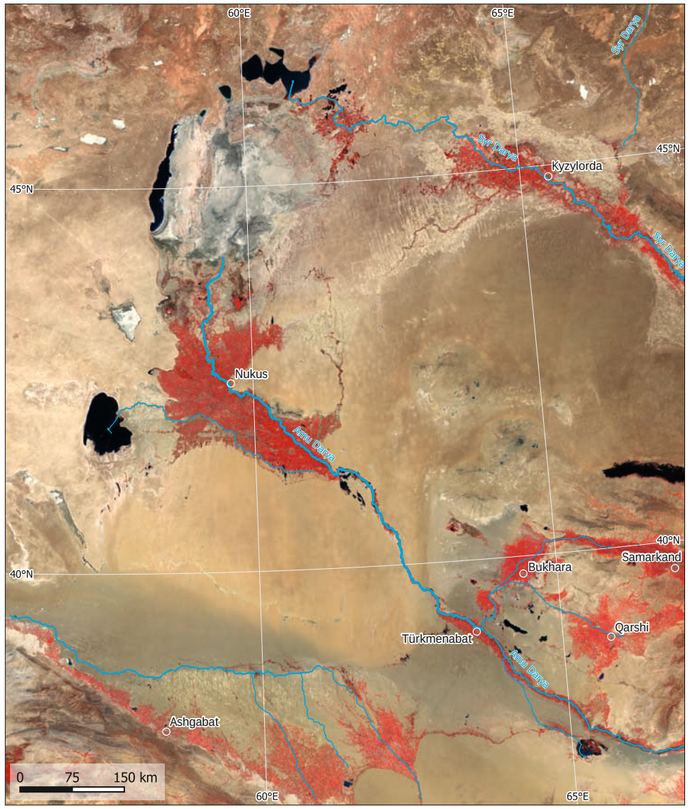

1. The false-colour infrared image of the region around the Aral Sea shows, where the water of its affluents is used for irrigation (Sentinel-2 mosaic, data acquired during first quarter of 2023).

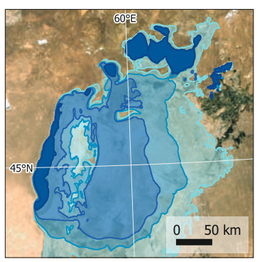

2. Area of Aral Sea in 1964, 1987, 2000, and 2023, derived from satellite data.

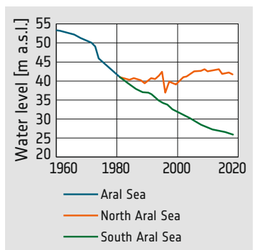

3. Receding water level of Aral Sea. A dam stabilised the North Aral Sea.

Aral Sea

Since the 1960s, the Aral Sea has been shrinking dramatically. This is primarily due to the diversion of water from the two main rivers that feed it, the Amu Darya and the Syr Darya, for agricultural irrigation purposes. The Soviet Union initiated large-scale irrigation projects to cultivate cotton and other crops in the arid region, diverting water away from the Aral Sea.

The shrinking of the Aral Sea has led to environmental and social consequences. As the water level dropped, the salinity of the lake increased. Fish populations declined drastically, leading to the collapse of the fishing industry in the region. Salty dust from the dry lakebed became airborne, leading to an increase in respiratory health problems and in the incidence of other diseases. The collapse of the fishing industry and the degradation of agricultural land have economic consequences for the people living around the Aral Sea. Once prosperous fishing villages have been abandoned, leading to unemployment and poverty in the region.

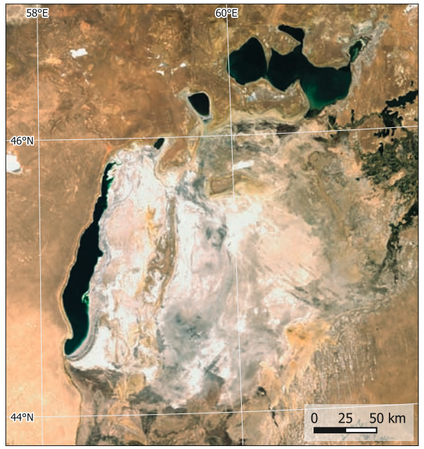

4. Aral Sea in 2023. Only the deeper part in the west and the North Aral Sea remain. Data: Sentinel-3.

5. Aral Sea in 1987. Data: Landsat 4.

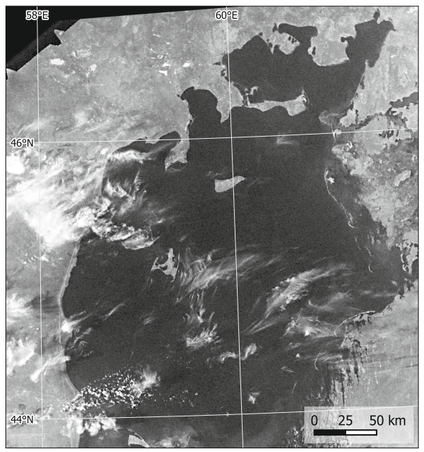

6. Taken in 1964 by the reconnaissance satellite Argon, this image is an important source documenting the change of the Aral Sea.

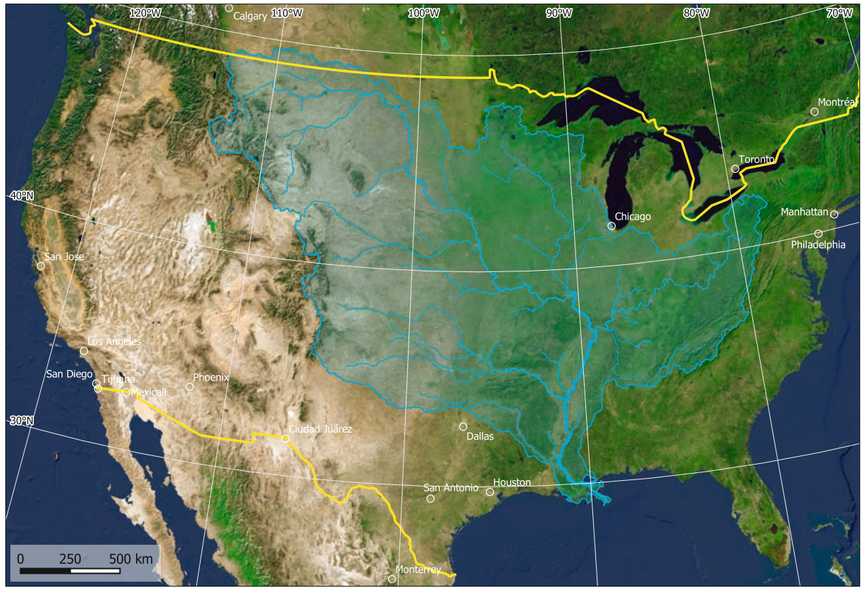

7. The Mississippi River catchment basin covers a large part of the area of the United States.

8. A dense network of offshore drilling platforms and oil pipelines has been installed to exploit the rich oil reserves in the Gulf of Mexico. Data: Sentinel-2, 2023-04-22.

Mississippi Delta

Land use changes in the Mississippi catchment and its delta have altered both landscape and hydrology, with implications for the environment and the human population. About 80% of the original wetlands in the Mississippi River Delta have been lost due to land conversion for agriculture, urbanisation, and infrastructure development.

Around 60% of the sediment load carried by the Mississippi River is now trapped behind dams, reducing sediment delivery to the delta and exacerbating land subsidence. Urbanisation along the river has fragmented natural habitats and increased impervious surfaces, leading to higher runoff volumes and flood risks in downstream areas. The city of New Orleans, located in the Mississippi delta, is particularly vulnerable to flooding, with over 40% of its land below sea level.

The oil industry is an important economic driver in the region, with offshore drilling platforms, refineries, and petrochemical plants dotting the coastline. This industry poses environmental risks, including habitat destruction, pollution, and the potential for oil spills. The 2010 Deepwater Horizon oil spill, for example, released an estimated 4.9 million barrels of oil into the Gulf of Mexico.

Hurricanes are a recurring threat to the Mississippi delta. Hurricane Katrina in 2005 and Hurricane Harvey in 2017 caused billions of dollars in damages and loss of life. Wetland loss and coastal erosion have reduced natural barriers protecting the coast, leaving communities increasingly vulnerable to storm surges and flooding.

9. Satellite images acquired since 1985 illustrate the dynamics of the Mississippi River delta.

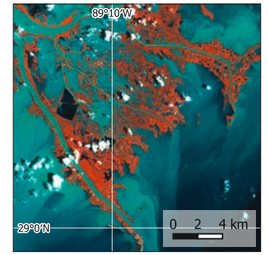

9a. Data: Landsat 4, 1985-05-04.

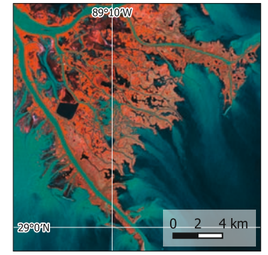

9b. Data: Landsat 5, 1995-07-19.

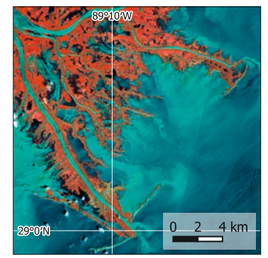

9c. Data: Sentinel-2, 2017-05-08.

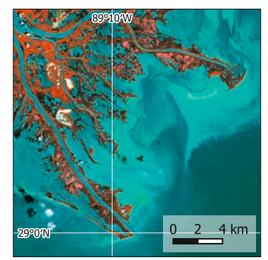

9d. Data: Sentinel-2, 2023-05-12.

1. Plattsmouth, U.S.A., 2023-03-21. Data: Sentinel-2.

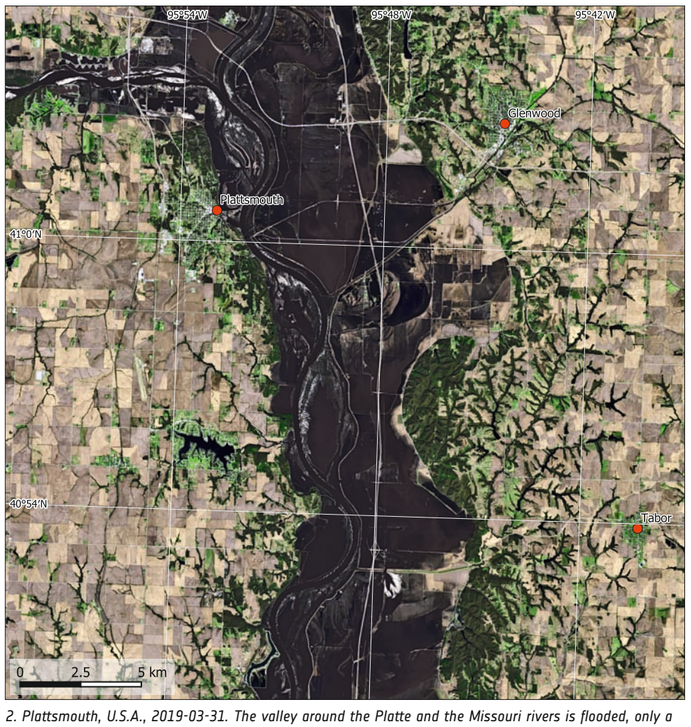

2. Plattsmouth, U.S.A., 2019-03-31. The valley around the Platte and the Missouri rivers is flooded, only a few infrastructure elements such as highways and dams remain dry. Data: Sentinel-2.

Plattsmouth, U.S.A.

The 2019 flooding around Plattsmouth, Nebraska, was a catastrophic event that brought immense devastation to the region. Triggered by a combination of factors, including heavy rainfall and snowmelt, the flooding inundated homes, farms, and infrastructure along the Missouri River.

Climate change played a role in this event, as rising global temperatures are leading to more extreme weather patterns, with heavier precipitation and increased risk of flooding. In the case of Plattsmouth, the area experienced record-breaking rainfall, with some areas receiving over 50 cm of rain in a single month. This excessive rainfall, combined with the saturated ground from earlier precipitation, overwhelmed the river's capacity to contain water.

The flooding affected over 2,000 homes and forced the evacuation of nearly 1,000 people in the Plattsmouth area. It caused millions of dollars in damages to homes, infrastructure, and agriculture, disrupting the lives of countless residents.

Satellite images captured the dramatic expansion of the floodwaters, which swallowed entire communities and vast swaths of farmland. Moreover, the data allow for accurately estimating the affected areas and the damage caused by the flood.

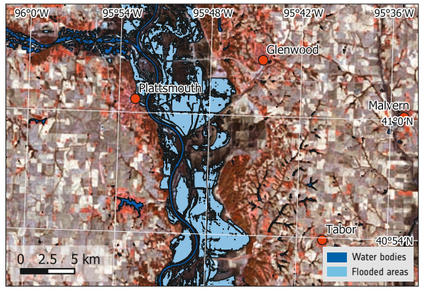

3. False-colour infrared image of Plattsmouth, 2019-03-31. Overlay: water surfaces derived from satellite data. Data: Sentinel-2.

4. View of Plattsmouth during the flood.

Venice, Italy

Venice, the famous "Floating City" of Italy, has been built on hundreds of islands in a lagoon near the Adriatic Sea. Due to this exposed situation the town has long struggled with flooding both from the sea and from the mainland.

To reduce the increasing risk of flooding from the sea, the Italian government decided to install MOSE *(Modulo Sperimentale Elettromeccanico, Experimental Electromechanical Module)*, an innovative flood protection system.

MOSE consists of three hydraulically operated barriers installed at the entrances to the Venetian Lagoon. Two of these entrances are visible in the overview satellite image. When water levels rise, sensors activate the system, filling the barriers with compressed air and forming a solid barrier against high tides and storm surges.

MOSE integrates advanced technology for monitoring and control while considering the ecological balance of the lagoon. As a pioneering example of adapting to climate change, MOSE demonstrates how coastal cities can adapt to the risks of rising sea levels, and, as well, how big the effort of adapting is.

So far, MOSE has been successfully activated several times. One example of the system in its activated state is shown in the satellite map from 2022.

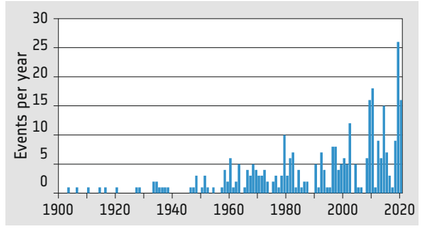

5. Development of the number of acqua alta events (high water levels) in Venice per year.

6. Venice. View of the closed MOSE barrier near Malamocco in the south of Lido.

7. Venice, Italy. Image acquired while the MOSE flood barriers were closed. Data: Sentinel-2, 2022-11-24.

8. Venice, Italy. True colour image of the central part of the lagoon with the MOSE flood barriers open. Differences in the ocean colour from sediments show sea currents. Data: Sentinel-2, 2021-11-04.

Arctic Sea Ice

Arctic sea ice is a vital component of Earth's climate system and contributes regulating global temperatures. Covering approximately 14 million square kilometres at its maximum extent in winter, it forms a reflective shield, bouncing back solar radiation and thus cooling the planet. During the summer months, Arctic sea ice shrinks to its lowest extent, reaching a minimum around September.

Arctic sea ice has diminished in recent years due to climate change. Its minimum extent during the summer months has receded to around 3-4 million square kilometres. Additionally, the thickness of Arctic sea ice has decreased by more than 40% since the 1980s, primarily due to the warming effects of climate change.

The diminishing Arctic sea ice contributes to the disruption of weather patterns, influences ocean circulation, and threatens the habitats of various Arctic species, including polar bears and walruses. On the other hand, the loss of sea ice opens up opportunities for shipping routes and resource extraction.

Satellite data plays an important role in monitoring the Arctic sea ice, providing accurate measurements of ice extent, thickness, and movement.

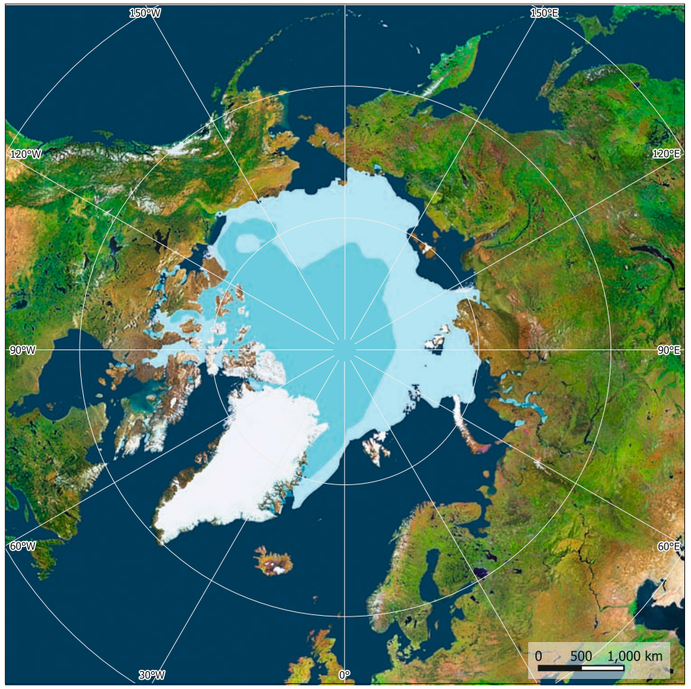

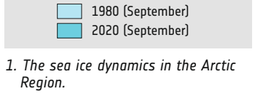

1. *The sea ice dynamics in the Arctic Region.*

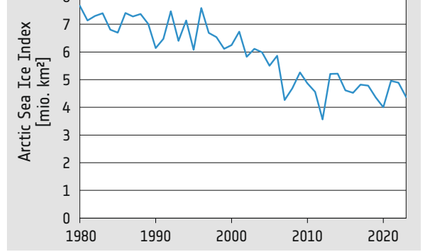

2. *Development of the Arctic area covered by sea ice during September (i.e. during the month with minimum sea ice coverage).*

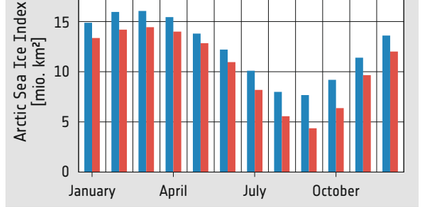

3. *Seasonal variation of the Arctic sea ice extent (blue: 1980, red: 2023).*

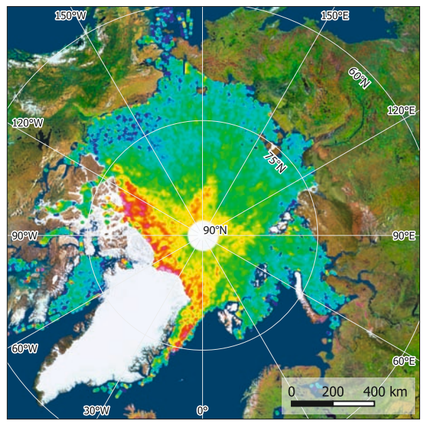

4. *Arctic sea ice thickness in Jan. 2011. Monthly average derived from data acquired by CryoSat.*

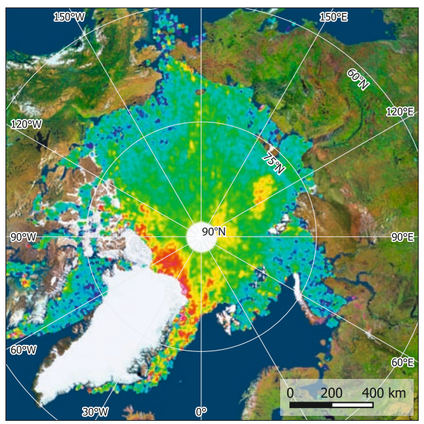

5. *Arctic sea ice thickness in Jan. 2024. Monthly average derived from data acquired by CryoSat.*

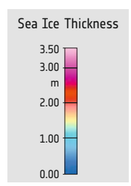

Greenland Ice Sheet

As part of the Arctic region, the Greenland Ice Sheet is the second largest in the world. Covering approximately 1.7 million square kilometres, which is 80% of the area of the island, it is one of the largest repositories of freshwater ice and plays an important role with respect to global climate and sea level. The Greenland Ice Sheet reaches a thickness exceeding 3 kilometres, harbouring an estimated volume of ice equivalent to roughly 7.2 metres of global sea level rise. Its sheer mass exerts a significant influence on regional weather patterns and ocean currents.

Scientific research utilizing satellite observations, ice core samples, and climate models has revealed clear trends in the Greenland Ice Sheet's dynamics. Accelerated melting driven by rising temperatures has led to increased runoff and iceberg calving, contributing to rising sea levels worldwide. The loss of ice mass from Greenland has been identified as one of the primary drivers of global sea level rise. Feedback mechanisms exacerbate the ice sheet's vulnerability to climate change. As ice melts and exposes darker surfaces, such as rock or water, the albedo effect intensifies, causing more solar radiation to be absorbed and accelerating further melting in a so-called positive feedback loop.

Satellite altimetry measurements provide insights into changes in ice sheet elevation, allowing to monitor variations in ice thickness. This data revealed thinning and mass loss particularly along Greenland's periphery, where warmer ocean waters accelerate ice melt from below. Satellite imagery offers information on surface features and melt patterns across the ice sheet. High-resolution optical and radar images capture details such as crevasses, melt ponds, and supraglacial lakes, which influence the ice sheet's development. Radar satellite remote sensing enables the monitoring of ice sheet movement through techniques like interferometric synthetic aperture radar (InSAR). By measuring precise changes in surface elevation, InSAR provides insights into ice flow velocities.

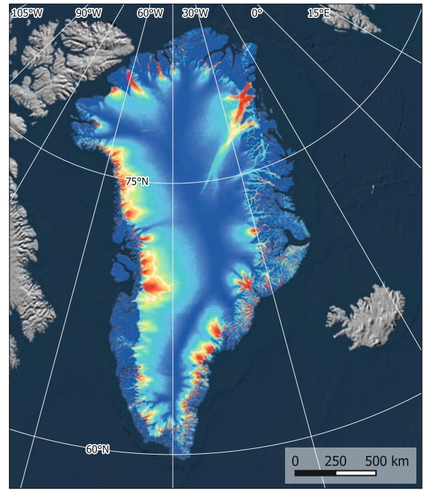

7. *Greenland, Ice sheet velocity in 2020 derived from radar satellite data. Data: Sentinel-1.*

6. *Greenland, Cumulative ice loss and its contribution to the global sea level rise (Data source: IMBIE Credit: ESA/NASA).*

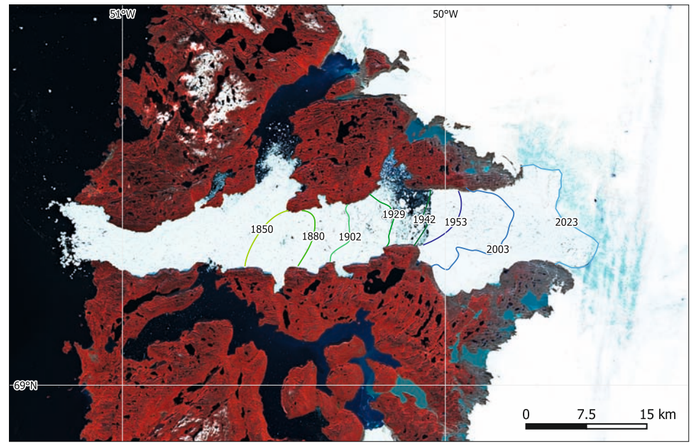

8. *False-colour infrared image of Jakobshavn Isbrae, Greenland. The overlay shows the retreat of the glacier edge since 1850. Data: Sentinel-2, 2023-09-01*

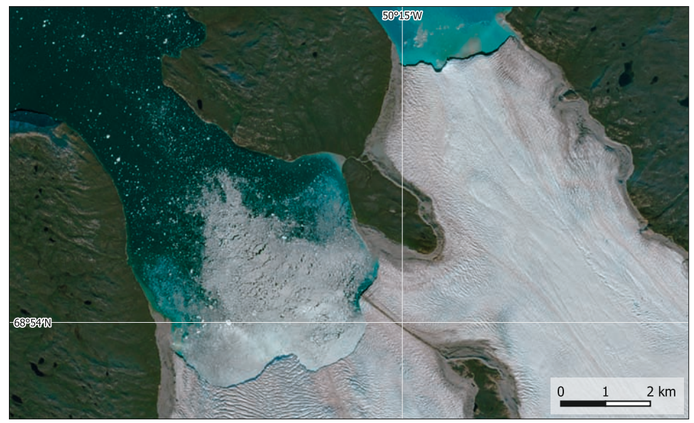

9. *True colour image of the edge of a glacier south of Jakobshavn Isbrae, Greenland, with calving icebergs. Data: Sentinel-2, 2023-09-01.*

1. *Sea ice extent around Antarctica in January and in July.*

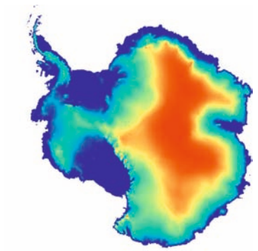

2. *Elevation of the Antarctic ice sheet as measured by CryoSat.*

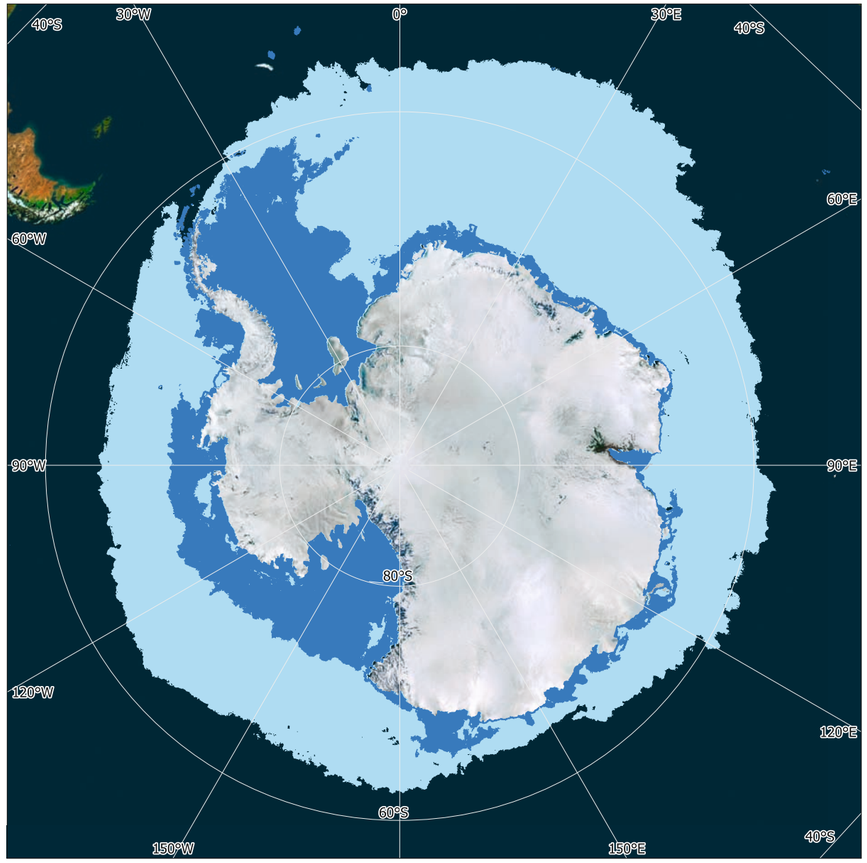

Antarctica

During the last decades, Antarctica, the largest desert on Earth, has gained increasing awareness in the scientific and political communities. This is due to its enormous importance for Earth's climate and for the consequences of climate change for humanity.

The ice sheet of Antarctica is the largest freshwater reservoir on Earth, containing more than 26 million cubic kilometres or 70% of all freshwater. Global warming leads to melting of the ice sheet, so far affecting mainly the smaller West Antarctic sheet. Between 2012 and 2017 every year 220 billion tons of ice melted, contributing to the sea level rise.

Where the glaciers of Antarctica meet the Antarctic Ocean, the ice shelves are located. Ice shelves are large and typically 100 to several hundred metres thick, stable ice bodies floating on the water. The warming of the oceans reduces the stability of the ice shelves and leads to the calving of large icebergs.

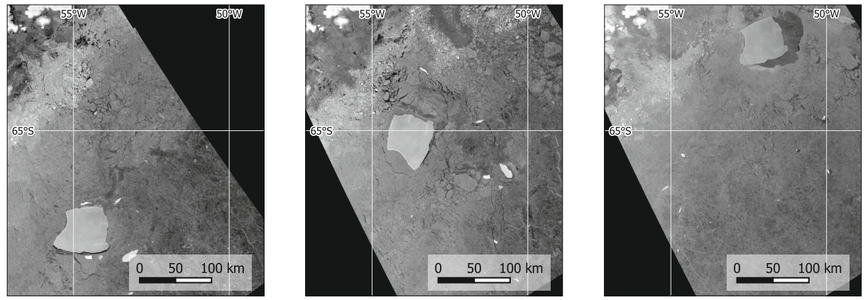

3. *Radar satellite images of the movement of iceberg A23a between August and October 2023. Data: Sentinel-1.*
Left: 2023-08-06
Centre: 2023-09-13
Right: 2023-10-19

Icebergs on the Move

The large tabular iceberg A23a calved from the Filchner-Ronne Ice Shelf in 1986. After its calving, the research base Druzhnaya I, which was placed on this iceberg, had to be removed and was renamed to Druzhnaya III. For many years the iceberg remained stuck on the sea bed before it started moving in 2020. With an area of almost 4,000 square kilometres it was by 2024 one of the largest icebergs ever monitored.

Late in 2020, A23a started its journey towards north, roughly following the coastline of the Antarctic Peninsula. In November 2023 the iceberg moved past the northern tip of the Antarctic Peninsula, heading toward north. During its tour away from Antarctica, A23a will reach warmer waters and will subsequently melt.

While the dissolution of the ice shelves does not directly contribute to the seawater level (the melted water replaces only the volume of the submerged part of the ice), it plays an important indirect role as the shelves act as a stabilising barrier for the glaciers flowing towards the sea. A loss of this barrier can lead to an enhanced ice flow.

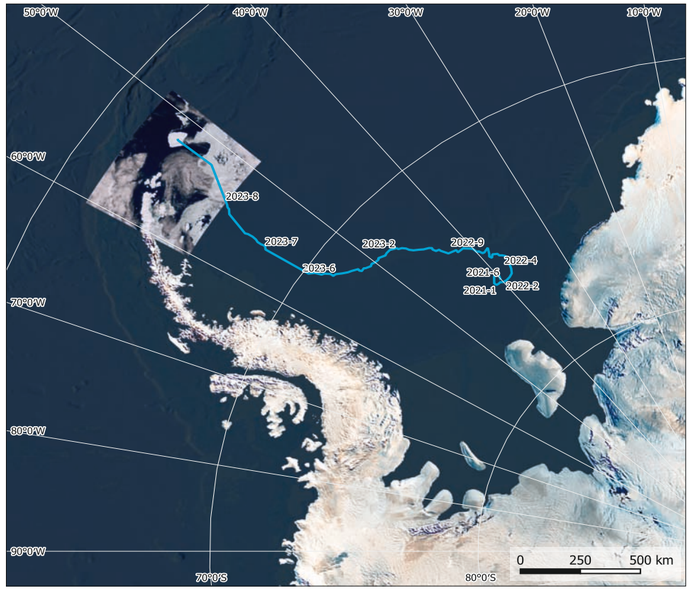

4. *Path of iceberg A23a during 2022 and 2023. Background image: Sentinel-3, 2023-11-15.*

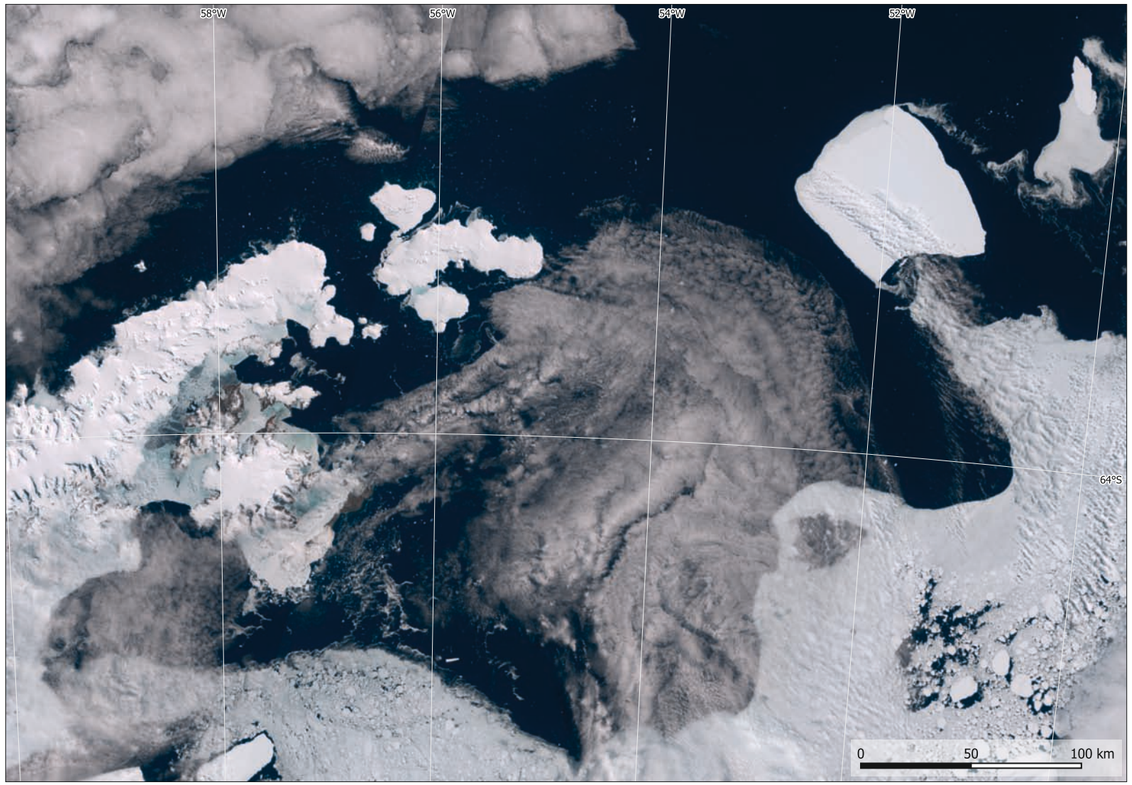

5. *Iceberg A23a passing the Antarctic Peninsula on its way towards the South Atlantic ocean. Data: Sentinel-3, 2023-11-15.*

1. Overview satellite image map of Alaska. The glaciers are concentrated in the mountain ranges along the south coast of Alaska. Data: Spot Vegetation

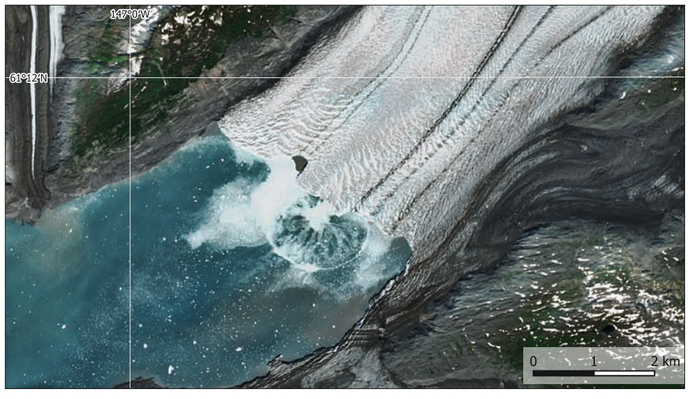

2. Detail satellite image of the terminus of the Columbia Glacier. Note the circular wave spreading from the centre of the terminus, where an iceberg has calved. Data: Sentinel-2, 2023-07-30.

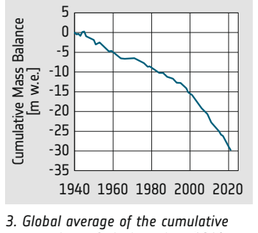

3. Global average of the cumulative mass loss of glaciers since 1940. The unit „metre of water equivalent" roughly corresponds to the loss of thickness of the glaciers.

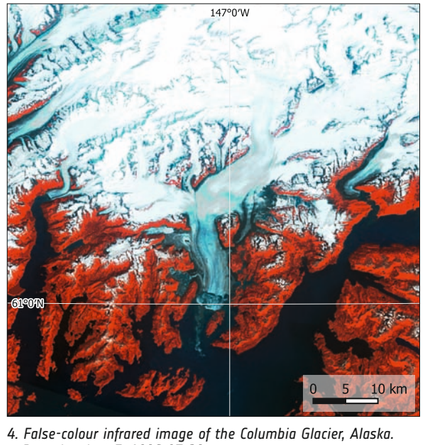

4. False-colour infrared image of the Columbia Glacier, Alaska. Data: Landsat 5, 1986-07-28.

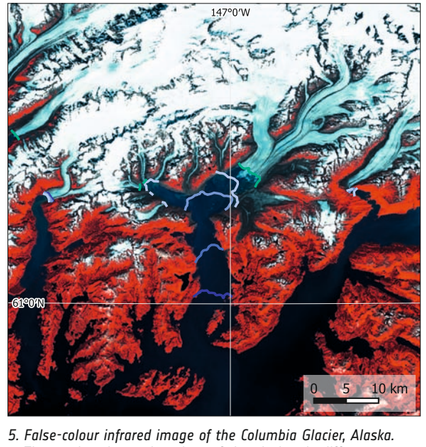

5. False-colour infrared image of the Columbia Glacier, Alaska. The overlay shows the edges of the glaciers in different years. Data: Sentinel-2, 2023-07-30.

Glacier Edge (year)
1986
1994
2011
2019
2023

Columbia Glacier, Alaska

For decades now glaciers all around the world have been retreating, a phenomenon directly linked with climate change. On an average, the glaciers worldwide have lost about 30 metres of their thickness since 1940. Currently, on an average, they are losing about one metre per year.

The retreat of several tidewater glaciers, which are glaciers ending in the sea, is particularly spectacular. Tidewater glaciers exist in Alaska, in Patagonia and along the coasts of Greenland. These glaciers end directly at sea level, therefore their environment is relatively warm during summer. As a consequence, the end zones of these glaciers are among the fastest flowing ice streams on Earth. Their lower end floats on the water of the sea and follows the tidal movement. This movement enhances the formation of cracks and of the calving of icebergs that float off into the sea.

The Columbia Glacier is located in Alaska. Descending from more than 3000 metres above sea level, it flows into the Prince William Sound at the coast of the Pacific Ocean. For a long time, the nose (or terminus) of the glacier remained stable near the mouth of Columbia Bay. However, since the 1980s it has retreated by more than 20 kilometres.

The Columbia glacier shows that the combination of different effects can lead to a highly dynamic evolution. At the beginning, the nose of the glacier was supported by the gravel of the end moraine. After the initial phase of the retreat it floated on water, making the tidal forces more effective and thus increasing the speed of the retreat, even more so as this allowed warmer water from the ocean to flow under the ice.

Aletsch Glacier, Switzerland

With a total length of almost 23 kilometres and an area of approximately 80 square kilometres, the Aletsch Glacier is the largest glacier in the Alps. Its ice reaches a thickness of up to 900 metres, forming a frozen river that winds its way through the rugged mountain landscape.

The effects of climate change are taking a toll on the Aletsch Glacier, as it is the case with most alpine glaciers. Over the past century, it has been retreating at an increasing rate of about 100 metres per year. Satellite data has shown that the Aletsch Glacier has lost almost 2 kilometres in length since the 1980s. Rising global temperatures are causing the glacier to lose more ice through melting than it gains through snowfall. This imbalance threatens not only the glacier's size but also the ecosystems that depend on it.

6. View of the Aletsch Glacier, showing the crevasses and the rubble of the moraines.

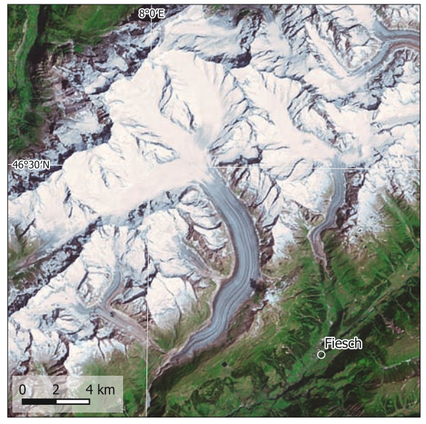

7. True colour image of the extent of the Aletsch Glacier in 1985. Data: Landsat 5, 1985-07-26.

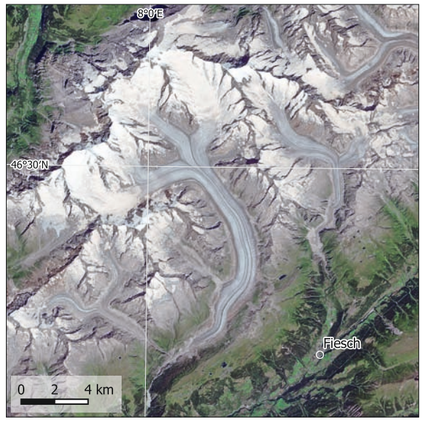

8. True colour image of the extent of the Aletsch Glacier in 2022. Data: Sentinel-2, 2022-07-13.

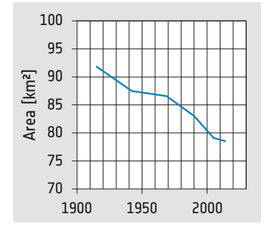

11. Aletsch Glacier, change in area since 1915.

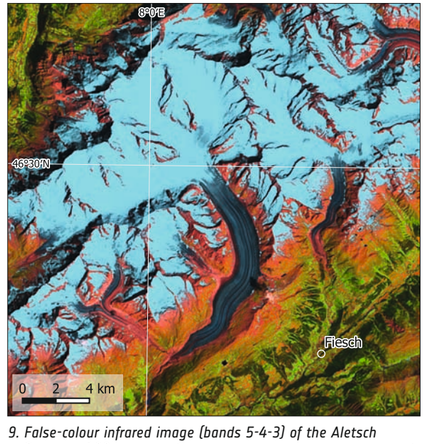

9. False-colour infrared image (bands 5-4-3) of the Aletsch Glacier in 1985, highlighting ice in dark blue and snow in light blue colours. Data: Landsat 5, 1985-07-26.

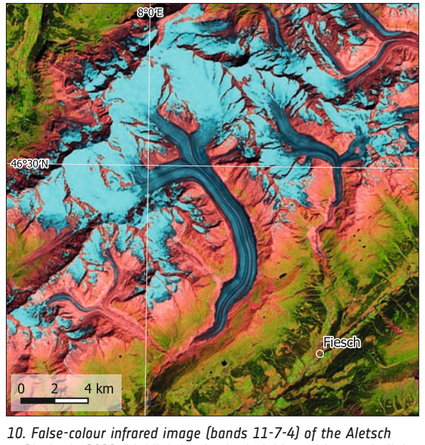

10. False-colour infrared image (bands 11-7-4) of the Aletsch Glacier in 2022, highlighting ice in dark blue and snow in light blue colours. Data: Sentinel-2, 2022-07-13.

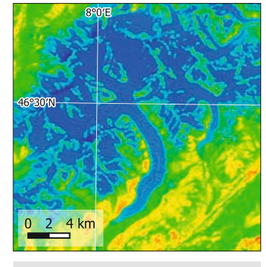

12. Thermal infrared image of the Aletsch Glacier in July 1985 (dark blue: temperature ~0 °C). Data: Landsat 5, 1985-07-26

ATMOSPHERE

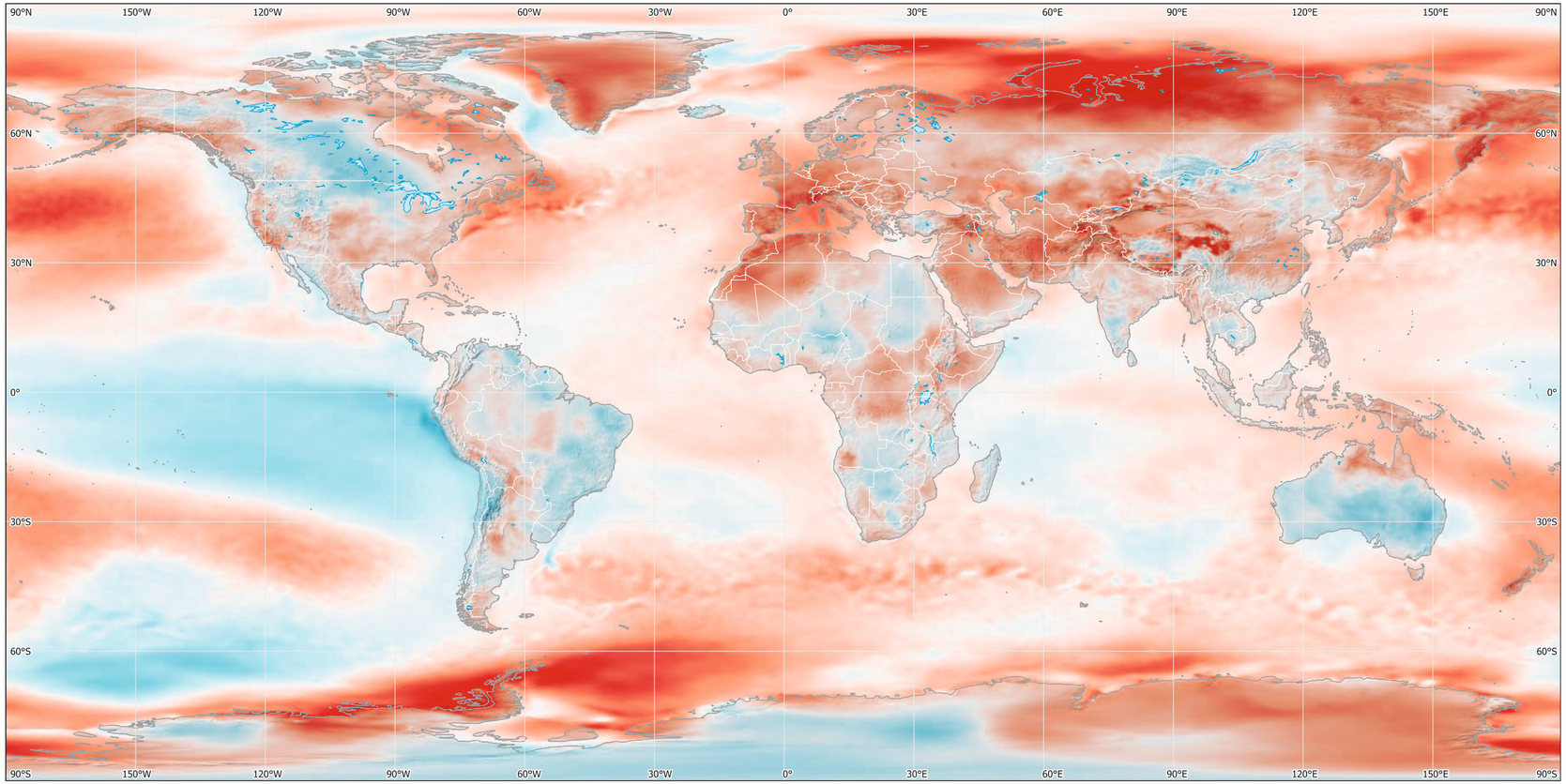

1. Global map of temperature anomalies measured in 2022 with respect to the period from 1960 to 1990.

Temperatures and Temperature Anomalies

Global temperatures are among the most prominent parameters of Earth's climate system, shaping weather patterns and ecosystems. Solar irradiation, the energy emitted by the sun, influences global temperatures by providing the energy necessary to sustain life and drive atmospheric processes.

Variations in solar output, driven by cyclic phenomena such as sunspots and solar flares, modulate the amount of energy reaching Earth's atmosphere. These fluctuations influence atmospheric circulation patterns, ocean currents, and the distribution of heat across the planet's surface.

The dominant driver of recent changes in global temperatures is the increase in greenhouse gas concentrations resulting from human activities. The combustion of fossil fuels, deforestation, and industrial processes have led to a rapid rise in atmospheric concentrations of carbon dioxide (CO_2), methane (CH_4), and other greenhouse gases.

This rise in greenhouse gases amplifies the natural greenhouse effect, trapping heat within Earth's atmosphere and causing global temperatures to escalate. Since the 1950s, the Earth's average surface temperature has increased by approximately 1.1 degrees Celsius, with significant variations across regions and seasons. The past decade (2010-2019) was the warmest on record.

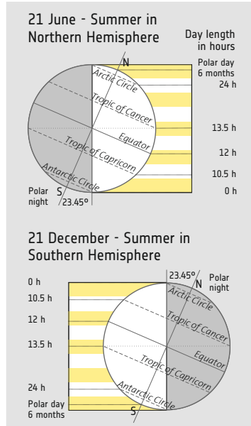

4. The angle of the Earth's axis with respect to the direction to the sun varies with the seasons, and with it the angle of solar irradiation and the length of the days. This influences the solar energy received at a point and, consequently, the temperature.

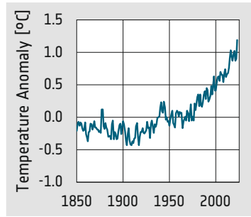

5. Annual mean temperature anomaly with respect to the period 1950-1980.

2. Global temperatures during north summer (July 2023).

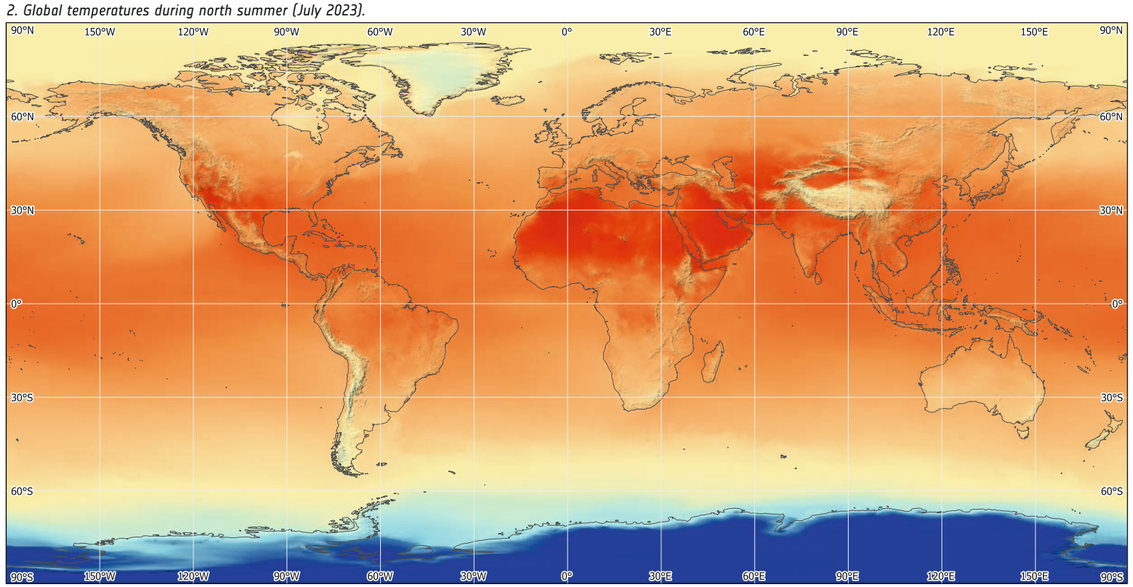

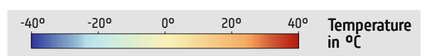

3. Global temperatures during north winter (January 2023).

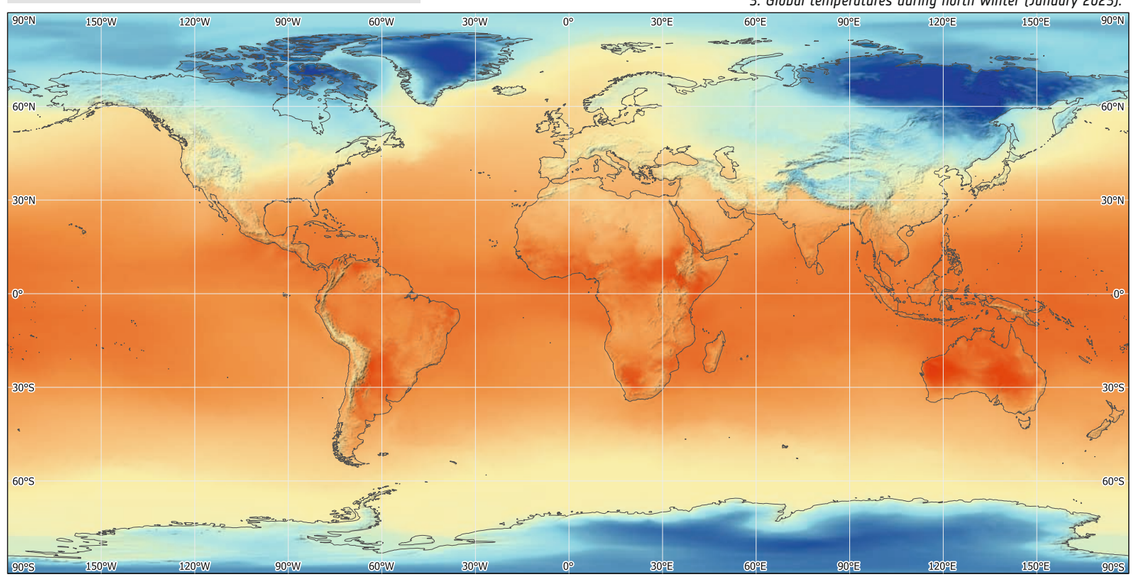

ATMOSPHERE

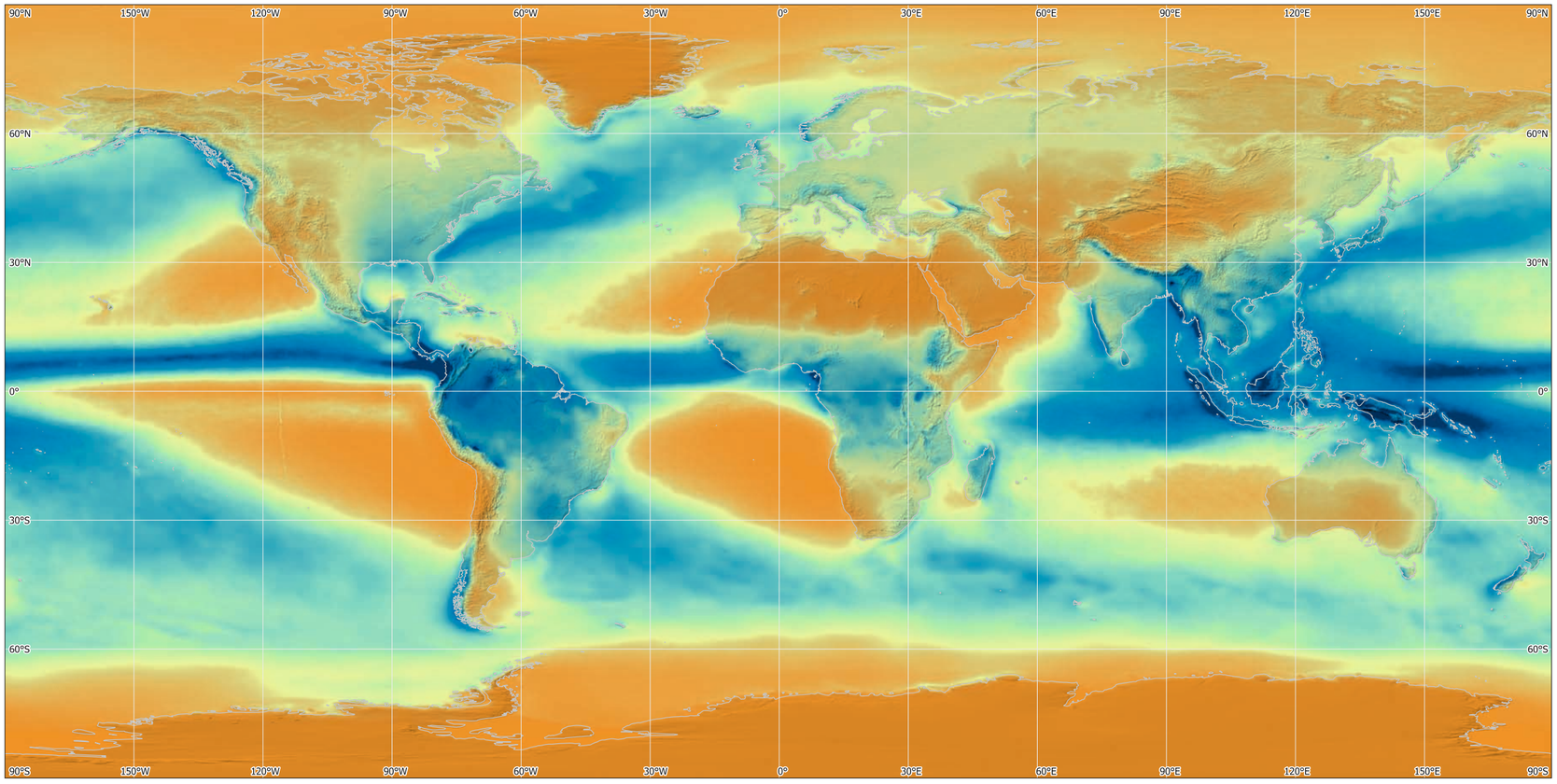

Precipitation [mm/year]

0 500 1,000 2,000 3,000 4,000

1. Average annual precipitation for the years 2000 to 2023 as measured by satellite.

Global Distribution of Precipitation

Precipitation distribution on Earth is influenced by several factors including latitude, proximity to large bodies of water, elevation, and prevailing wind patterns. Equatorial regions typically experience high levels of precipitation due to the convergence of warm, moist air masses, resulting in abundant rainfall throughout the year. Conversely, regions near the poles tend to have lower precipitation rates due to colder temperatures and limited moisture availability.

Coastal areas often receive significant precipitation as moist air from oceans is forced to rise over landmasses, leading to enhanced cloud formation and rainfall. In contrast, interior continental regions may experience more variable precipitation patterns, with some areas receiving ample rainfall while others are relatively dry due to rain shadows caused by mountain ranges or prevailing wind patterns.

Cloud Cover (%)

0 25 50 75 100

3. Mean cloud cover, Jan. 2016

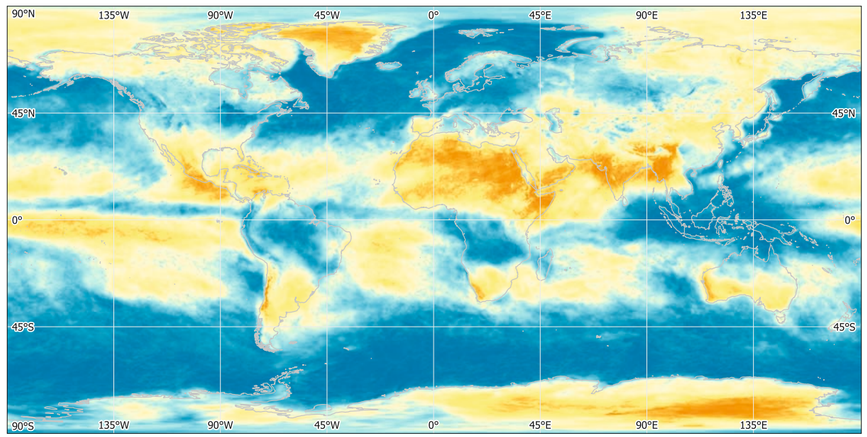

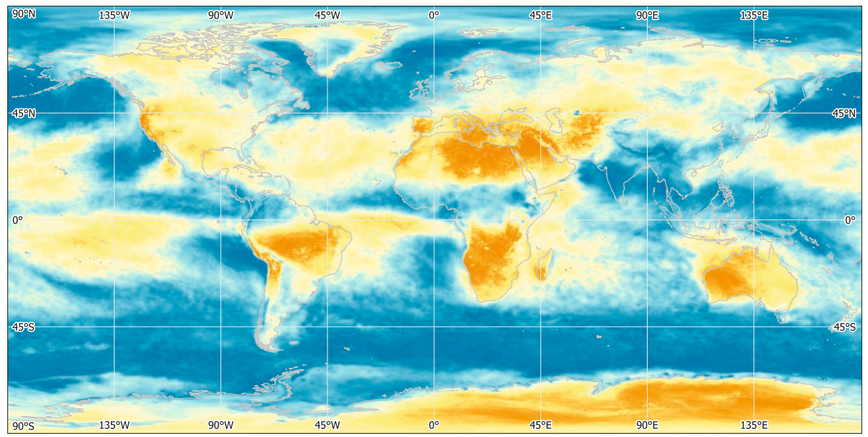

4. Mean cloud cover, July 2016.

Cloud Formation and Precipitation

The relationship between climate, cloud cover, and precipitation is a complex interplay that influences Earth's ecosystems and weather patterns. Climate is linked to atmospheric phenomena such as cloud formation and precipitation. Cloud cover, the extent to which clouds cover the Earth's surface, plays an important role in the planet's energy balance by reflecting sunlight back into space and trapping outgoing heat. Precipitation, including rainfall, snowfall, and other forms of moisture, is a fundamental component of the Earth's water cycle as well as of regional climates and ecosystems.

These interconnected processes are essential for climate change, weather patterns, and their impacts on human societies and natural environments. Earth observation satellites monitor these phenomena on a global scale. Equipped with advanced sensors, these satellites provide data on cloud cover, precipitation rates, and atmospheric conditions across different spatial and temporal scales.

Satellite observations offer insights into the spatial distribution and temporal variability of cloud cover, allowing to study cloud formation processes, their interactions with atmospheric circulation patterns, and their role in the Earth's climate. Satellite-based measurements of precipitation provide crucial information for water resource management, flood forecasting, and agricultural planning.

By combining satellite observations with advanced climate models, scientists can improve our understanding of the complex feedback mechanisms between climate, cloud cover, and precipitation. In this context, Earth observation satellites serve as important tools for monitoring and studying the Earth's climate system.

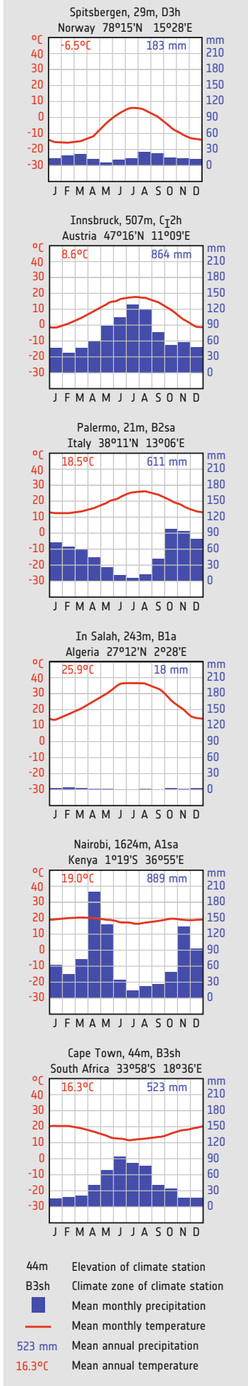

2. Climate diagrams for areas of interest at different latitudes.

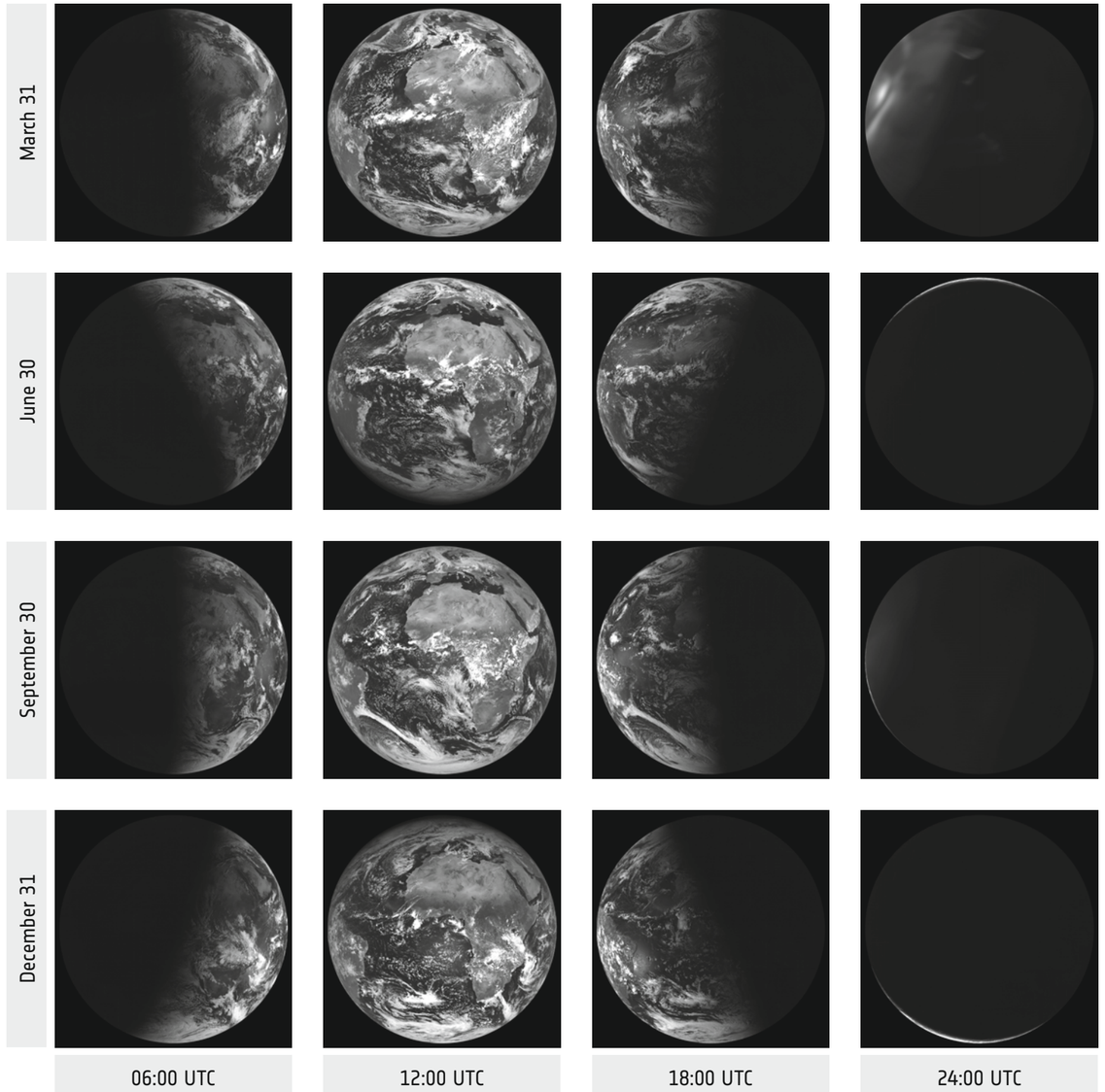

1. Seasonal and diurnal changes of illumination of the Earth. Meteosat (0° meridian, visible light)

The Earth in Visible Light

Meteosat satellites provide insights into Earth's dynamics through visible spectrum imagery, capturing the planet's surface features and atmospheric conditions with remarkable detail. In the visible spectrum, these images reveal a view of natural phenomena, illustrating the ever-changing landscape influenced by seasonal variations and diurnal cycles.

During the course of a year, Meteosat imagery shows the dynamic interplay of Earth's seasons. The change of the angle of irradiation of sunlight is very well visible. During the spring and autumn equinoxes the full hemisphere is illuminated at 12:00 UTC. Additionally, seasonal changes in the vegetation and snow cover are visible.

The diurnal cycle with its sequence of day and night can be followed in Meteosat imagery, too. Seasons and times of day intersect in Meteosat imagery. In high latitudes, the transition from polar night to polar day during summer results in continuous daylight, while winter months remain dark. In equatorial regions, the diurnal cycle remains relatively constant throughout the year.

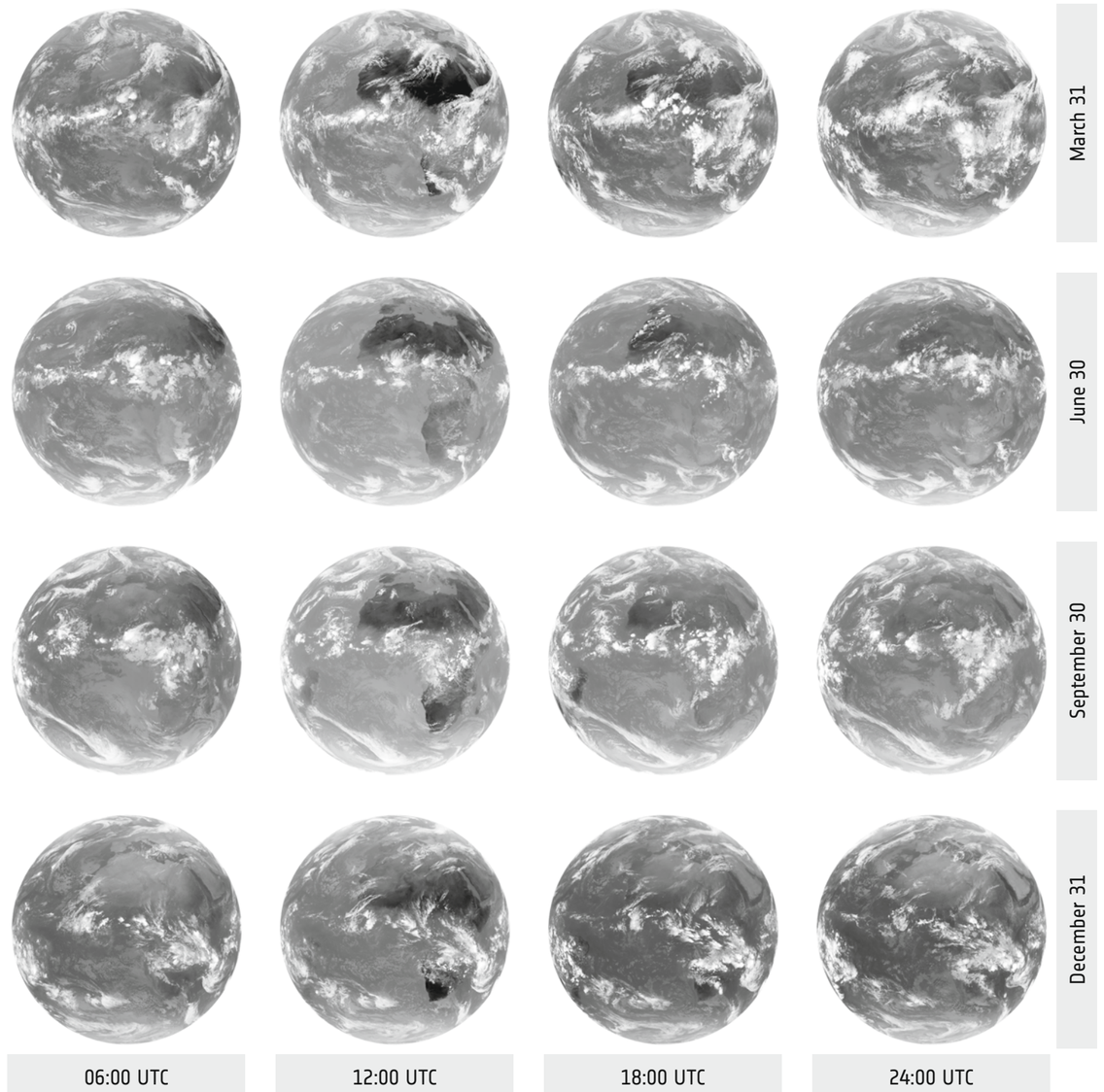

2. Changes of temperature distribution and migration of ITC during the year. Higher temperatures appear darker. Meteosat (0° Meridian, thermal infrared band).

The Earth in Infrared Light

Infrared Meteosat imagery shows clouds and atmospheric dynamics, offering insights into weather patterns, climate phenomena, and the behaviour of the Intertropical Convergence Zone (ITC). Operating in the infrared spectrum, these images detect thermal radiation emitted by Earth's surface and atmosphere, providing a perspective on cloud cover and atmospheric temperatures.

Cloud cover dominates infrared Meteosat imagery, appearing as shades of gray or white against a darker background. Different cloud types, such as cumulus, stratus, and cirrus, exhibit distinct thermal signatures, allowing to discern their height, thickness, and composition. Thick, high-altitude clouds appear colder in infrared imagery, while low-lying clouds and fog usually are warmer.

The Intertropical Convergence Zone (ITC), a region near the equator where trade winds converge, appears in the images as a band of thunderstorms and cumulonimbus clouds. The position of the ITC shifts over the year with the tilt of the Earth's axis, influencing global weather patterns and precipitation distribution.

ATMOSPHERE

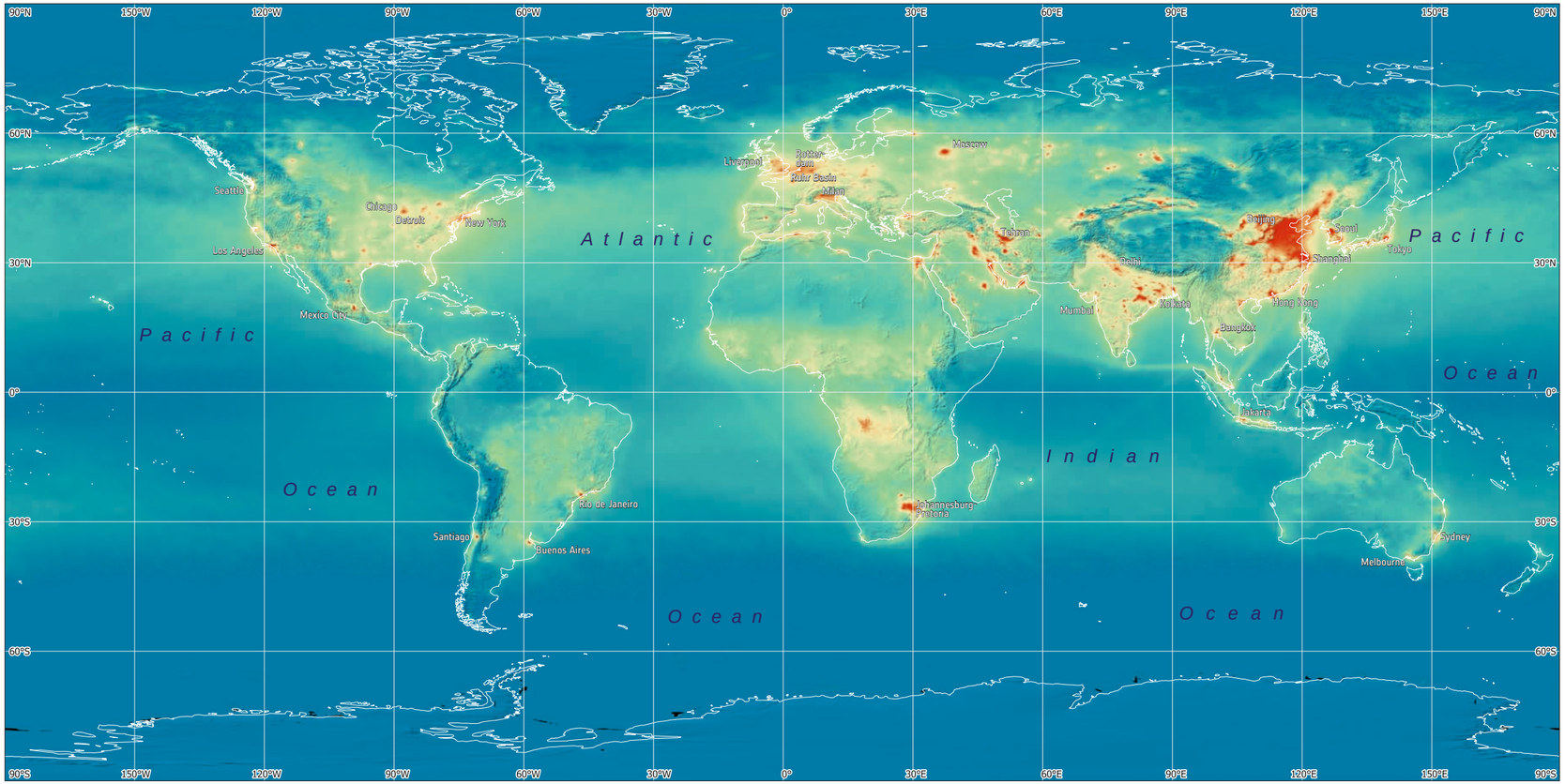

Nitrogen dioxide (NO_2) in µmol / m^2

200 100 50 20 10 0

1. Global map of nitrogen dioxide (NO_2). distribution. NO_2 is produced by high-temperature combustion processes in industry and traffic and reflects the industrial activity of a region. Data: Sentinel-5P.

Components of the Atmosphere

The atmosphere consists mainly of nitrogen (N_2, 78.08%), oxygen (O_2, 20.95%), and argon (Ar, 0.93%). The remaining 0.04% are made of the so-called trace gases, which despite their small concentrations play important roles in the atmosphere. Carbon dioxide (CO_2), methane (CH_4), and nitrous oxide (N_2O) are important greenhouse gases contributing to global warming. During the last decades especially CO_2 has gained awareness, as its concentration has increased from 320 ppm (parts per million) in the 1960s to 420 ppm in 2023.

Ozone (O_3) plays an important role in the stratosphere. It acts as a filter for the solar ultraviolet (UV) radiation, which can destroy biomolecules. The antarctic ozone hole, an O_3-deficit occurring every year around October, was intensified by the man-made trace gas CFC (chlorofluorocarbon).

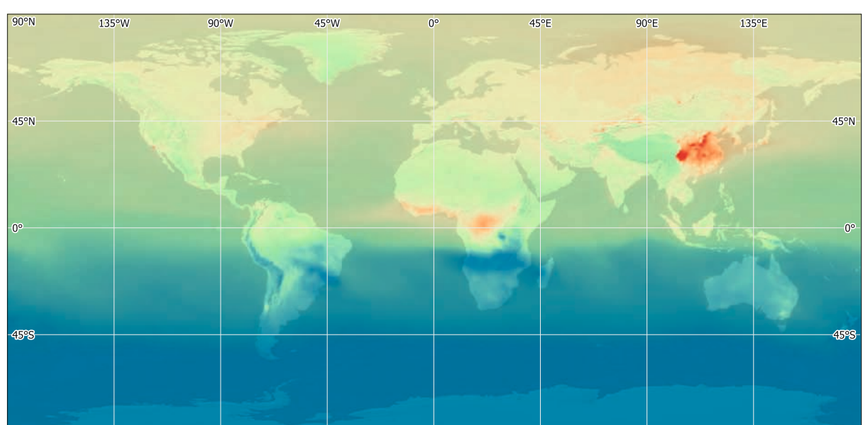

2. Global map of carbon dioxide (CO_2) distribution in January 2020.

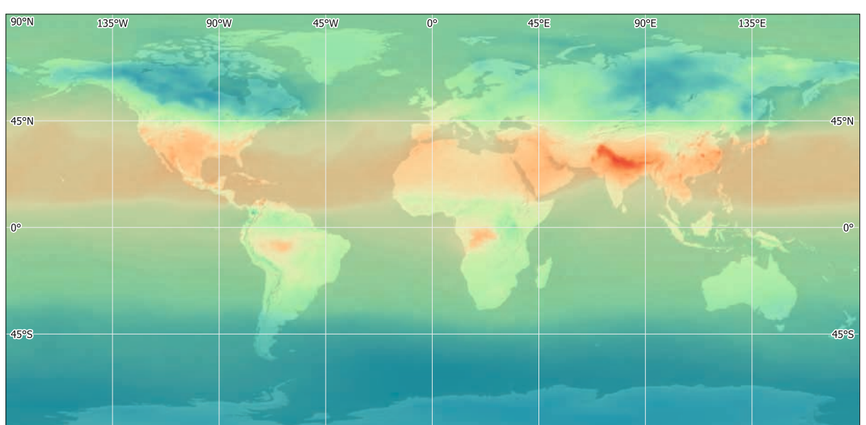

3. Global map of carbon dioxide (CO_2) distribution in July 2020.

Carbon Dioxide (CO_2) Concentration [ppm]

<408 410 412 414 416 418 420<

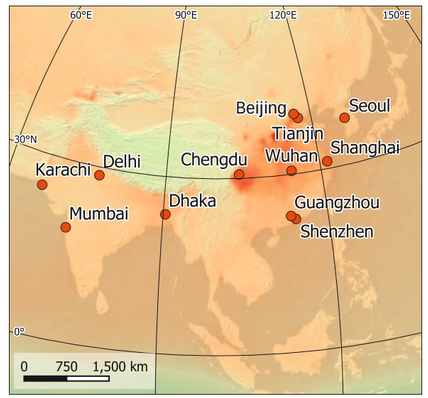

Methane (CH_4) Concentration [ppb]

<1,700 1,750 1,800 1,850 1,900 1,950 2,000<

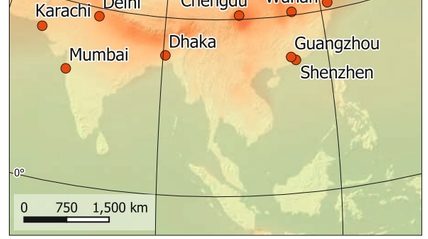

4. Seasonal variation of the methane (CH_4) concentration in south-east Asia, January 2020 (top) and July 2020 (bottom). Rice cultivation is one of the most important sources of CH_4.

5. Development of the Antarctic ozone hole since 1970.

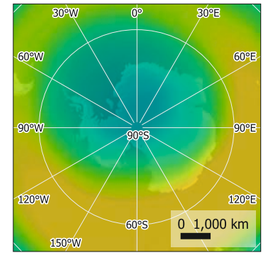

5a. Antarctic ozone hole, Oct. 1970.

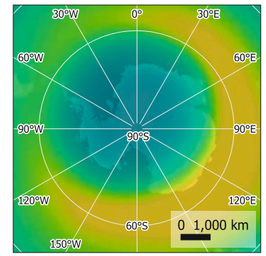

5b. Antarctic ozone hole, Oct. 1980.

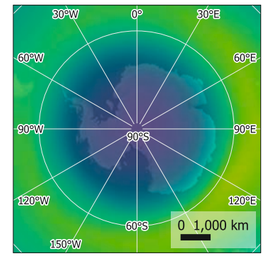

5c. Antarctic ozone hole, Oct. 1990.

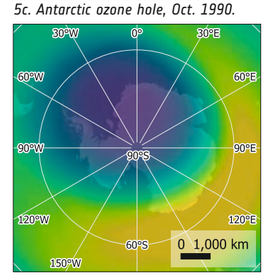

5d. Antarctic ozone hole, Oct. 2000.

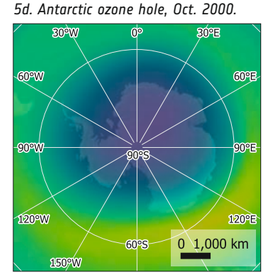

5e. Antarctic ozone hole, Oct. 2010.

Ozone Concentration Total Column [Dobson units]

<100 200 300 400<

ATMOSPHERE

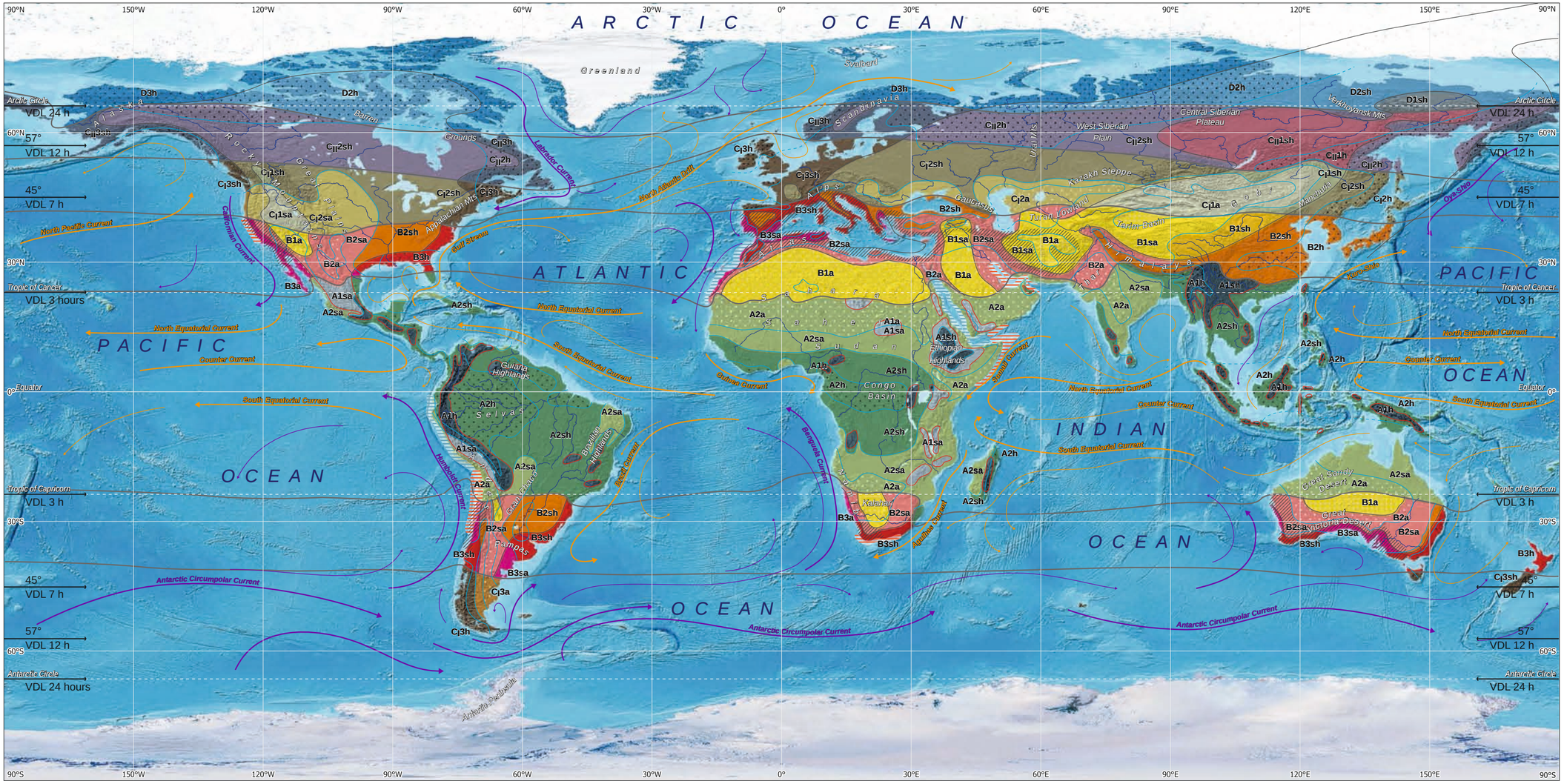

1. Global map of climate zones according to Lauer and Frankenberg.

Climate zones

C_I3sh	Example: C_I3sh is a maritime, semi-humid, warm temperate climate
57° / VDL 12 h	Annual variation of day length (VDL) in hours (solar climatic boundary)
	Thermally adapted climatic boundary with influences of mountains and sea currents taken into account
	C: Degree of continentality (in %) as measure of the annual temperature variations
	Humid months: precipitation > evaporation from the landscape
	Region of subtropical winter rain
	Coastal fogs (winter/summer)

Ocean currents

- Cold mainstream
- Cold current
- Warm mainstream
- Warm current

Climate Zones

The term climate comprises all meteorological features responsible for the long-term average state of the atmosphere on a certain place. The climate is influenced by a wealth of factors. Most important, the geographic position influences the temperature – the longer the distance from the equator and the higher the altitude, the lower the temperature.
The distance from the ocean, the continentality, is of similar importance – land masses heat up and cool down faster than the water of the ocean, which makes the temperature variations in the continent larger than at the coasts. Therefore in coastal regions the summers usually are cooler and the winters milder.

Regions with similar climatic conditions are assigned to the same climate zone. The classification of climates by Lauer and Frankenberg (1987) defines in a first approach the tropical, sub-tropical, temperate, and polar climate zones.

The criteria for classification refer to the real vegetation. The basic principle of climate grading is the inclusion of solar-climatic conditions of radiation and illumination. The borderline of the tropes is defined by the fluctuation of temperature. The border is located where the variation between summer and winter (annual amplitude) is larger than the variation between day and night (diurnal amplitude). Tropical climates are therefore diurnal climates, whereas non-tropical climates are annual climates. According to this climatic classification, the Earth can be divided roughly into four climatic zones, defined by the solar radiation, tropical, subtropical, temperate and polar climates. These zones are subclassified based on their thermal properties.

The climate system of the Earth is highly complex – weather satellites are of high value for measuring atmospheric conditions and extrapolating the development based on these measurements. This covers measuring cloud cover, temperatures and humidity as well as the concentration of ozone and greenhouse gases with their long-term impact on the development of the climate.

Climate Zone (global solar irradiation)	Climate region (heat balance)	Water balance (number of humid months) a (arid) 0-2	sa (semi-arid) 3-5	sh (semi-humid) 6-9	h (humid) 10-12	Climatic boundary
A Tropical	1 Cold tropics					Absolute Frost Line
	2 Warm tropics					VDL 3 hrs.
B Subtropical	1 high-continental					c=200%
	2 continental					c=100%
	3 maritime					VDL 7 hrs.
C Mid-Latitudes I warm temperate	1 high-continental					c=200%
	2 continental					c=100%
	3 maritime					VDL 12 hrs.
C Mid-Latitudes II cool temperate	1 high-continental					c=200%
	2 continental					c=100%
	3 maritime					VDL 24 hrs.
D Polar regions	1 high-continental					c=200%
	2 continental					c=100%
	3 maritime					Snow Line
	Glaciers					

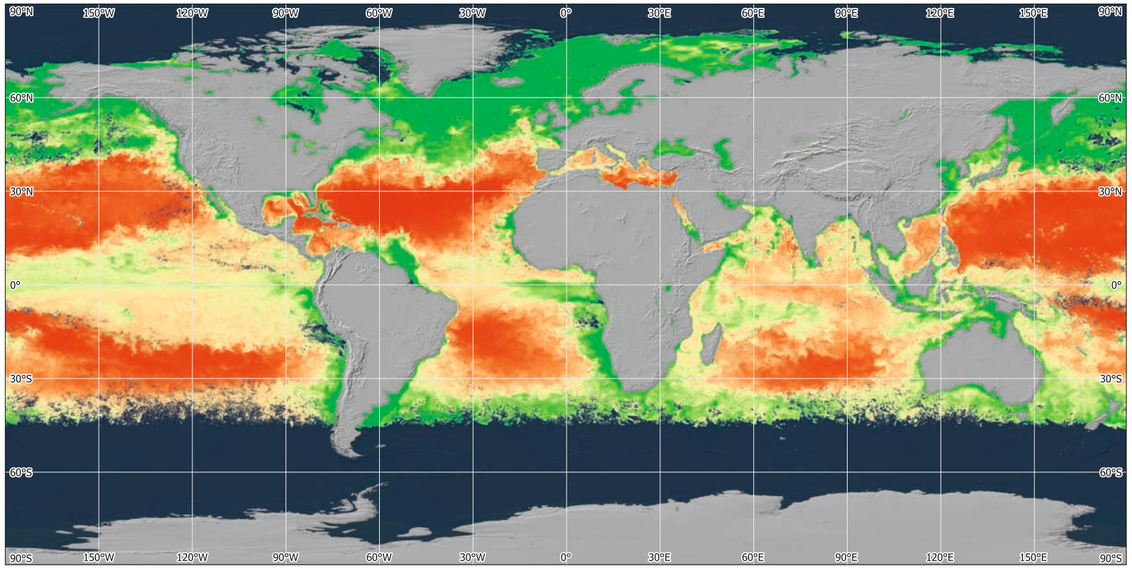

1. Chlorophyll-a concentration in the ocean surface, June 2023. Data: Sentinel-3.

Chlorophyll-α Concentration [mg/m³]

- 0.000 - 0.049
- 0.050 - 0.074
- 0.075 - 0.099
- 0.100 - 0.134
- 0.135 - 0.179
- 0.180 - 0.249
- 0.250 - 0.374
- 0.375 - 0.599
- 0.600 - 64.99
- 65.0 <

2. Chlorophyll-a concentration in the ocean surface, December 2023. Data: Sentinel-3.

Life in Water

Phytoplankton are microscopic marine plants crucial to aquatic ecosystems, serving as primary producers and oxygen sources. Their abundance varies seasonally and depends on the availability of nutrients. Under specific conditions like nutrient influx and warm temperatures they can rapidly proliferate, causing algal blooms. These blooms consume oxygen, leading to hypoxic conditions harmful to aquatic life. Some phytoplankton species produce toxins, posing risks to human health through contaminated seafood.

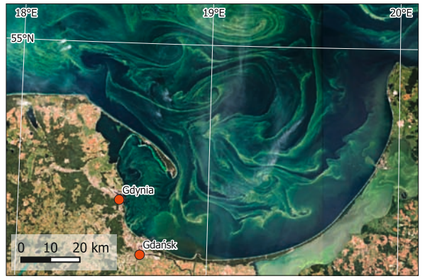

3. Swirls of an algal bloom in the Baltic Sea near Gdańsk, Poland. Data: Sentinel-2, 2019-07-20.

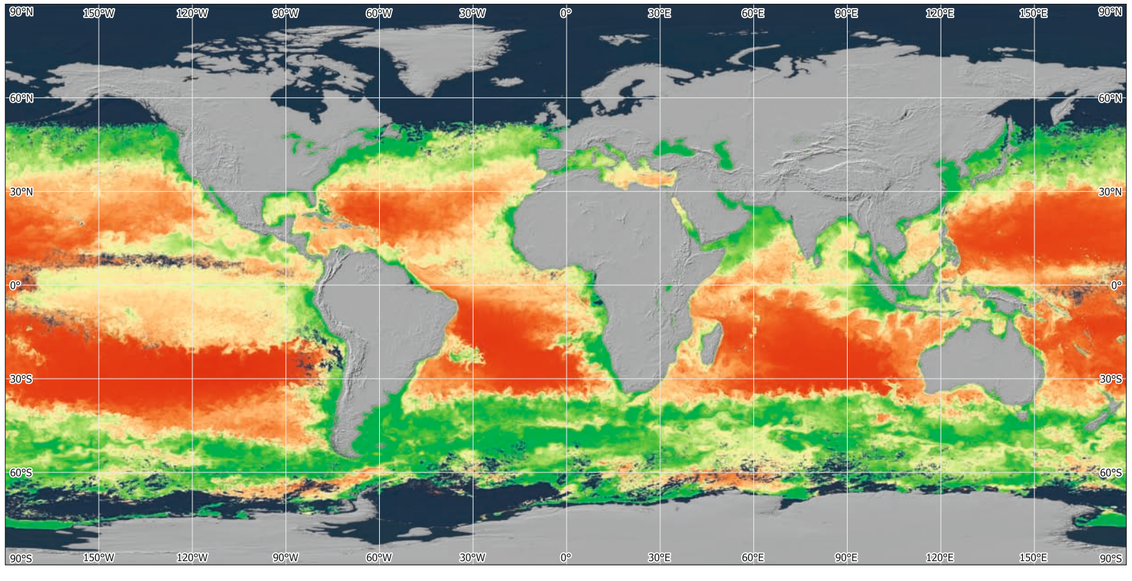

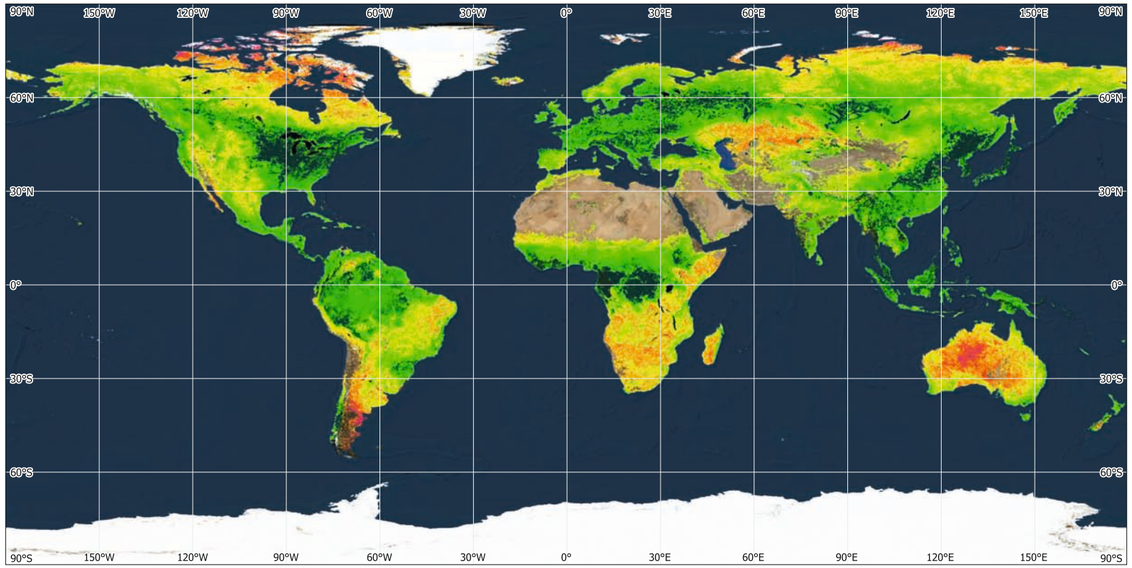

4. Vegetation intensity shown by the Chlorophyll terrestrial index, July 2018. Data: Sentinel-3.

Land Vegetation

Plants are covering the largest part of the solid surface of Earth, well adapted to the respective conditions given by the climate and the soils of the region. The importance of solar energy for the plants' life cycles is reflected by the large seasonal differences in the chlorophyll content of the vegetation. The differences are smallest in the tropical regions, where the solar irradiance remains relatively constant. From deciduous forests to superblooms the dynamics of vegetation shows a wide spectrum of different phenomena.

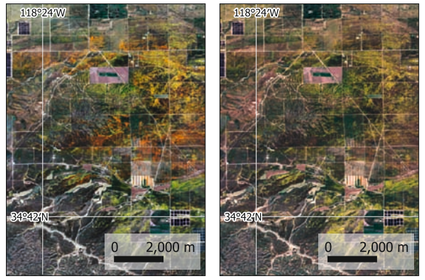

6. Colours during (2023-04-08, left) and after a superbloom event (2023-04-13, right) in California, U.S.A. Data: Sentinel-2.

Terrestrial Chlorophyll Concentration (arbitrary units)

- 3.3
- 2.8
- 2.0
- 1.4
- 1.2
- 1.0
- 0.9

5. Vegetation intensity shown by the Chlorophyll terrestrial index, January 2018. Data: Sentinel-3.

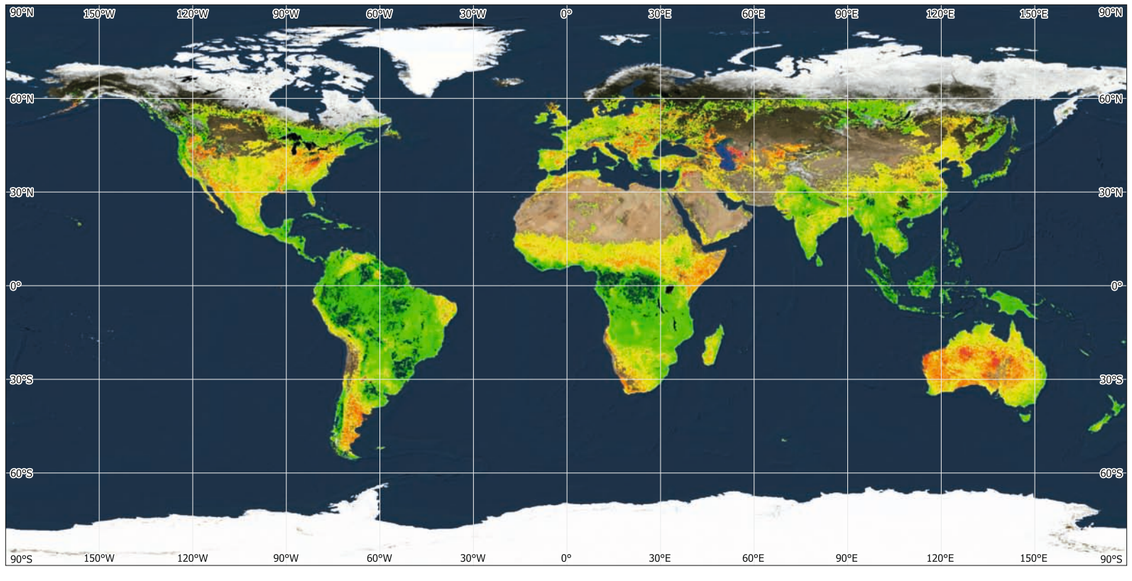

BIOSPHERE

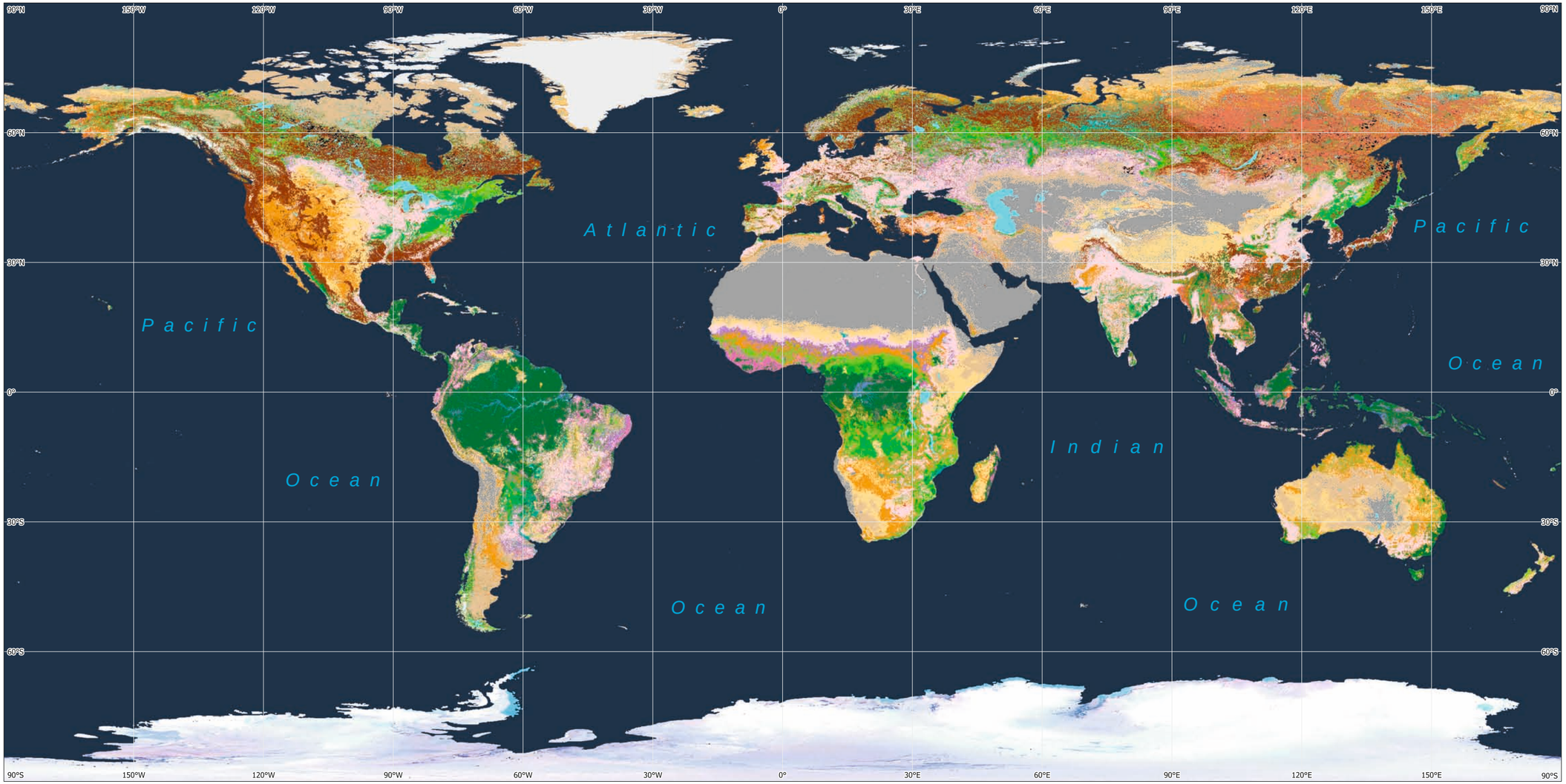

1. Global landcover/land use map derived from satellite data.

- Snow and ice
- Water surface
- Sparse herbaceous or sparse shrub cover
- Tree cover, conifer, deciduous
- Tree cover, mixed-leave type
- Tree cover, broad-leaved, deciduous, closed
- Tree cover, conifer, evergreen
- Tree cover, burnt
- Mosaic: tree cover / other natural vegetation
- Bare ground
- Artificial surface and associated area
- Cultivated and managed area
- Herbaceous cover, closed-open
- Regularly flooded shrub and/or herbaceous cover
- Tree cover, broad-leaved, deciduous, open
- Tree cover, broad-leaved, evergreen
- Mosaic: cropland / tree cover / other natural vegetation
- Mosaic: cropland / shrub and/or grass cover
- Shrub cover, closed-open, evergreen
- Shrub cover, closed-open, deciduous
- Tree cover, regularly flooded, saline water
- Tree cover, regularly flooded, fresh water
- No data

2. Kiruna, Sweden. Tree cover, extensive agriculture, mining (Sentinel-2, 2023-09-08).

3. Pärnu, Estonia. Pine, birch and spruce, intensive Forestry (Sentinel-2, 2023-09-26).

4. Thessaloniki, Greece. Cultivation of crops and fruits (Sentinel-2, 2023-09-20).

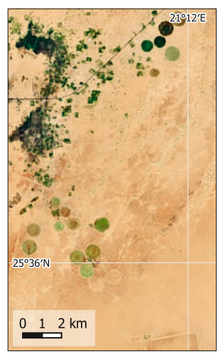

5. Tazirbu, Libya. Agriculture in the oasis based on irrigation (Sentinel-2, 2023-09-27).

6. Abéché, Chad. Cattle raising in the savannah around the city (Sentinel-2, 2023-09-24).

7. Boende, D.R. Congo. Shifting cultivation in the rain forest (Sentinel-2, 2023-09-08).

8. Marchand, South Africa. Irrigation agriculture along the river (Sentinel-2, 2023-03-31).

Global Land cover and Land Use

Land cover refers to physical characteristics of the Earth's surface, including vegetation, water bodies, and bare ground. In its natural state, it depends on the soils, climate, and the fauna inhabiting a region.

Land use, on the other hand, describes how humans utilize the land, such as for agriculture, urban development, or conservation. In many cases land use is closely related to changes in the land cover, such as deforestation, the increase of agricultural land and the growth of sealed surfaces due to the development of settlements. Changes in land cover and land use can impact ecosystems, biodiversity, and the climate.

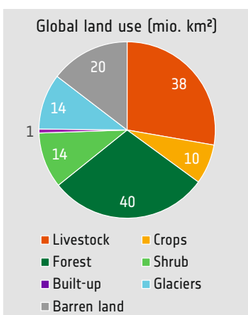

9. Land surfaces covered by important land cover/land use classes (areas in million km²).

1. The Mar de Plástico around El Ejido, Spain. Data: Sentinel-2, 2022-09-10.

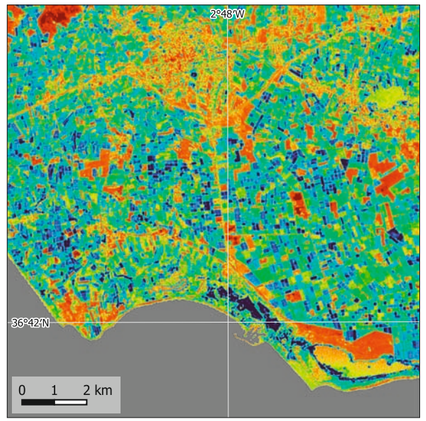

2. Soil Moisture Index (NDMI) of the region of El Ejido. Data: Sentinel-2, 2022-09-10 (left).

Soil Moisture
dry moist

3. The Mar de Plástico around El Ejido, Spain, in 1985. Data: Landsat 5, 1985-10-17 (right).

4. View of the plastic greenhouses near El Ejido.

El Mar de Plástico — El Ejido, Spain

Famous for its extended greenhouses, the so-called Mar de Plástico. The region has a dry, mild, Mediterranean climate and is further sheltered on the north by the Sierra de Gador mountains. With just slightly more than 200 mm of annual precipitation, the agriculture relies on groundwater replenished by water from the adjacent Sierra.

Covering an area of 30,000 hectares, the region has undergone significant changes, which is well visible in the satellite images. An important player in Spain's economy, the Mar de Plástico sustains over 40,000 jobs. Most producers are family companies with areas of about 1 to 1.5 ha. Mainly vegetables (e.g. tomatoes) are grown in an artificial sandy soil. The development of the Mar de Plástico has different impacts. The social landscape is in flux, with shifting employment dynamics and community structures, partly related with illegal migration. Simultaneously, ecological considerations arise, including water usage patterns and concerns about chemical runoff, prompting a deeper exploration of the delicate balance between progress and environmental sustainability.

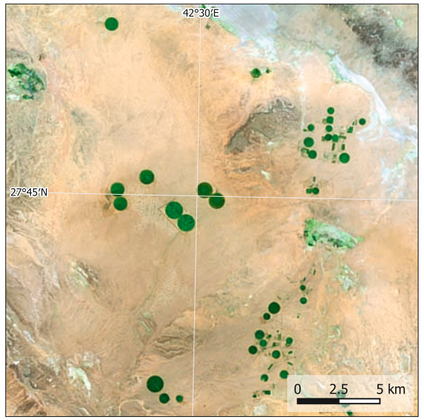

5. First center-pivot irrigation fields near Ha'il, Saudi Arabia, in 1985. Data: Landsat 5, 1985-04-15.

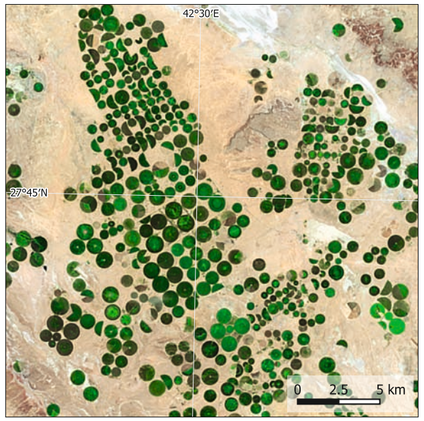

6. Until 1995, the number of irrigated fields has grown significantly. During this period the export of wheat reached its maximum. Data: Landsat 5, 1995-04-27.

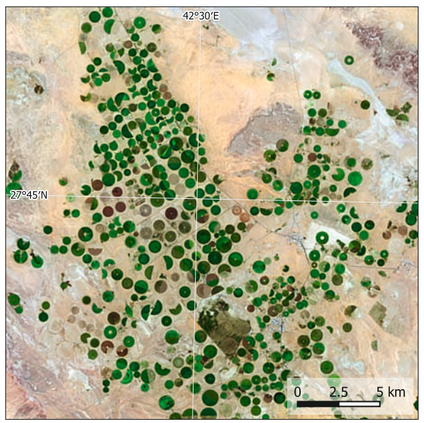

7. After 1995, the intensity of cultivation decreased due to the economic situation as well as due to problems with salination. Data: Landsat 5, 2015-04-18.

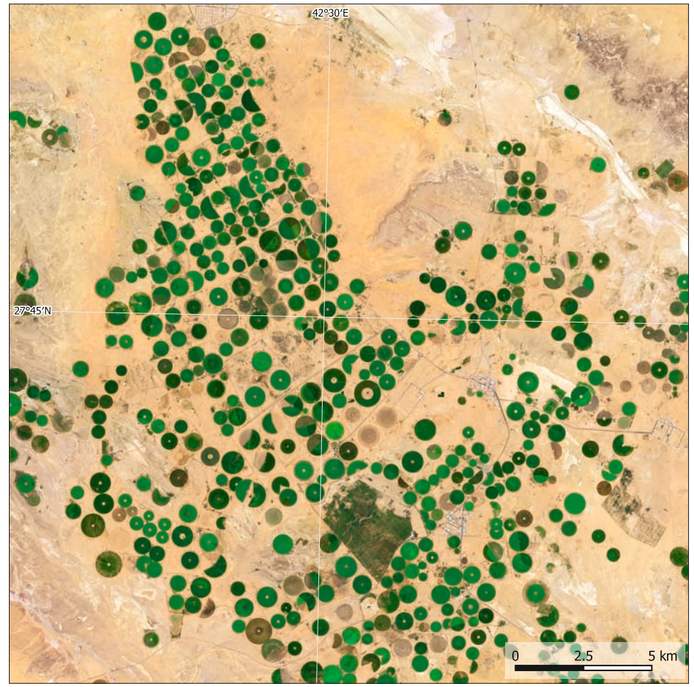

Desert Agriculture — Ha'il, Saudi Arabia

Saudi Arabia is one of the most arid countries in the world and is mostly covered by deserts. The desert environment goes hand in hand with a relatively low population density. The economy of the country largely depends on the export of fossil fuels (oil and gas), but Saudi Arabia has been exporting wheat, too. With the exception of oases, agriculture in Saudi Arabia has been mostly based on extensive farming. With the exploitation of fossil groundwater deposits for irrigation it was possible to intensify the production of wheat and other crops.

The area around the town of Ha'il is located above a large groundwater layer that has been exploited with increasing intensity since the 1970s. While the originally applied techniques led to the evaporation of a large part of the water combined with significant salination of the soil, the methods used now are better adapted to the environment. Nevertheless, the use of fossil groundwater will end once the groundwater layers are depleted.

The satellite images show a good contrast between vegetation and the surrounding desert, as the numerous centre-pivot irrigation fields show. They are very well suited to monitor the development of the irrigated fields and the crop status. This makes it possible to use the data for precision farming, as they allow to tell where the supply of water and fertilizers need to be optimised.

8. Situation of irrigation fields near Ha'il, Saudi Arabia, in 2023. Data: Sentinel-2, 2023-04-26.

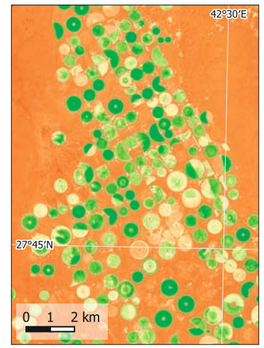

9. The NDVI (normalised difference vegetation index) helps monitoring the status of the crops.

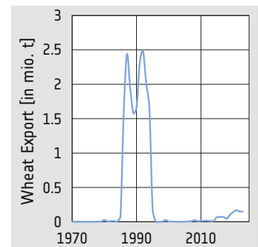

10. Development of the export of wheat from Saudi Arabia.

1. Campo Novo de Rondônia, Brazil, 1991-06-28. Image taken by Landsat 5 shows the "fishbone" structures during the initial phase of deforestation.

2. Campo Novo de Rondônia, Brazil. Aerial view of fires during deforestation.

Rondônia, Brazil

Rondônia is one of the states of Brazil, located in the southwestern part of the Amazon basin. The state has seen a population increase from about 40,000 inhabitants in 1950 to more than 1.8 million in 2021. This development went hand in hand with a change in the vegetation cover. Originally almost 90% of the surface was covered by rainforest. By now it has become one of the best known examples of deforestation in the Amazon basin. About one third of the area is still covered by forests.

The satellite maps show the development around Campo Novo de Rondônia, which in 2020 had 14,200 inhabitants. The image series shows how the deforestation is initiated with the construction of roads, along which settlers start to clear the forests to gain agricultural land. Only in the southern part of the area shown in the satellite maps forests have remained – this is a part of the Uru-Eu-Uaw-Uaw Indigenous Territory, established by the government of Brazil to protect the indigenous population. First contact with one of the tribes living here, the Uru-Eu-Uaw-Uaw people, happened as late as 1981.

3. Area deforested in Brazil per year.

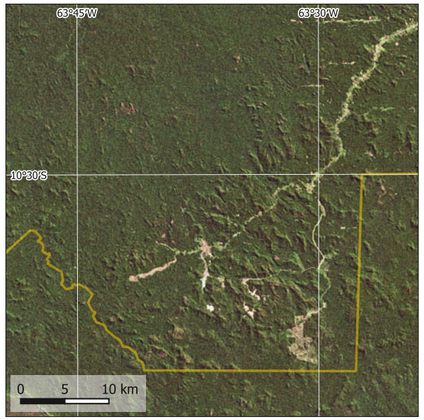

4. Campo Novo de Rondônia in 1984. Yellow lilne: border of the Uru-Eu-Uaw-Uaw Indigenous Territory. Data: Landsat 5, 1984-06-24.

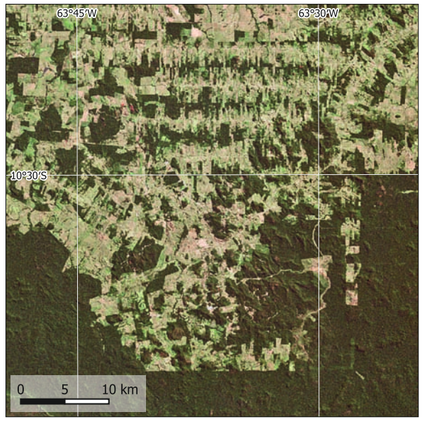

5. Campo Novo de Rondônia in 2010. Large parts of the area have been deforested to develop agricultural land. Data: Landsat 5, 2010-05-15.

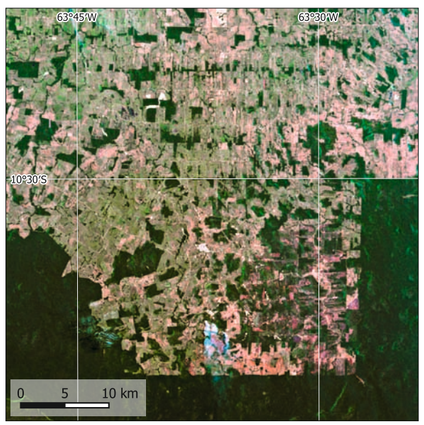

6. Campo Novo de Rondônia in 2023. Most of the forest in the north has been removed, only in the Uru-Eu-Uaw-Uaw Indigenous Territory a large and mostly homogeneous forest area has remained. Data: Sentinel-2, 2023-10-07.

British Columbia, Canada

Forest fires are a recurring concern in the Canadian province of British Columbia. Forest fires occur when vegetation, dry conditions, and other factors combine, resulting in uncontrolled flames that spread across large areas.

In 2023, forest fires in Canada during the first half of the year have affected an area of 48,000 km², compared to the area of 21,000 km² burned during an average year. Climate change is assumed to have played a significant role, creating hotter and drier conditions that increase the risk of fire ignition and spread. Lightning strikes and human activities, such as campfires and negligence, have also been contributing factors.

The impacts of forest fires are far-reaching. They pose a threat to wildlife habitats, degrade air quality, and damage watersheds. Particles released into the air can travel thousands of kilometres. Forest fires affect local communities, disrupt transportation, and impact the economy, particularly the timber industry.

7. Number of forest fires and burned area per year in Canada. In 2023 the burned area has increased dramatically.

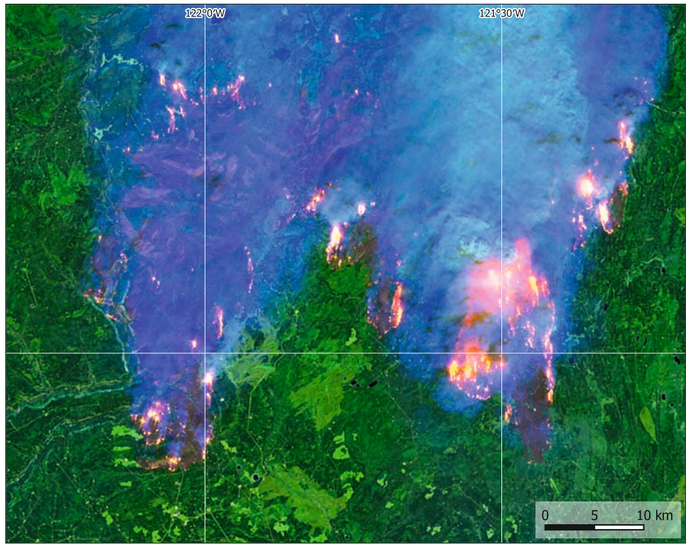

8. False-colour infrared detail image of a fire front in British Columbia. Data: Sentinel-2, 2023-05-18.

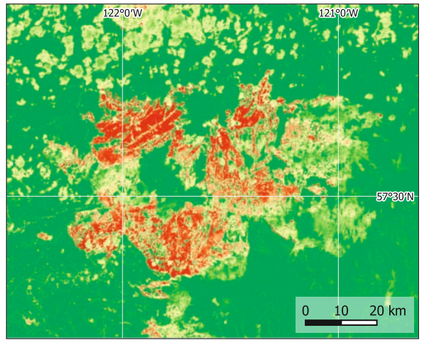

9. Burnt area index of a forest fire in British Columbia. Data: Sentinel-2, 2023-06-07.

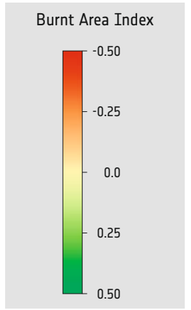

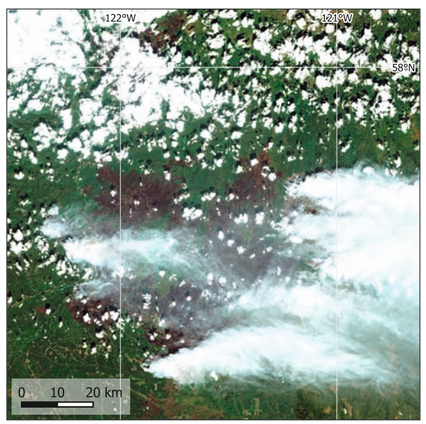

10. True colour visualisation of a forest fire in British Columbia. Data: Sentinel-2, 2023-06-07.

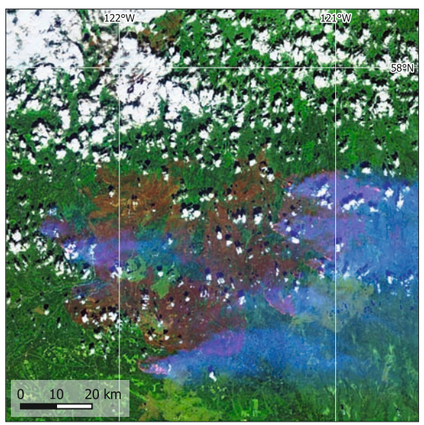

11. Smoke-penetrating false-colour infrared image of a forest fire in British Columbia. Data: Sentinel-2, 2023-06-07.

12. Large forest fires can be very difficult to combat.

1. *Overview satellite image of the southern coast of the Bohai Bay showing the aquaculture areas along the coast. The colours of the sea show a high sediment load of the shallow waters. Data: Sentinel-2, 2023-04-29*

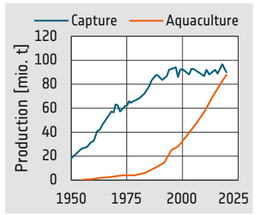

2. *Growing demand and shrinking natural resources have led to a shift of production from capture fisheries to aquaculture.*

Aquaculture – Bohai Bay

Global aquaculture has been steadily increasing over the years, producing fish, shrimp, mussels, and aquatic plants. The global production reached almost 90 million metric tons in 2020 (FAO), half of the total seafood production for human consumption. Top aquaculture-producing countries are China, India, Indonesia, Vietnam, Bangladesh, and Norway. This industry provides livelihoods for millions of people and is a vital source of food and income.

Aquaculture is an important contributor to the economy of the Bohai Bay region, with China being the largest producer of farmed seafood in the world. Including algae, China produced over 64 million metric tons of farmed seafood in 2020. The Bohai Bay is surrounded by extensive flat coastal areas suitable for aquaculture, with farms ranging from small-scale traditional operations to large commercial enterprises.

4. *Section of the south coast of the Bohai Bay in 2007, the land use has changed significantly. Data: Landsat 5, 2007-05-05.*

5. *Section of the south coast of the Bohai Bay during the initial phase of aquaculture activities in 1989, showing the extended mudplains of the original intertidal zone. Data: Landsat 5, 1989-05-17.*

3. *The radar satellite image of the southern coast of the Bohai Bay shows the intensive land use in a mix of settlements, agriculture and aquaculture. Offshore activities such as fishing boats and wind farms show up as bright dots in the sea. Data: Sentinel-1, 2023-04-26.*

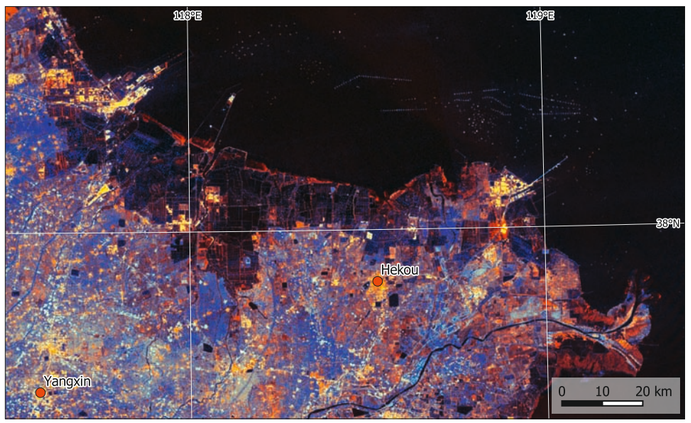

6. *Ilha de Orango, Bissago Archipel, during high tide. Data: Sentinel-2, 2023-04-24.*

7. *Ilha de Orango during low tide. Extended mudplains are visible. Data: Sentinel-2, 2023-04-14.*

Nature Protection

Nature protection is important for preserving biodiversity and maintaining the health of ecosystems. Effective nature protection requires collaborative efforts at local, national, and international levels. This involves implementing policies that balance conservation with socioeconomic needs, engaging stakeholders, and raising awareness about the importance of biodiversity conservation. In these tasks, satellites have become an important tool. This becomes clear when considering unique habitats like mangroves and alpine regions.

Mangroves are vital coastal ecosystems and serve as nurseries for marine life, protect against coastal erosion, and store carbon. They face threats from human activities such as urbanisation, aquaculture, and pollution. Conservation efforts focus on establishing protected areas, restoring degraded habitats, and involving local communities in sustainable management practices.

Similarly, alpine habitats, with their biodiversity and water regulation functions, are under pressure from climate change, tourism, and land-use changes. Conservation initiatives aim to preserve these ecosystems by creating protected zones and promoting sustainable economic procedures.

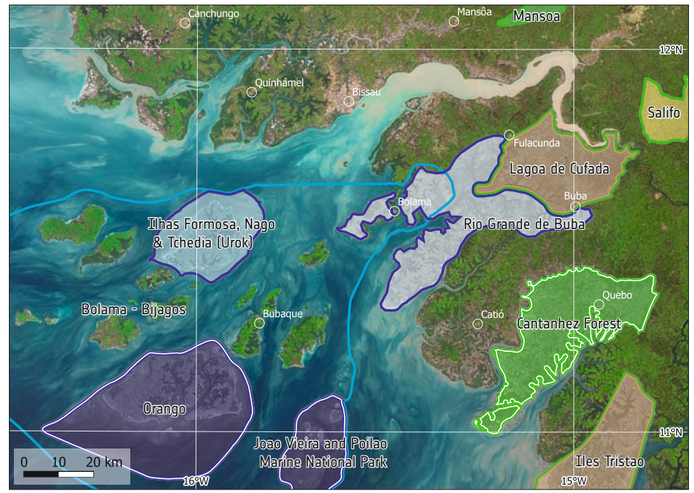

9. *The false-colour infrared image shows the mangroves in darker red. Data acquired by Sentinel-2, 2023-04-24.*

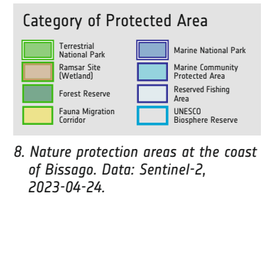

8. *Nature protection areas at the coast of Bissago. Data: Sentinel-2, 2023-04-24.*

10. *View of the intertidal plain along the coastline of Bissago.*

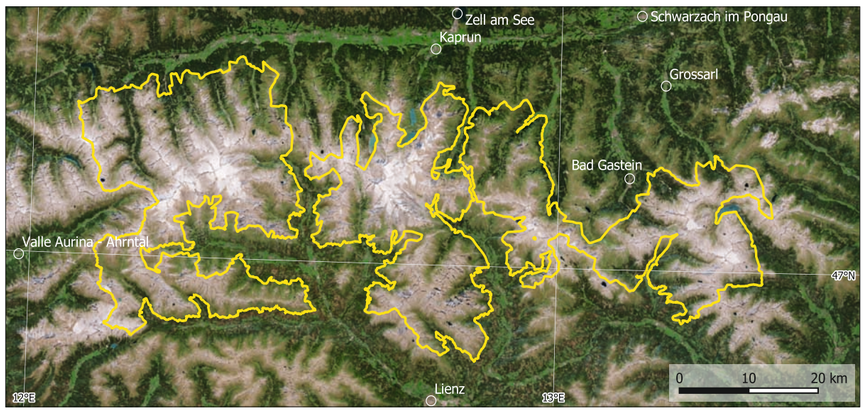

11. *View of Grossglockner, the highest peak in the National Park Hohe Tauern.*

12. *The National Park Hohe Tauern in Austria extends over the high alpine parts of the country. Data: Sentinel-2, 2023.*

ANTHROPOSPHERE

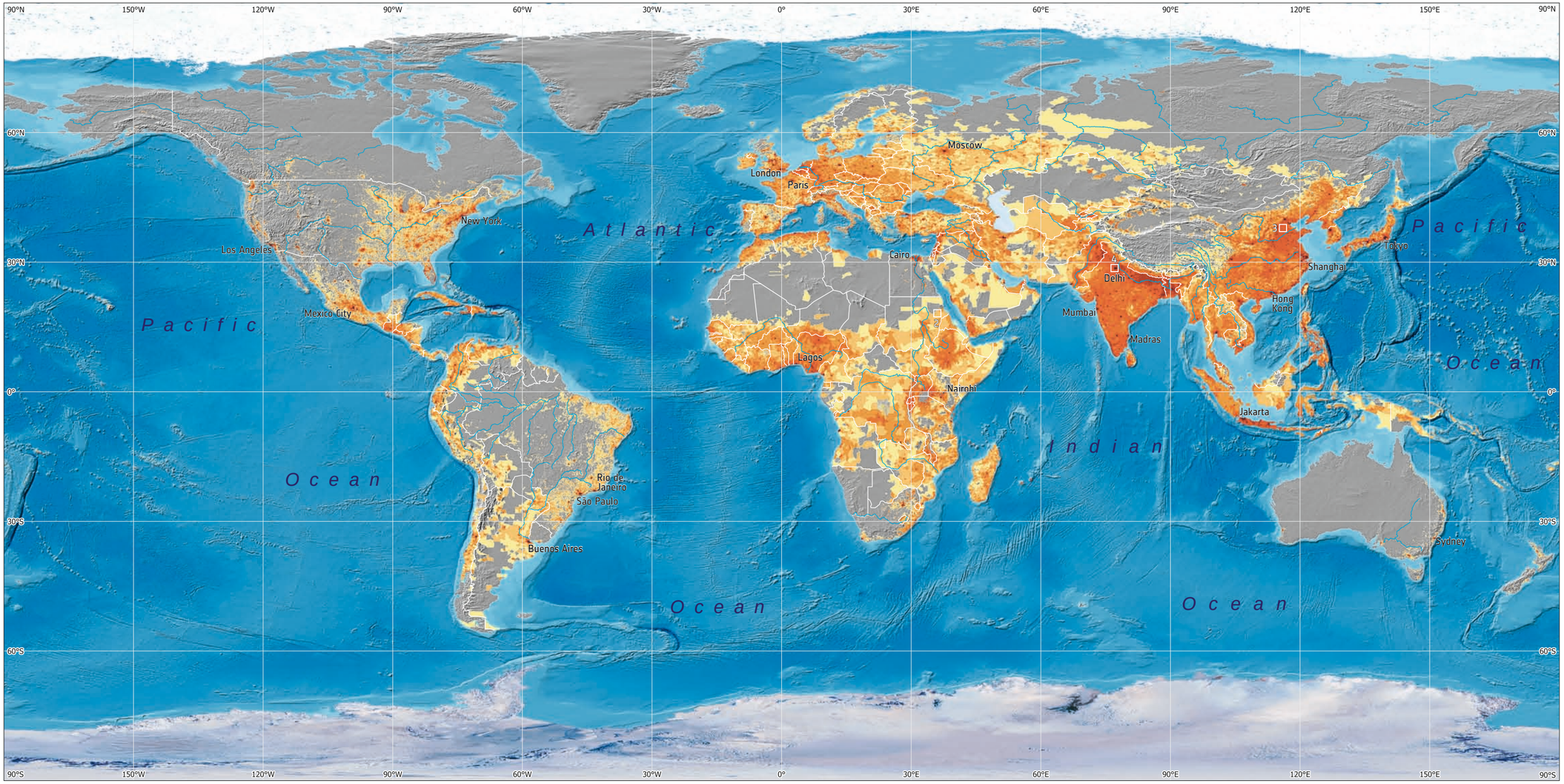

1. *Population Density (Data: Gridded Population of the World, 2020).*

Inhabitants per km²

- <3
- 3 - 10
- 10 - 30
- 30 - 100
- 100 - 300
- 300 - 1,000
- 1,000 - 3,000
- > 3,000

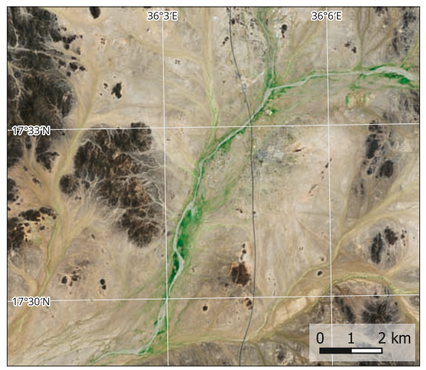

2. *Derudeb, Sudan. Data: Sentinel-2, 2024-04-13. Population density 3-10 inhabitants per km².*

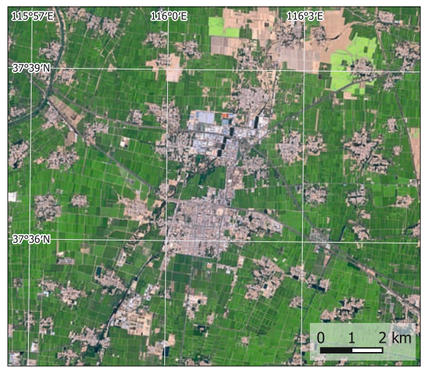

3. *Longhuazhen, China. Data: Sentinel-2, 2024-04-18. Population density 100-300 inhabitants per km².*

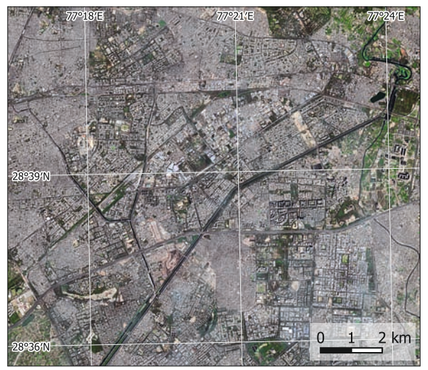

4. *Delhi, India. Data: Sentinel-2, 2024-03-19. Population density > 3,000 inhabitants per km².*

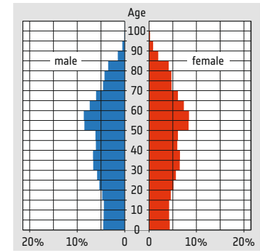

5a. *Population pyramid, Germany 2022.*

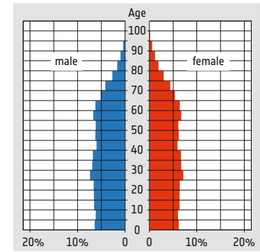

5b. *Population pyramid, United States of America 2021.*

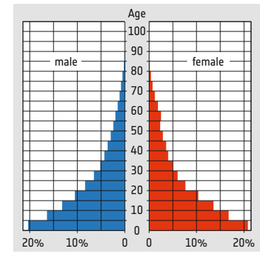

5c. *Population pyramid, Niger 2021.*

Population Distribution and Growth

The human population of Earth is distributed very unevenly. Large areas have almost no inhabitants, mainly the deserts, polar regions and dense forests. This stands in stark contrast with the densely populated regions e.g. in eastern China, the Ganges Delta in India, and western Europe.

The global population has seen an enormous increase especially during the last 100 years. While many societies on Earth are stagnating and ageing, there are young societies that are quickly growing. Most population scenarios show that a maximum number of 10 to 11 billion humans will be reached during the upcoming decades.

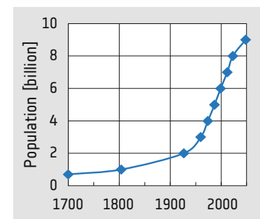

6. *Development of the global population (in billion) since 1700. The dots mark the years in which full billions were reached.*

1. Niamey, Niger, in 1984. Data: Landsat 4, 1984-10-13.

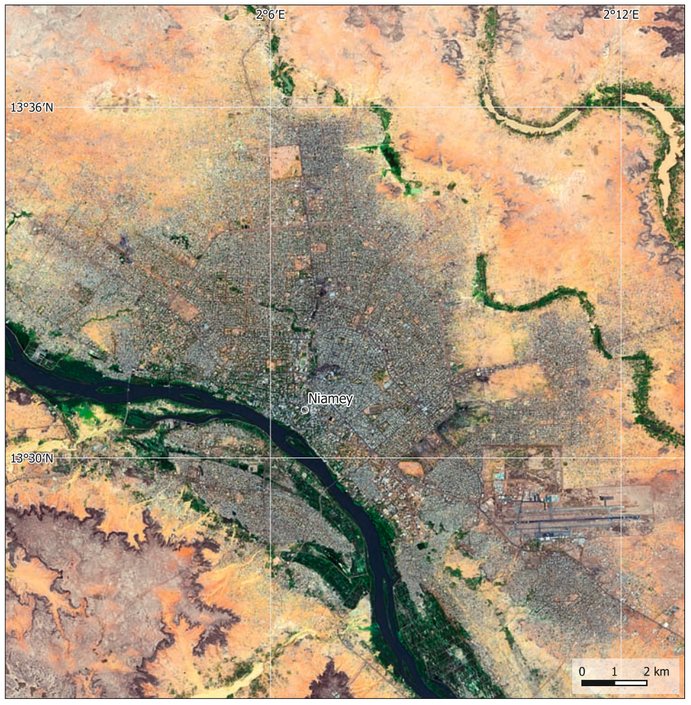

2. Niamey, Niger, in 2023. The city area has increased significantly, accompanied by the development of large infrastructure projects. Data: Sentinel-2, 2023-02-27.

Niamey, Niger

Niamey, the capital city of Niger, has seen a remarkable population development over the years. Situated on the banks of the Niger River, the city has grown significantly since Niger gained independence in 1960. By the turn of the century, it had become one of the fastest-growing cities in Africa.

Several factors have contributed to Niamey's population boom, including improved health care services and educational opportunities. The most important factor is rural-to-urban migration. These factors have increased the city's overall population and have also influenced the age structure with its average age of 21 years. This youthful population is a resource for the city's development, offering workforce and potential for innovation. However, it also presents enormous challenges in terms of providing education, employment, and health care.

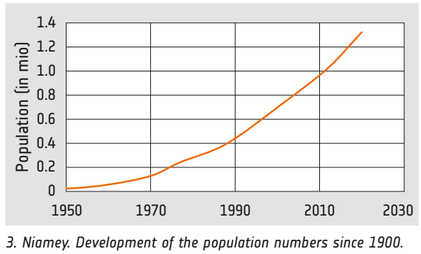

3. Niamey. Development of the population numbers since 1900. Note the sharp rise starting in the middle of the 20th century.

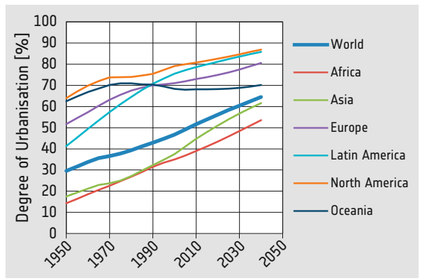

4. Recorded and prospected development of the degree of urbanisation in different parts of the world.

5. Niamey Bridge crossing the Niger River, one of the infrastructure projects of the city.

City development in China

The city of Suqian lies in the Jiangsu Province, East China, and is a typical example of the rapid urban development and growth in that country. Suqian's roots can be traced back to ancient times when it served as a transportation hub along the Grand Canal, connecting northern and southern China. Over the centuries, it evolved into a regional centre for trade and commerce.

In recent decades, Suqian has experienced an economic boom, which is reflected in the land use changes visible in the satellite images. The gross domestic product (GDP) grew from 1 billion Euro in 2000 to over 30 billion Euro in 2020. This growth has been driven by investments in industry, agriculture, and technology, with annual export values exceeding 20 billion Euro. The city's strategic location, excellent infrastructure, and business-friendly policies have attracted over 10,000 domestic and international enterprises.

Suqian has committed itself to sustainable development and green initiatives, including the establishment of over 800 square kilometres of forest coverage and the adoption of renewable energy sources, meeting 30% of its energy needs. Urban planning efforts have already resulted in a reduction in pollution levels and an increase in green spaces.

6. View of Suqian.

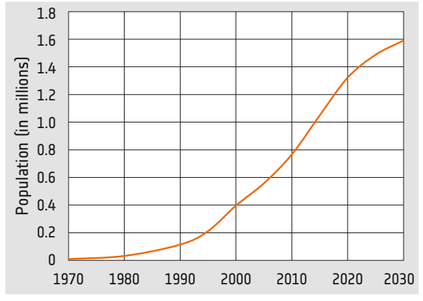

7. Suqian. Development of the population figures since 1970. The rapid growth started with the opening of China after 1990.

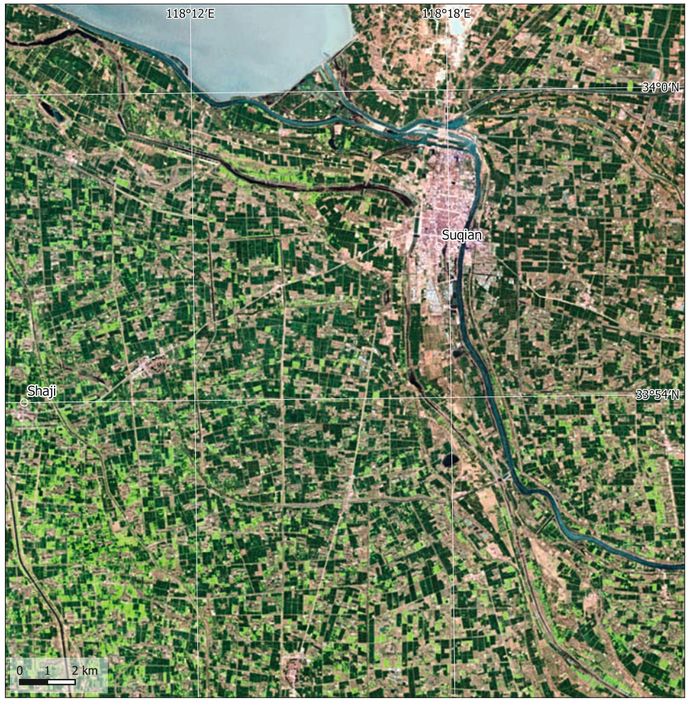

8. Suqian, China, in 1987. Data: Landsat 4, 1987-04-21.

9. Suqian, China, in 2023. Data: Sentinel-2, 2023-04-16.

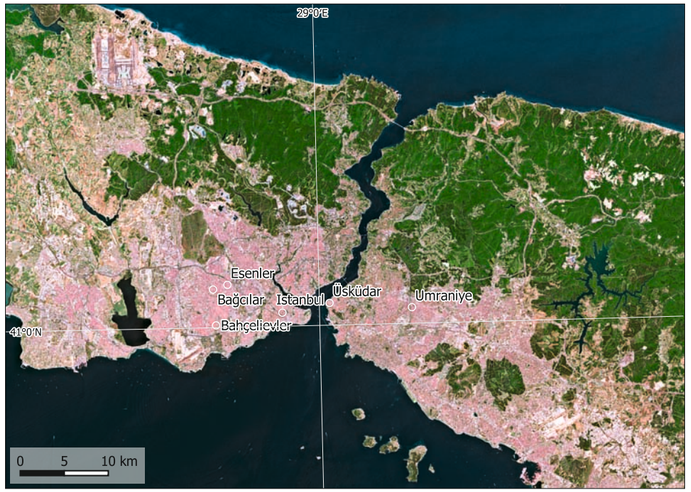

1. Overview satellite image map of the Bosporus and Istanbul, Türkiye. Data: Sentinel-2, 2023-07-23.

New Airport of Istanbul, Türkiye

Opened in 2019, the New Istanbul Airport has quickly become the busiest airport in Europe in terms of passenger traffic with more than 64 million passengers in 2022. The construction of the New Istanbul Airport was an enormous financial undertaking, costing over 10 billion Euros.

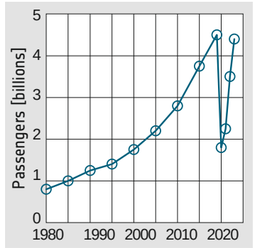

2. During the last decades, the global number of flight passengers has seen a significant increase. A short interruption of this development was caused by the Covid-19 pandemic of 2020/22.

The airport is designed for the long haul, with a potential capacity to serve more than 200 million passengers every year once it reaches full operation. This makes it one of the world's busiest airports, highlighting Istanbul's role as an important global travel and trade centre. The New Istanbul Airport is expected to have a profound economic influence and to make a substantial contribution to Turkey's growth. Additionally, it generates thousands of job opportunities directly and indirectly.

The satellite map shows the huge impact of the airport on the landscape. Located about 30 kilometres northwest of the city centre, the new airport has replaced forests and agricultural land on an area of almost 40 square kilometres. Additionally, the road network serving the airport was enhanced substantially.

3. Aerial view of the new Airport İstanbul Havalimanı, looking West.

4. Region northwest of Istanbul, Türkiye. True colour satellite image showing the forests and agricultural land before the construction of the new airport. Data: Landsat 5, 2010-09-18.

5. Construction site of the new Istanbul Airport in 2017. True colour satellite image highlighting the extent of the construction work. Data: Sentinel-2, 2017-07-24.

6. Istanbul Airport, Türkiye, in 2023. True colour satellite image map, data: Sentinel-2, 2023-07-23.

Suez Canal, Egypt

The Suez Canal is an artificial waterway connecting the Mediterranean Sea to the Red Sea. Opened in 1869, the canal dramatically shortened the maritime route between Europe and Asia, allowing ships to avoid the lengthy and hazardous journey around Africa. The canal's strategic location has made it a vital link between the East and the West, contributing significantly to global commerce.

In March 2021, the Ever Given, a container ship measuring 400 metres in length and capable of carrying over 20,000 containers, ran aground in the southern section of the canal due to adverse weather conditions. This led to the temporary closure of the canal, causing a significant disruption to the global supply chains. Optical and radar satellites captured the Ever Given, blocking the entire canal, and the traffic jam caused by the accident for ships waiting at the entrances to the canal.

7. Suez, Egypt, with the southern end of Suez Canal, on 2021-03-29. The true colour satellite image shows the container vessel Ever Given stuck in the canal, blocking all traffic. Data: Sentinel-2.

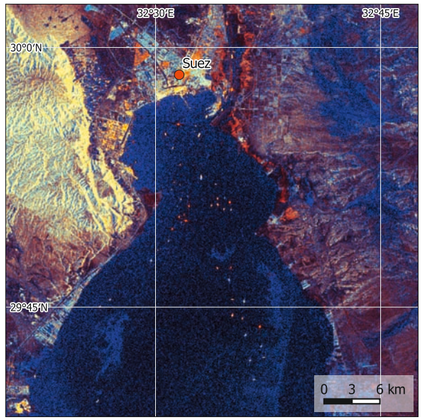

8. Radar image of Suez, Egypt, with the southern end of Suez Canal on 2021-03-21. The image shows normal traffic through the canal and only a few waiting vessels. Data: Sentinel-1.

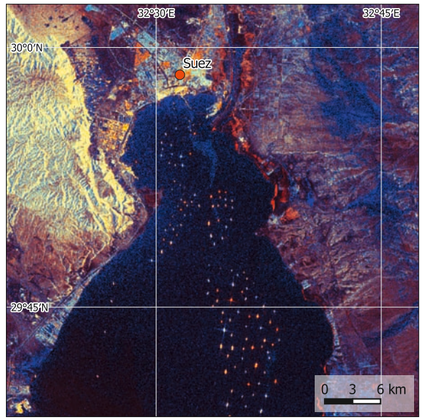

9. Radar image of Suez, Egypt, with the southern end of Suez Canal on 2021-03-27. A traffic jam has built up due to the blocking of the canal. Data: Sentinel-1.

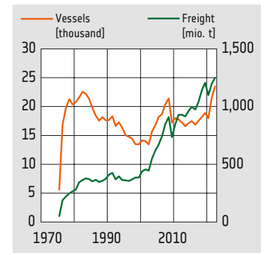

10. The increasing importance of international traffic is reflected by the development of the transport of goods through the Suez Canal. At the same time, the number of vessels passing the canal has changed much less, because larger vessels have been used.

11. The Ever Given, a container vessel of the Evergreen shipping company. With its length of almost 400 metres it is one of the world's largest container ships and can transport more than 20,000 standard containers.

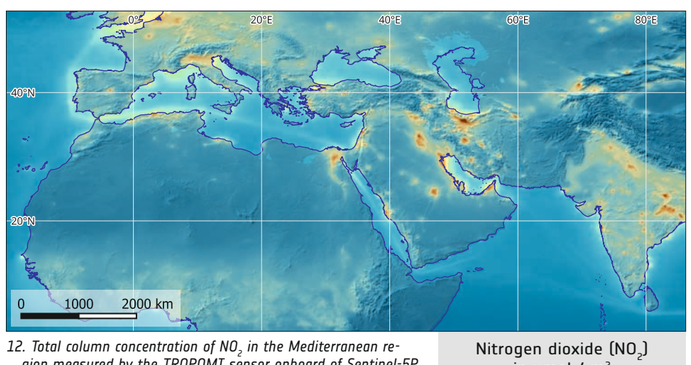

12. Total column concentration of NO_2 in the Mediterranean region measured by the TROPOMI sensor onboard of Sentinel-5P. NO_2 is produced by combustion processes in industry and traffic. The combustion gases of ships are visible as a faint band of NO_2 around the Iberian peninsula and continuing eastwards.

ANTHROPOSPHERE

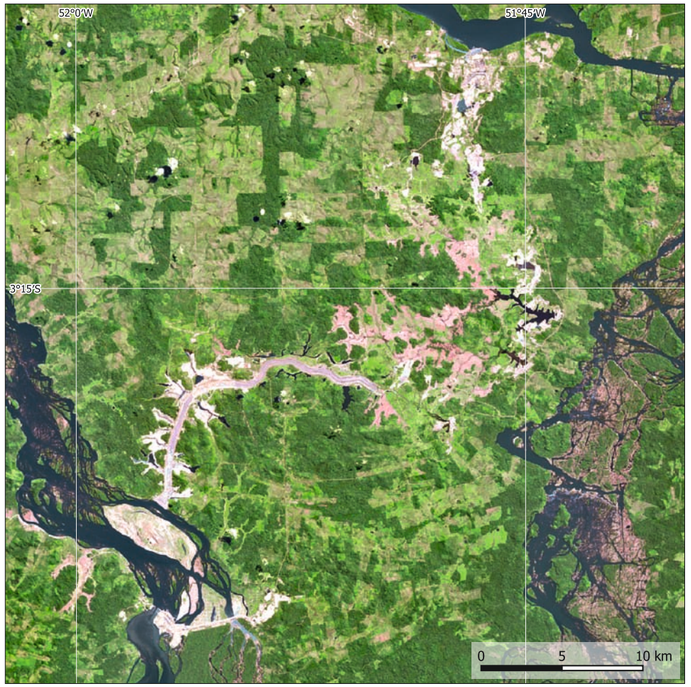

1. Construction works along the Rio Xingu near Altamira in 2015. Data: Landsat 5, 2015-07-15.

2. Rio Xingu near Altamira in 2011. True colour satellite image showing the forests and agricultural land before the construction of the dam. Data: Landsat 5, 2011-07-27.

3. Rio Xingu near Altamira after completion of the dam. True colour satellite image showing water bodies, forests, and agricultural land. Data: Sentinel-2, 2017-07-28.

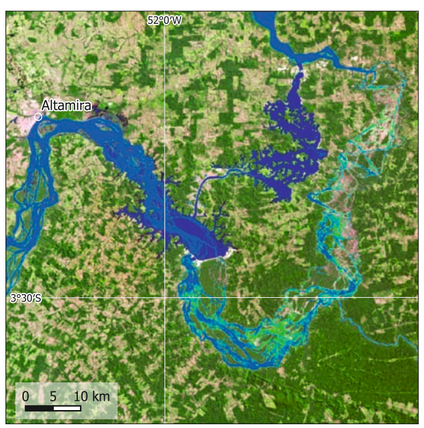

4. Rio Xingu near Altamira after completion of the dam. The overlay shows the new water surfaces (blue) and the water courses fallen dry (light green). True colour satellite image, data: Sentinel-2, 2017-07-28.

Hydropower — Belo Monte Dam, Brazil

The Belo Monte Power Station in Brazil's northern state of Pará is one of the largest hydroelectric power plants in the world. Its construction began in 2011 and was completed in 2019. The power station is using the water of the Xingu River, a major tributary of the Amazon River. The total installed capacity of more than 11,000 megawatts (MW) is enough to supply electricity to over 60 million people. The power station has 18 power generating units, each with a capacity of 611 MW.

The construction of the Belo Monte Power Station has been highly controversial. Environmentalists and indigenous groups have raised concerns about the impact of the power station on the local ecosystem and on the livelihoods of the indigenous people in the area. The construction of the power station involved the flooding of a large area of forest and the displacement of thousands of people. Moreover, the changed water regime has impacted the ecosystem of Rio Xingu below the dam. Despite these concerns, the Brazilian government has defended the construction of the Belo Monte Power Station as necessary to meet the country's energy needs and to promote economic development. The power station has also been promoted as a way to reduce Brazil's dependence on fossil fuels and to help combat climate change.

5. View of the Belo Monte powerhouse during construction.

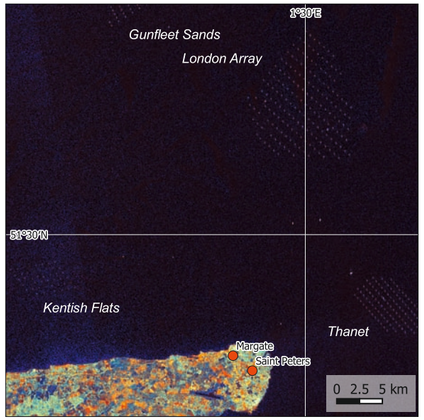

6. Radar image of windfarms in the Thames estuary. Data: Sentinel-1, 2024-03-02.

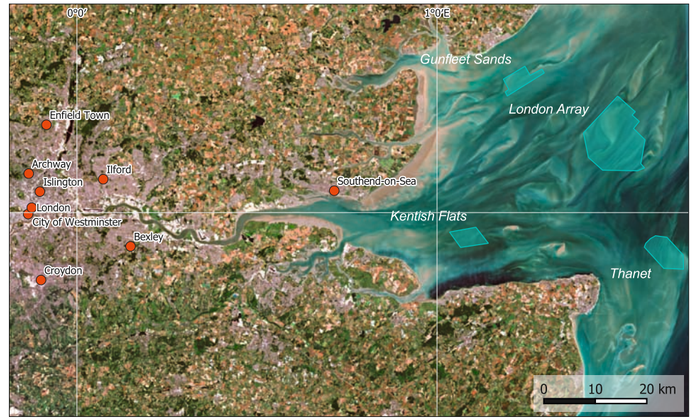

7. Overview satellite image of the Thames estuary with its offshore windfarms. Data: Sentinel-2, 2023-07-07.

Harvesting wind energy over the sea

The Thames Estuary, located in southeastern England, has become a prominent site for the installation of offshore wind farms. These wind farms exploit the strong and consistent wind currents present in the estuary.

Their proximity to densely populated areas like London ensures efficient distribution of generated electricity, minimizing transmission losses. Secondly, the offshore location reduces visual and noise pollution compared to onshore wind farms. Offshore wind farms contribute to the renewable energy targets, helping to reduce carbon emissions and combat climate change. The development of wind farms in the Thames Estuary also poses challenges, including potential impacts on marine ecosystems and wildlife habitats.

From lignite mining to solar energy production

Situated in the German state of Saxony, the solar farm near Böhlen (Solarpark Böhlen) uses solar radiation to generate clean and sustainable electricity. As the largest of its kind in Germany, the solar power plant comprises photovoltaic (PV) panels that convert sunlight directly into electrical energy. The installation covers approximately 100 hectares of an abandoned open-pit lignite mine, hosting over 300,000 photovoltaic panels. With a total installed capacity exceeding 100 megawatts (MW), this facility is capable of generating enough clean electricity to power over 30,000 homes.

The installation of the solar power plant near Böhlen aligns with Germany's ambitious *Energiewende* (energy transition) goals, aiming to shift away from fossil fuels towards renewable sources.

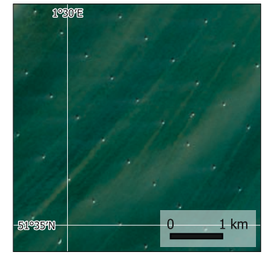

8. Detail of the Sentinel-2 image of the London Array windfarm. The tidal currents stir up sediments.

9. The region south of the German city of Leipzig has seen intensive open pit lignite mining, which has shaped the landscape. Parts of the former mining areas have been recultivated and transformed into recreational zones. Sentinel-2, 2017-05-27.

10. A part of the area of a former lignite mine now hosts a solar power plant (Solarpark Böhlen), others parts are used as recreational areas. Data: Sentinel-2, 2024-01-28.

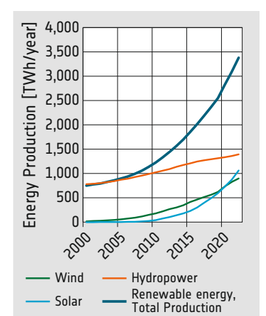

11. The global production of electric energy from renewable sources, especially from wind and solar energy, is growing quickly.

A

absorption – The process in which radiant energy is retained by a substance.

active system (active sensor) – A remote-sensing system that transmits its own radiation to detect an object or area for observation and receives the reflected or transmitted radiation. Example: radar.

aerosol – A colloid of solid or liquid particles suspended in a gas (e.g. smoke, fog).

albedo – The ratio of the outgoing solar radiation reflected by an object to the incoming solar radiation incident upon it.

altimeter – An active instrument used to measure the altitude of a satellite above a fixed level. Coupled with exact orbit knowledge this enables determination of the topography.

amplitude – The magnitude of the displacement of a wave from a mean value. For a simple harmonic wave, it is the maximum displacement from the mean.

apogee – Point of the elliptic orbit of a satellite where its distance from the Earth is maximal.

aquatic – related to water.

aquaculture – Cultivation of aquatic organisms, i.e. breeding, raising, and harvesting fish, shellfish, and aquatic plants.

Ariane – Launch vehicles developed for ESA by a subsidiary of the European Aeronautic Defence and Space Company (EADS) and launched from the Kourou Space Centre in French Guyana.

arid – Dry. A climate sub-type in which there is a severe excess of evaporation over precipitation.

ASAR *(Advanced Synthetic Aperture Radar)* – a radar sensor on the satellite ENVISAT operating in C-band.

ASTER *(Advanced Spaceborne Thermal Emission and Reflection Radiometer)* – An imaging instrument on NASA's Terra. ASTER is used to obtain detailed maps of land surface temperature, emissivity, reflectance, and elevation.

atmospheric windows – The range of wavelengths at which the atmospheric gases only slightly absorb radiation. Atmospheric windows allow the Earth's radiation to escape into space unless clouds absorb the radiation.

attenuation – The decrease in the power of a signal in transmission. Attenuation may be expressed in decibels, and can be caused by interferences such as rain, clouds, or radio frequency signals.

AVHRR *(Advanced Very High Resolution Radiometer)* – A five-channel scanning instrument that quantitatively measures electromagnetic radiation on NOAA environmental satellites. Determines cloud cover and surface temperature. Visible and infrared detectors observe vegetation, clouds, lakes, shorelines, snow, and ice.

azimuth – The direction, in degrees referenced to true north, that an antenna must be pointed to receive a satellite signal. The angular distance is measured in a clockwise direction.

B

backscatter – Process by which up to 25% of radiant energy from the sun is reflected or scattered away from the surface by clouds.

band – A region of the electromagnetic spectrum to which a remote sensor responds; a multispectral sensor makes measurements in a number of spectral bands.

bandwidth – The total range of frequency required to pass a specific modulated signal without distortion or loss of data.

bathymetry – Mapping the topography of the ocean floor.

biodiversity – biological diversity, variety of all living things and their interactions in an area.

biomass – ecology: total mass of living biological organisms in a given area or ecosystem; energy production: biological mass used as a renewable energy source.

Biomass – Part of the Earth Explorer Mission of ESA, created to observe and analyse the world's forests using radar technology.

C

calibration – Act of comparing an instrument's measuring accuracy to a known standard.

C-Band – part of the electromagnetic microwave spectrum between 500 MHz and 1000 MHz.

chlorophyll – Molecule in green plants giving them their colour. It allows plants to absorb energy from the sun as they undergo the process of photosynthesis.

climate – Average weather conditions for a particular location over a long period of time, e.g. 30 years.

climate change – Long-term shifts in temperatures and weather patterns due to natural or man-made effects.

climate model – Computer model to calculate and project the climate for a specific period.

Copernicus – former name GMES *(Global Monitoring for Environment and Security)*, the EU's Copernicus Earth observation programme.

CryoSat – ESA research satellite mapping the Earth's cryosphere and collecting data in particular on the volume of the ice sheets in the Arctic and Antarctic (since 2010).

D

declination – The angular distance from the equator to the satellite.

degradation – Decline of the value of a biophysical environment due to human-induced processes.

delta – Triangularly shaped river mouth formed by sediments carried by the river.

demography – statistical study of human populations (size, ethnic composition, ages), and of their changes.

digital elevation model (DEM) – A representation of the topography of the Earth in digital format, i.e. by coordinates and numerical descriptions of altitude.

diurnal – In a daily cycle.

DMSP *(Defense Meteorological Satellite Program)* – U.S. Air Force meteorological satellite program with satellites circling in sun-synchronous orbit. Imagery is collected in the visible- to near-infrared band (0.4 to 1.1 µm) and in the thermal-infrared band (about 8 to 13 µm) at a resolution of about 3 km.

Dobson Unit (DU) – The standard unit for ozone amounts in the atmosphere. One DU is 2.7 x 1016 ozone molecules per cm² and refers to a layer of ozone that would be 0.001 cm thick under conditions of standard temperature (0°C) and pressure.

E

EAC – European Astronaut Centre, Cologne; central ESA facility for training astronauts.

EarthCARE – Scheduled space mission to research aerosols and clouds and their impact on radiation in the Earth's atmosphere, as part of the Living Planet Programme of the ESA. Launch date: 2024.

Earth Explorer – An ESA mission and part of the Living Planet Programme, which comprises the satellite missions providing new observation data on the Earth.

Earth observation satellite – Satellites observing the Earth from space.

eccentricity *e* – Describes the shape of an orbit. The satellite orbit is an ellipse, with eccentricity defining the shape of the ellipse. When *e* = 0, the ellipse is a circle. When *e* is near 1, the ellipse is very long and skinny.

electromagnetic radiation – Energy propagated as time-varying electric and magnetic fields at the speed of light. Light and radar are examples of electromagnetic radiation differing only in their wavelengths (or frequency).

electromagnetic spectrum – The entire range of radiant energies or wave frequencies from the longest to the shortest wavelengths. The spectrum usually is divided into seven sections: radio, microwave, infrared, visible, ultraviolet, x-ray, and gamma-ray radiation.

elliptical orbit – Bodies in space orbit in elliptical rather than circular orbits because of factors such as gravity and drag. The point where the orbiting satellite is closest to Earth is the perigee, the point where the satellite is farthest from Earth is called apogee.

emissivity – The ratio of the radiation emitted by a surface to that emitted by a black body at the same temperature.

Enhanced Thematic Mapper Plus (ETM+) – An eight-band multispectral scanning radiometer onboard the Landsat 7 satellite that provides high-resolution imaging information of the Earth's surface.

Envisat *(Environmental Satellite)* – ESA satellite mission, 2002-2012; large platform monitoring the environmental changes on Earth and in the atmosphere, scientific mission to study Earth observation applications.

equatorial – Region near the equator.

erosion – Surface processes (e.g. water flow or wind) removing soil, rock, or dissolved material from the Earth's crust and transporting it to another location where it is deposited.

ERS *(European Remote Sensing Satellite)* – two radar satellites operated by ESA, 1991-2011, precursors to Sentinel-1.

ESA – European Space Agency

ESOC – European Space Operations Centre

ESRIN – European Space Research Institute

ESTEC – European Space Research and Technology Centre

extensive (farming) – Agricultural production system that uses small inputs of labour, fertilizers, and capital, and producing small output relative to the land area being farmed.

F

false-colour – A colour imaging process which produces an image of a colour that does not correspond to the true or natural colour of the scene (as seen by our eyes).
far infrared (FIR) – Electromagnetic radiation, longer than the thermal infrared, with wavelengths between about 25 and 1000 micrometres.

field of view – The range of angles that are scanned or sensed by a system or instrument, measured in degrees of arc.

fluvial – Related to rivers.

Fraction of Photosynthetically Active Radiation (FPAR) – Radiation between 400 and 700 nm used by the green canopy in the photosynthetic process.

frequency *f* – Number of cycles and parts of cycles completed per second; $f = 1/T$, where T is the length of one cycle in seconds.

freshwater – Liquid or frozen water containing low concentrations of salts and other dissolved solids.

gross domestic product (GDP) – Monetary value of final goods and services produced in a country in a given period of time (e.g. a year), a measure of the economic power of a country.

G

Galileo – European satellite navigation system, consisting of 30 satellites in 3 orbits.

gamma ray – High energy electromagnetic radiation, especially as emitted by a nucleus in a transition between two energy levels.

geocoding – One element of georeferencing, where data with no georeference are translated into the desired reference system.

Geographic Information System (GIS) – A system for archiving, retrieving, and manipulating data that has been stored and indexed according to the geographic coordinates of its elements. The system generally can utilize a variety of data types, such as imagery, maps, table, etc.

geomorphology – study of the origin and evolution of topographic and bathymetric features generated by processes operating at or near Earth's surface.

geostationary – Describes an orbit in which a satellite is always in the same position with respect to the rotating Earth. The satellite travels around the Earth in the same direction, at an altitude of approximately 35,790 km because that produces an orbital period equal to the period of rotation of the Earth. Used for weather satellites and most commercial telecommunications satellites.

geosynchronous – Synchronous with respect to the rotation of the Earth.

GOES *(Geostationary Operational Environmental Satellite)* – Observes the U.S. and adjacent ocean areas from vantage points 35,790 km above the equator at 75 degrees west and 135 degrees west. GOES satellites have an equatorial, Earth-synchronous orbit with a 24-hour period, a visible resolution of 1 km, and an IR resolution of 4 km.

GPS *(Global Positioning System)* – A system consisting of 25 satellites in 6 orbital planes at 20,000 km altitude with 12 hr periods, used to provide highly precise position, velocity and time information.

GOME *(Global Ozone Monitoring Experiment)* – Instrument aboard ERS.

greenhouse gas – Gaseous substances in the atmosphere affecting radiation and contributing to the warming of the Earth's atmosphere, known as the greenhouse effect.

ground resolution – Describes the length of the side of a single square pixel in an image. The smaller this value is, the more precise and detailed the image.

ground track – The inclination of a satellite, together with its orbital altitude and the period of its orbit, creates a track defined by an imaginary line connecting the satellite and the Earth's centre.

H

hotspot – Area of the Earth's mantle from which hot plumes rise upward, forming volcanoes on the overlying crust.

I

inclination – Inclination is the angle between a satellite orbit and the equator.

indigenous – Group of people native to a specific region.

infrared radiation (IR) – Infrared is electromagnetic radiation with wavelengths from about 0.7 to 1000 µm (between visible and microwave radiation), subdivided into visible and near-infrared, mid-infrared and far infrared.

interferometry – Data analysis method exploiting the phase difference between two optical beams; used e.g. to derive elevation differences or changes.

ISS *(International Space Station)* – A joint project between 16 countries designed as a scientific laboratory in space.

K

Ku-band – Radar and microwave band in which the wavelengths vary between 1.67 and 2.4 cm.

L

land cover – The characteristics of a land surface as determined by its spectral signature (the unique way in which a given type of land cover reflects and absorbs light).

Landsat – Land Remote-Sensing Satellite, operated by the U.S. Earth Observation Satellite Company (EOSAT). Commercialized under the Land Remote-Sensing Commercialisation Act of 1984, Landsat is a series of satellites (formerly called ERTS) designed to gather data on the Earth's resources in a regular and systematic manner.

land use – The characteristics of a land surface as determined by its use (the unique way in which a given type of land is – or is not – exploited by man).

M

MERIS *(Medium Resolution Imaging Spectrometer)* – Instrument aboard Envisat for the observation of the ocean and vegetation.

METEOSAT *(METEOrological SATellite)* – Europe's geostationary weather satellite, launched by the European Space Agency and operated by Eumetsat.

microwave – Electromagnetic radiation with wavelengths between about 1000 µm and 1 m.

middle infrared (MIR) – Electromagnetic radiation between the near infrared and the thermal infrared, about 2-5 µm.

MODIS *(Moderate-resolution Imaging Spectroradiometer)* – Sensor flying aboard Terra and viewing the entire surface of the Earth every 1-2 days, making observations in 36 spectral bands, at moderate resolution (0.25 – 1 km), of land and ocean surface temperature, primary productivity, land surface cover, clouds, aerosols, water vapor, temperature profiles, and fires.

multispectral – Comprising data from different spectral bands.

Multispectral Scanner (MSS) – A line-scanning instrument flown on Landsat satellites that continually scans the Earth in a 185 km swath. On Landsat 1, 2, 4, and 5, the MSS had four spectral bands in the visible and near-infrared with an IFOV of 80 metres. Landsat-3 had a fifth band in the thermal infrared with an IFOV of 240 metres.

multitemporal – Comprising data from different points in time.

N

NASA *(National Aeronautics and Space Administration)* – NASA, established in 1958 with Headquarters in Washington D.C., is the agency responsible for the public space program of the USA. Its mission is to plan, direct, and conduct aeronautical and space activities.

NDVI *(normalized difference vegetation index)* – A method for converting satellite-based measurements into surface vegetation types. The NDVI uses a complex ratio of reflectance in the red and near-infrared portions of the spectrum to accomplish this. It is a quantity that measures greenness and vigour of vegetation.

near infrared (NIR) – Electromagnetic radiation with wavelengths from just longer than the visible (about 0.7 µm) to about 2 µm.

NOAA *(National Oceanic and Atmospheric Administration)* – NOAA was established in 1970 within the U.S. Department of Commerce. It is focused on the conditions of the oceans and the atmosphere. The two main components are the NWS *(National Weather Service)* and NESDIS *(National Environmental Satellite, Data, and Information Service).*

O

ocean colour – The ability of phytoplankton to appear as different colours in certain bands of the electromagnetic spectrum because of their chlorophyll concentrations.

Operational Land Imager (OLI) – Multispectral imaging sensor on board Landsat 8 and 9.

orbit – The path described by a heavenly body in its periodic revolution. Earth satellite orbits with inclinations near 0° are called equatorial orbits because the satellite stays nearly over the equator. Orbits with inclinations near 90° are called polar orbits because the satellite crosses nearly over the north and south poles.

orbital plane – An imaginary gigantic flat plane containing an Earth satellite's orbit. The orbital plane passes through the centre of the Earth.

P

panchromatic – Sensitive to all or most of the visible spectrum.

passive microwave radiometer – A system sensing only microwave radiation emitted by the object being viewed or reflected by the object from a source other than the system.

passive system – A system sensing only radiation emitted by the object being viewed or reflected by the object from a source other than the system.

payload – The instruments that are accommodated on a spacecraft.

perigee – The point of an orbit where a satellite is closest to the Earth.

period – Time required for a satellite to make one complete orbit.

phytoplankton – Plant-like components of the plankton community forming a key part of ocean and freshwater ecosystems.

pixel – 'Picture element', ground area corresponding to a single element of a digital image data set.

platform – A satellite that can carry instruments.

polar orbit – An orbit with an orbital inclination of near 90° where the satellite ground track will cross both polar regions once during each orbit.

GLOSSARY

pollutant – substance that pollutes something, especially water, the atmosphere, or soil.

precipitation – Water falling from the atmosphere to the ground in liquid (rain) or solid (snow, hail) form.

PROBA *(Project for On-Board Autonomy)* – small scale technology demonstration satellite of ESA, carrying several Earth observation instruments with ground resolutions down to 20 m (CHRIS, multispectral) and 5 m (HRV, panchromatic).

R

radar interferometry – The study of interference patterns caused by radar signals; a technique that enables scientists to generate three dimensional images of the Earth's surface.

radiation – Energy transfer in the form of electromagnetic waves or particles that release energy when absorbed by an object.

radiation budget – A measure of inputs and outputs of radiative energy relative to a system, such as Earth.

reflectance – The proportion of irradiated electromagnetic radiation reflected by a surface.

reflection – The return of light or sound waves from a surface. If a reflecting surface is plane, the angle of reflection of a light ray is the same as the angle of incidence.

remote sensing – The technology of acquiring data and information about an object or phenomena by a device without physical contact. Earth remote sensing refers to gathering information about the Earth and its environment from a distance.

repetition rate (orbital period) – Time required for a satellite to complete one orbit.

resolution – In the case of imagery, it describes the area represented by each pixel of an image. The smaller the area represented by a pixel, the more accurate and detailed the image.

runoff – Draining away of water or substances carried in it from the surface of an area.

S

SAR *(synthetic aperture radar)* – A high-resolution ground-mapping technique that effectively synthesizes a large receiving antenna by processing the phase of the reflected radar return.

salination – Increase of the salt concentration in soils, reducing their fertility.
salinity – Salt content of (ocean) water or soil.

satellite – A free-flying object orbiting the Earth, another planet, or the sun.

satellite image map – Map created on the basis of satellite image data.

saturation – State of a system, such as a solution, containing as much of another substance, such as a solute, as is possible at a given temperature.

S-band – Frequency range from 4 to 2 GHz (7 to 20 cm wavelength) within the microwave (radar) portion of the electromagnetic spectrum. S-band radars are used for medium-range meteorological applications, e.g. rainfall measurements.

scanning radiometer – An imaging system consisting of lenses, moving mirrors, and solid-state image sensors used to obtain observations of the Earth and its atmosphere.

scattering – The process by which electromagnetic radiation interacts with and is redirected by the molecules of the atmosphere, ocean, or land surface.

scatterometer – A high-frequency radar instrument that transmits pulses of energy towards the ocean and measures the backscatter from the ocean surface. It detects wind speed and direction over the oceans by analysing the backscatter from the small wind-induced ripples on the surface of the water.

scene – Object space illuminated by a sensor.

sea surface temperature (SST) – The temperature of the layer of seawater (approx. 0.5 m deep) near the surface.

sedimentation – Deposition of sediments such as sand or silt transported by water, wind, or glaciers.

sensor – Device producing an output in response to incident radiation. Sensors aboard satellites obtain information about features and objects on Earth by detecting radiation reflected or emitted in different bands of the electromagnetic spectrum.

Sentinel – Series of Earth Observation satellites under responsibility of ESA in the Copernicus programme.

shortwave radiation – The radiation received from the sun and emitted in the spectral wavelengths less than 4 µm. It is also called solar radiation.

SMOS *(Soil Moisture and Ocean Salinity Mission)* – ESA's second Earth Explorer Opportunity mission to gather global observation data for the modelling of weather, climate and ocean currents.

soil – biologically active, porous medium that covers the uppermost layer of Earth's crust.

solar constant – The constant expressing the amount of solar radiation reaching the Earth from the sun, approximately 1370 W/m².

solar radiation – Energy received from the sun. The energy comes in many forms, such as visible light. Other forms of radiation include radio waves, infrared, ultraviolet waves, and x-rays.

spectral band – A finite segment of wavelengths in the electromagnetic spectrum.

spectral signature – This refers to the particular form or shape evinced by the power spectrum calculated from the data comprising the time series of a process.

SPOT *(Systeme Pour l'Observation de la Terre)* – French, polar-orbiting Earth observation satellites with ground resolution of 10 m. SPOT images are available commercially and are intended for such purposes as environmental research and monitoring or ecology management.

SRTM *(Shuttle Radar Topography Mission)* – A Space Shuttle mission that used C-band and X-band interferometric synthetic aperture radars (IFSARs) to acquire topographic data over 80% of Earth's land mass (between 60°N and 56°S) in February 2000.

sun-synchronous – A sun synchronous orbit is a nearly polar orbit. Every time it crosses the Equator, it does it at the same local time.

sustainability – Meeting the needs of the present without compromising the ability of future generations to meet their needs.

Sustainable Development Goals (SDGs) – call to action adopted by the United Nations in 2015 to protect the planet and improve the lives and prospects humanity.

Swarm – Earth Explorer Mission of the ESA, to observe the magnetic field of the Earth.

swath – The area observed by a satellite as it orbits the Earth.

T

tectonic – related to processes that result in the structure and properties of the Earth's crust and its evolution through time.

terrestrial radiation – The total infrared radiation emitted by the Earth and its atmosphere in the temperature range of approximately 200-300 K.

Thematic Mapper (TM) – Multispectral imaging sensor with 7 spectral bands on board of Landsat 4 and Landsat 5, acquiring data in the visible and infrared parts of the electromagnetic spectrum. The ground resolution of the visible and short-wave infrared bands is 30 m/pixel, the thermal band 120 m/pixel.

thermal infrared (TIR) – Electromagnetic radiation with wavelengths between 3 and 25 µm.

toxin – Naturally occurring poisonous substance produced by living cells or organisms, e.g. algae.

TRMM *(Tropical Rainfall Measuring Mission)* – Satellite programme launched by NASA and NASDA in 1997 to acquire data on tropical precipitation.

U

ultraviolet radiation (UV) – Part of the electromagnetic spectrum with wavelengths below the violet region; it contains about 5% of the energy radiated by the sun and is the main source of energy in the stratosphere and in the mesosphere.

urbanisation – Increase in the proportion of people living in towns and cities due to people moving from rural areas to urban areas.

USGS *(United States Geological Survey)* – US American office responsible for the acquisition and distribution of geoinformation.

V

VHR *(Very High Resolution)* – Earth observation data with a ground resolution of 1 m and better.

VISSR *(Visible/Infrared Spin Scan Radiometer)* – Multispectral imagining system with high resolution, deployed onboard of GOES weather satellites (until GOES-7).

visible light – The part of the electromagnetic spectrum visible to the human eye (0.4 µm to 0.7 µm).

W

water vapour – water in its gaseous state; in the atmosphere the most important factor of the natural greenhouse effect.

wave – Moving changes of a parameter, periodical in space and time, e.g. electromagnetic radiation.

wavelength – Distance between two maxima of a wave.

weather satellite – Earth observation satellite that observes meteorological processes.

X

X-band – Radar frequency band between 12.5 and 8 GHz (wavelength 2,4-3,75 cm).

GEOGRAPHICAL INDEX

IMAGE AND DATA SOURCES

8.1: ESA • **8.2** *[Modis | Mosaic]*: NASA Goddard Space Flight Center • **8.3**, **9.4**: ESA • **9.5**: ESA - Harwell Campus • **9.6**: ESA • **9.7**: ESA - A. Van Der Geest • **9.8**: ESA • **9.9**: ESA - Philippe Sebirot • **9.10**: ESA - Stephane Corvaja • **9.11**, **9.12**, **10.1**: ESA • **10.2**: ESA/D. Ducros • **10.3**: ESA/DLR/FU Berlin (G. Neukum) • **10.4**: NASA, ESA, CSA, STScI, J. Diego (Instituto de Física de Cantabria, Spain), J. D'Silva (U. Western Australia), A. Koekemoer (STScI), J. Summers & R. Windhorst (ASU), and H. Yan (U. Missouri) • **10.5**: ESA/ATG medialab • **11.6**: ESA/CNES/Arianespace • **11.7**: ESA/David Ducros, Jacky Huart • **11.8**, **12.1** *[GOCE | Mosaic]*: ESA • **12.2** *[Aeolus | 06.05.2020]*: ESA/VirES • **12.3** *[SMOS | 01.09.2023]*: ESA CCI/Climate from Space • **12.4**, **13.5**, **13.6**, **13.7**, **14.1**, **14.1**, **14.1**: ESA • **14.2**: Copernicus • **15.7**: ESA/P. Carril • **15.3a**: ESA/ATG medialab • **15.3b** *[Sentinel-1 | 06.02.2024]*: Copernicus • **15.4a**: ESA • **15.4b** *[Sentinel-2 | 08.07.2023]*: Copernicus • **15.5a**: ESA • **15.5b** *[Sentinel-3 | 08.06.2023]*: Copernicus • **15.6a**: ESA/P. Carril • **15.6b** *[Sentinel-5P | 08.07.2023]*: Copernicus • **16.1**: eoVision • **16.2**: Union of Concerned Scientists • **16.3**: ESA • **17.4**, **17.5**, **18.4**: eoVision/ESA • **18.1a** *[Sentinel-2 | 21.03.2022]*, **18.1b** *[Sentinel-2 | 21.03.2022]*, **18.1c** *[Sentinel-2 | 21.03.2022]*, **18.1d** *[Sentinel-2 | 21.03.2022]*, **18.1e** *[Sentinel-2 | 21.03.2022]*, **18.2a** *[Sentinel-2 | 21.03.2022]*, **18.2b** *[Sentinel-2 | 21.03.2022]*, **18.3a** *[Sentinel-2 | 21.03.2022]*, **18.3b** *[Sentinel-2 | 21.03.2022]*, **18.3c** *[Sentinel-2 | 21.03.2022]*, **19.5** *[Sentinel-1 | 23.03.2022]*, **19.6** *[Sentinel-1 | 23.03.2022]*, **19.7** *[Sentinel-1 | 23.03.2022]*, **19.8** *[Sentinel-1 | 23.03.2022]*: Copernicus • **19.9**: eoVision/ESA • **20.1** *[Sentinel-2 | 21.03.2022]*, **20.2** *[Sentinel-2 | 21.03.2022]*, **20.3** *[Sentinel-2 | 21.03.2022]*, **20.4** *[Sentinel-2 | 21.03.2022]*: Copernicus • **21.5** *[Modis | Mosaic]*, **21.6a** *[Modis | Mosaic]*, **21.6b** *[Modis | Mosaic]*, **21.6c** *[Modis | Mosaic]*, **21.6d** *[Modis | Mosaic]*: NASA Goddard Space Flight Center • **21.7a**: BEV • **21.7b** *[Sentinel-2 | 19.06.2023]*: Copernicus • **21.7c**: BEV • **22.1** *[Modis | Mosaic]*: NASA Goddard Space Flight Center • **22.2** *[DMSP OLS | Mosaic]*: NASA/NOAA/USGS • **22.3** *[07.12.1972]*: Ron Evans/Harrison Schmitt, NASA • **22.4** *[Modis | Mosaic]*, **24.1** *[Modis | Mosaic]*: NASA Goddard Space Flight Center • **24.2** *[Sentinel-2 | 02.08.2023]*: Copernicus • **24.3** *[Modis | Mosaic]*: NASA Goddard Space Flight Center • **25.4**: eoVision, based on work of American Museum of Natural History • **25.5**: eoVision, based on work by Hannes Grobe • **25.6** *[Sentinel-2 | 26.08.2023]*: Copernicus • **25.7** *[Modis | Mosaic]*: NASA Goddard Space Flight Center • **26.1**: USGS • **26.2** *[Sentinel-2 | 22.10.2023]*: Copernicus • **26.3**, **26.3**, **26.4**, **26.4**, **27.5**: USGS • **27.5** *[Sentinel-2 | 24.09.2023]*, **27.6** *[Sentinel-2 | 24.09.2023]*, **27.7**: Copernicus • **27.8**, **27.9** *[Landsat 7 | 06.06.2000]*: USGS • **28.1** *[Sentinel-2 | June 2022]*, **28.2** *[Sentinel-2 | 03.06.2022]*, **28.3** *[Sentinel-2 | 21.06.2022]*, **28.4** *[Sentinel-5P | 21.06.2022]*: Copernicus • **28.5**: Branca, S., M. Coltelli, G. Groppelli and F. Lentini (2011). Geological map of Etna Volcano • **28.6**: gnuckx • **29.7** *[Sentinel-2 | 21.08.2021]*, **29.8** *[Sentinel-2 | 30.09.2021]*, **29.9** *[Sentinel-2 | 03.01.2022]*, **29.10** *[Sentinel-2 | 03.01.2022]*: Copernicus • **29.11**: eoVision • **29.12** *[Modis | Mosaic]*: NASA; Carracedo et al. 1998 • **29.13** *[Sentinel-2 | 21.08.2021]*, **30.1** *[Sentinel-2 | 15.06.2023]*: Copernicus • **30.2** *[Landsat 5 | 05.06.1992]*: USGS • **30.3**: Tzorn • **30.4** *[2022]*: Boliden Summary Report • **30.5** *[2024]*: USGS, Mineral Commodity Summaries 2024 • **31.6** *[Landsat 5 | 03.09.2011]*: USGS • **31.7** *[Sentinel-2 | 03.06.2023]*, **31.8** *[Sentinel-1 | 25.05.2023]*, **31.9** *[Sentinel-2 | 03.06.2023]*: Copernicus • **31.10**: Jason Houston (iLCP Redsecker Response Fund/CEES/CINCIA) • **32.1** *[Sentinel-2 | 15.08.2023]*, **32.2** *[Sentinel-2 | 01.07.2020]*: Copernicus • **32.3** *[Landsat 5 | 22.08.2010]*, **32.4** *[Landsat 5 | 28.07.2001]*, **32.5** *[Landsat 4 | 12.06.1990]*: USGS • **32.6**: Copernicus • **32.7**: Energy Institute - Statistical Review of World Energy (2023) • **33.8** *[Landsat 4 | 25.01.1985]*, **33.9** *[Landsat 5 | 03.01.2000]*: USGS • **33.10** *[Sentinel-2 | 18.01.2023]*: Copernicus • **33.11**: Energy Institute - Statistical Review of World Energy (2023) • **33.12** *[Sentinel-2 | 18.01.2023]*: Copernicus • **34.1** *[Multisensor | January 2023]*: Copernicus Marine Service/OSTIA • **34.3** *[Multisensor | 25.12.2015]*, **34.4** *[Multisensor | 25.12.2011]*: Copernicus/ESA SST CCI • **35.2** *[Multisensor | July 2023]*: Copernicus Marine Service/OSTIA • **35.5** *[Multisensor | 01.07.2014]*: Copernicus/ESA SST CCI • **35.6**: NOAA • **36.1** *[Sentinel-2 | July 2023]*: Copernicus • **36.2**: Copernicus Land Monitoring Service • **37.3** *[Landsat 5 | 10.06.1985]*: USGS • **37.4** *[Sentinel-2 | 25.06.2023]*: Copernicus • **37.5**: Mohamed Eissa • **37.6** *[Sentinel-2 | 05.11.2017]*, **37.7** *[Sentinel-2 | 14.11.2022]*, **38.1** *[Sentinel-2 | 2023]*, **38.2** *[Sentinel-3 | 2023]*: Copernicus • **38.3**: Kamshat Tusspova et al., Water 12/2020. • **38.4** *[Sentinel-3 | 2023]*: Copernicus • **38.5** *[Landsat 4 | 1987]*, **38.6** *[Argon | 1964]*: USGS • **39.7** *[Modis | Mosaic]*: NASA Goddard Space Flight Center • **39.8** *[Sentinel-2 | 22.04.2023]*: Copernicus; U.S. Department of the Interior, BOEM (Bureau of Ocean Energy Management) • **39.9** *[Landsat 4 | 04.05.1985]*, **39.10** *[Landsat 5 | 19.07.1995]*: USGS • **39.11** *[Sentinel-2 | 08.05.2017]*, **39.12** *[Sentinel-2 | 12.05.2023]*, **40.1** *[Sentinel-2 | 21.03.2023]*, **40.2** *[Sentinel-2 | 31.03.2019]*, **40.3** *[Sentinel-2 | 31.03.2019]*: Copernicus • **40.4**: US Army Corps of Engineers (Omaha) • **41.5**: Città di Venezia, Alte Maree • **41.6**: Fusi Sandro • **41.7** *[Sentinel-2 | 04.11.2021]*, **41.8** *[Sentinel-2 | 24.11.2022]*: Copernicus • **42.1** *[1980-2020]*, **42.2**, **42.3**: NSIDC • **42.4** *[CryoSat | January 2011]*, **42.5** *[CryoSat | January 2024]*: CPOM • **43.6**: Copernicus Climate Change Service • **43.7** *[Sentinel-1 | 2020]*: Coperniucs/ENVEO • **43.8** *[Sentinel-2 | 01.09.2023]*, **43.9** *[Sentinel-2 | 01.09.2023]*: Copernicus • **44.1** *[2004]*: NSIDC • **44.2** *[CryoSat | 2012]*: ESA/Helm et al., The Cryosphere, 2014 • **44.3.1** *[Sentinel-1 | 06.08.2023]*, **44.3.2** *[Sentinel-1 | 13.09.2023]*, **44.3.3** *[Sentinel-1 | 19.10.2023]*, **45.4** *[Sentinel-3 | 15.11.2023]*, **45.5** *[Sentinel-3 | 15.11.2023]*: Copernicus • **46.1** *[Modis | Mosaic]*: NASA Goddard Space Flight Center • **46.2** *[Sentinel-2 | 30.07.2023]*: Copernicus • **46.3** *[2023]*: WGMS Fluctuation of Glaciers database • **46.4** *[Landsat 5 | 28.07.1986]*: USGS • **46.5** *[Sentinel-2 | 30.07.2023]*: Copernicus • **47.6**: Dirk Beyer • **47.7** *[Landsat 5 | 26.07.1985]*: USGS • **47.8** *[Sentinel-2 | 13.07.2022]*: Copernicus • **47.9** *[Landsat 5 | 26.07.1985]*: USGS • **47.10** *[Sentinel-2 | 13.07.2022]*: Copernicus • **47.11** *[2023]*: WGMS Fluctuation of Glaciers database • **47.12** *[Landsat 5 | 26.07.1985]*: USGS • **48.1** *[Multisensor | 2022]*: Copernicus/C3S/ECMWF • **48.2** *[Multisensor | July 2023]*, **48.3** *[Multisensor | January 2023]*: Copernicus Atmosphere Monitoring Service • **49.4**: eoVision/ESA • **49.5**: NOAA/NCEI • **50.1** *[Multisensor | 2000-2023]*: NASA • **50.3** *[NOAA AVHRR | January 2023]*: EUMETSAT/CM SAF • **51.2**, **51.2**, **51.2**, **51.2**, **51.2**, **51.2**: climatecharts.net • **51.4** *[NOAA AVHRR | 01.07.2023]*: EUMETSAT/CM SAF • **52.1** *[Meteosat MSG | 2004]*, **53.2** *[Meteosat MSG | 2004]*: EUMETSAT • **54.1** *[Sentinel-5P | 2023]*, **54.2** *[Multisensor | January 2020]*, **55.3** *[Multisensor | July 2020]*, **55.4a** *[Sentinel-5P | January 2020]*, **55.4b** *[Sentinel-5P | July 2020]*: Copernicus Atmosphere Monitoring Service information • **55.5a** *[Multisensor | October 1970]*, **55.5b** *[Multisensor | October 1980]*, **55.5c** *[Multisensor | October 1990]*, **55.5d** *[Multisensor | October 2000]*, **55.5e** *[Multisensor | October 2010]*: Copernicus Climate Change Service, Climate Data Store • **56.1**: W. Lauer, P. Frankenberg; USGS • **56.1**, **56.1**: 0 • **58.1** *[Sentinel-3 | June 2023]*, **58.2** *[Sentinel-3 | December 2023]*: Copernicus Marine Service Information, provided by OCTAC/PML production centre • **58.3** *[Sentinel-2 | 20.07.2019]*, **59.4** *[Sentinel-3 | July 2018]*, **59.5** *[Sentinel-3 | January 2018]*, **59.6a** *[Sentinel-2 | 08.04.2023]*, **59.6b** *[Sentinel-2 | 13.04.2023]*: Copernicus • **60.1** *[2019]*: Copernicus Land Monitoring Service • **60.2** *[Sentinel-2 | 08.09.2023]*, **60.3** *[Sentinel-2 | 26.09.2023]*, **60.4** *[Sentinel-2 | 20.09.2023]*, **60.5** *[Sentinel-2 | 27.09.2023]*, **60.6** *[Sentinel-2 | 24.09.2023]*, **61.7** *[Sentinel-2 | 08.09.2023]*, **61.8** *[Sentinel-2 | 31.03.2023]*: Copernicus • **61.9** *[2024]*: Our World in Data • **62.1** *[Sentinel-2 | 10.09.2022]*, **62.2** *[Sentinel-2 | 10.09.2022]*: Copernicus • **62.3** *[Landsat 5 | 17.10.1985]*: USGS • **62.4**: ANE • **63.5** *[Landsat 5 | 15.04.1985]*, **63.6** *[Landsat 5 | 27.04.1995]*, **63.7** *[Landsat 5 | 18.04.2015]*: USGS • **63.8** *[Sentinel-2 | 26.04.2023]*, **63.9** *[Sentinel-2 | 26.04.2023]*: Copernicus • **63.10**: U.S. Dept. Agriculture • **64.1** *[Landsat 5 | 28.06.1991]*: USGS • **64.2**: Bruno Kelly/Amazônia Real • **64.3**: INPE • **64.4** *[Landsat 5 | 24.06.1984]*, **64.5** *[Landsat 5 | 15.05.2010]*: USGS • **64.6** *[Sentinel-2 | 07.10.2023]*: Copernicus • **65.7**: National Forestry Database • **65.8** *[Sentinel-2 | 18.05.2023]*, **65.9** *[Sentinel-2 | 07.06.2003]*, **65.10** *[Sentinel-2 | 07.06.2003]*, **65.11** *[Sentinel-2 | 07.06.2003]*: Copernicus • **65.12**: Cameron Strandberg • **66.1** *[Sentinel-2 | 29.04.2023]*: Copernicus • **66.2** *[2022]*: FAO, The state of world fisheries and aquaculture 2022 • **66.3** *[Sentinel-1 | 26.04.2023]*: Copernicus • **66.4** *[Landsat 5 | 05.05.2007]*, **66.5** *[Landsat 5 | 17.05.1989]*: USGS • **67.6** *[Sentinel-2 | 24.04.2023]*, **67.7** *[Sentinel-2 | 14.04.2023]*, **67.8** *[Sentinel-2 | 24.04.2023]*, **67.9** *[Sentinel-2 | 24.04.2023]*: Copernicus • **67.10**: Powell.Ramsar • **67.11**: Bsmuc64ger • **67.12** *[Sentinel-2 | July 2023]*: Copernicus • **68.1**: Gridded Population of the World (GPW) v4; NASA/SEDAC • **68.2** *[Sentinel-2 | 13.04.2024]*, **68.3** *[Sentinel-2 | 18.04.2024]*, **69.4** *[Sentinel-2 | 19.03.2024]*: Copernicus • **69.6**: UNDESA, 2013 • **69.5a**, **69.5b**, **69.5c**: LivePopulation.com • **70.1** *[Landsat 4 | 13.10.1984]*: USGS • **70.2** *[Sentinel-2 | 27.02.2023]*: Copernicus • **70.3**: worldpopulationreview.com • **70.4** *[2018]*: UNDESA, World Urbanization Prospects 2018 • **70.5**: Noah Maxwell • **71.6**: Sinopitt Xu • **71.7** *[2015]*: UNDESA • **71.8** *[Landsat 4 | 21.04.1987]*: USGS • **71.9** *[Sentinel-2 | 05.07.2023]*, **72.1** *[Sentinel-2 | 23.07.2023]*: Copernicus • **72.2**: ICAO, ACI/Moodie-Davitt-Report • **72.3**: Kulttuurinavigaattori • **72.4** *[Landsat 5 | 18.09.2010]*: USGS • **72.5** *[Sentinel-2 | 24.07.2017]*, **72.6** *[Sentinel-2 | 23.07.2023]*, **73.7** *[Sentinel-2 | 29.03.2021]*, **73.8** *[Sentinel-1 | 21.03.2021]*, **73.9** *[Sentinel-1 | 27.03.2021]*: Copernicus • **73.10**: Suez Canal Authority • **73.11**: Wolfgang Fricke • **73.12** *[Sentinel-5P | 2023]*: Copernicus (S5P-PAL; STAC?) • **74.1** *[Landsat 5 | 15.07.2015]*, **74.2** *[Landsat 5 | 27.07.2011]*: USGS • **74.3** *[Sentinel-2 | 26.07.2017]*, **74.4** *[Sentinel-2 | 26.07.2017]*: Copernicus • **74.5**: Fernanda Brandt • **75.6** *[Sentinel-1 | 02.03.2024]*, **75.7** *[Sentinel-2 | 07.07.2023]*, **75.8** *[Sentinel-2 | 07.07.2023]*, **75.9** *[Sentinel-2 | 27.05.2017]*, **75.10** *[Sentinel-2 | 28.01.2024]*: Copernicus • **75.11** *[2024]*: IRENA - International Renewable Energy Agency •

Explanation for Image and Data Sources:

19.8 *[Sentinel-1 | 23.03.2022]:* Copernicus

19.8	page number . consecutive number of figure
[satellite | acquisition date]	in case figure is satellite image, satellite model and acquisition date is specified
Copernicus	data source/image credit
•	separator

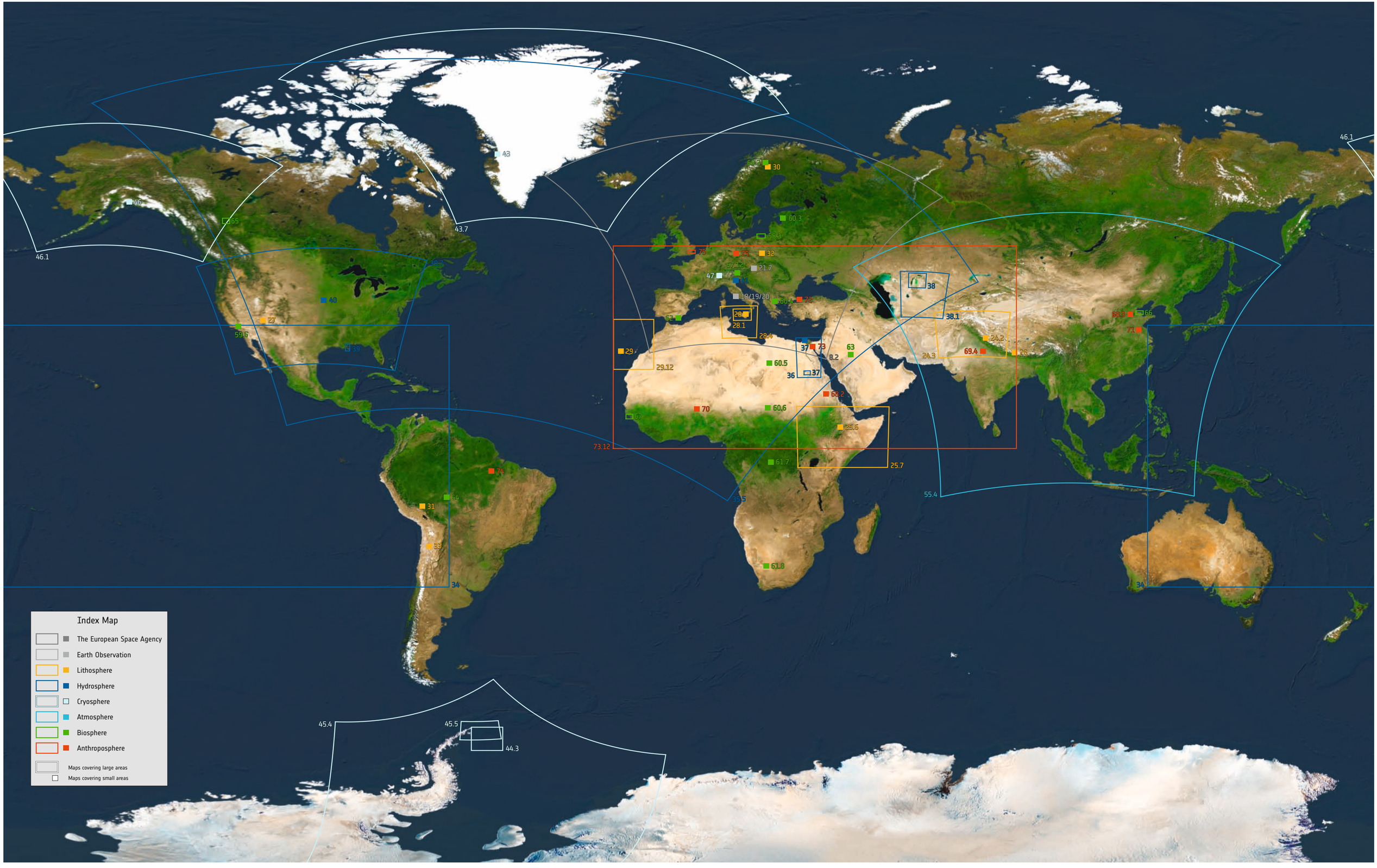
Index Map
The European Space Agency
Earth Observation
Lithosphere
Hydrosphere
Cryosphere
Atmosphere
Biosphere
Anthroposphere
Maps covering large areas
Maps covering small areas
46.1
43
43.7
46
65
39.7
40
27
59.6
39
74
64
31
38
34
30
60.3
58.9
75
75
32
21.7
47
19/19/20
60.4
72
32
28.1
28.4
29
29.12
60.5
37
73
63
8.2
36
37
68.2
70
60.6
67
73.12
25.6
61.7
25.7
35.5
61.8
38
38.1
24.2
69.4
24.3
28
58.3
66
71
55.4
34
45.4
45.5
44.3
46.1